Title
Ultraviolet Behavior of Supergravity Amplitudes

Permalink
https://escholarship.org/uc/item/1hm152b2

Author
Edison, Alex

Publication Date
2019

Peer reviewed|Thesis/dissertation

UNIVERSITY OF CALIFORNIA

Los Angeles

Ultraviolet Behavior of Supergravity Amplitudes

A dissertation submitted in partial satisfaction

of the requirements for the degree

Doctor of Philosophy in Physics

by

Alexander Christian Edison

2019

ABSTRACT OF THE DISSERTATION

Ultraviolet Behavior of Supergravity Amplitudes

by

Alexander Christian Edison

Doctor of Philosophy in Physics

University of California, Los Angeles, 2019

Professor Zvi Bern, Chair

In this manuscript, we detail three recent calculations addressing the ultraviolet behavior of supersymmetric quantum gravity. First, we revisit the classic calculation of the two-loop pure gravity divergence. We argue that the $\frac{1}{\epsilon}$ divergence is regulator and duality dependent. In its place, we propose that examining the running of the scaling parameter, $\log\mu$, is a duality and regulator independent approach to assessing gravity divergences in four dimensions. We explicitly calculate the $\log\mu$ coefficient at two loops for gravity with any particle content, explicitly verifying the divergences for pure gravity, and the finiteness for supersymmetric gravities. Second, we analyze fully-integrated $\mathcal{N}=4$ supergravity at one loop using the double copy. We find that there are evanescent effects at one loop that come directly from evanescent terms in pure-Yang–Mills. Using this observation, we lay the groundwork for deeper analysis of the $U(1)$ anomaly with respect to the observed evanescent behavior. Finally, we tackle the long-standing question of the critical dimension of $\mathcal{N}=8$ supergravity at five loops. We construct an integrand using the generalized double copy, expand the integrand in large loop momentum, and reduce the resulting integrals using $\mathfrak{sl}(L)$ integration-by-parts relations. This procedure yields a critical dimension of $d_c = 24/5$.

The dissertation of Alexander Christian Edison is approved.

Terence Chi-Shen Tao

Michael Gutperle

Per J. Kraus

Zvi Bern, Committee Chair

University of California, Los Angeles

2019

For my grandfather Larry.

Contents

List of Figures

List of Tables

Contribution of authors

Chapter 1 is based, with minimal changes, on Ref. [1]. It includes calculations and contributions from my advisor Zvi Bern, and from Lance Dixon and Huan-Han Chi of Standford. Chapter 2 is based on Ref. [2] with Zvi Bern, Julio Parra-Martinez, and David Kosower. Chapter 3 is based on work done with Zvi Bern, JJ Carrasco, Wei-Ming Chen, Henrik Johansson, Julio Parra-Martinez, Radu Roiban, and Mao Zeng that appeared in Ref. [3]

.

Vita

Institution	Position	Year
Bowdoin College	Bachelor of Arts in Physics	2013
UCLA	Teaching Assisstant/Graduate Student Researcher	2013-2019

My Publications

- Z. Bern, H.-H. Chi, L. Dixon, and A. Edison, "Two-Loop Renormalization of Quantum Gravity Simplified", Phys. Rev. **D95**, 046013 (2017), arXiv:1701.02422 `[hep-th]`.

- Z. Bern, A. Edison, D. Kosower, and J. Parra-Martinez, "Curvature-squared multiplets, evanescent effects, and the U(1) anomaly in $N = 4$ supergravity", Phys. Rev. **D96**, 066004 (2017), arXiv:1706.01486 `[hep-th]`.

- Z. Bern, J. J. Carrasco, W.-M. Chen, A. Edison, H. Johansson, J. Parra-Martinez, R. Roiban, and M. Zeng, "Ultraviolet Properties of $\mathcal{N} = 8$ Supergravity at Five Loops", Phys. Rev. **D98**, 086021 (2018), arXiv:1804.09311 `[hep-th]`.

Chapter 1

Two-Loop Renormalization of Quantum Gravity Simplified

The coefficient of the dimensionally regularized two-loop R^3 divergence of (nonsupersymmetric) gravity theories has recently been shown to change when non-dynamical three forms are added to the theory, or when a pseudo-scalar is replaced by the anti-symmetric two-form field to which it is dual. This phenomenon involves evanescent operators, whose matrix elements vanish in four dimensions, including the Gauss-Bonnet operator which is also connected to the trace anomaly. On the other hand, these effects appear to have no physical consequences in renormalized scattering processes. In particular, the dependence of the two-loop four-graviton scattering amplitude on the renormalization scale is simple. In this chapter, we explain this result for any minimally-coupled massless gravity theory with renormalizable matter interactions by using unitarity cuts in four dimensions and never invoking evanescent operators.

1.1 Introduction

Recent results show that the ultraviolet structure of gravity is much more interesting and subtle than might be anticipated from standard considerations. One example of a new ultraviolet surprise is the recent identification of "enhanced ultraviolet cancellations" in certain supergravity theories [4–6], which are as yet unexplained by standard symmetries [7–9]. Another recent example is the lack of any simple link between the coefficient of the dimensionally-regularized two-loop R^3 ultraviolet divergence of pure Einstein gravity [10–12] and the renormalization-scale dependence of the renormalized theory [13]. While the value of the divergence is altered by a Hodge duality transformation that maps anti-symmetric tensor fields into scalars, the renormalization-scale dependence is unchanged. In contrast, for the textbook case of gauge theory at one loop the divergence and the renormalization-scale dependence—the beta function—are intimately linked. In Ref. [13], a simple formula for the renormalization-scale dependence of quantum gravity at two loops was found to hold in a wide variety of gravity theories. In this chapter we explain this formula via unitarity.

As established by the seminal work of 't Hooft and Veltman [14], pure gravity has no ultraviolet divergence at one loop. This result follows from simple counterterm considerations: after accounting for field redefinitions, the only independent potential counterterm is equivalent to the Gauss-Bonnet curvature-squared term. However, in four dimensions this term is a total derivative and integrates to zero for a topologically trivial background, so no viable counterterm remains. Hence pure graviton amplitudes are one-loop finite. Amplitudes with four or more external matter fields are, however, generally divergent.

At two loops pure gravity does diverge, as demonstrated by Goroff and Sagnotti [10, 11] and confirmed by van de Ven [12]. The pure-gravity counterterm, denoted by R^3, is cubic in the Riemann curvature. The two-loop divergence was recently reaffirmed in pure gravity [13], and was also studied in a variety of other theories, by evaluating the amplitude for four identical-helicity gravitons. The actual value of the dimensionally-regularized R^3

divergence changes when three-forms are added to the theory, even though they are not dynamical in four space-time dimensions. More generally, when matter is incorporated into the theory, the coefficient of the R^3 divergence changes under a Hodge duality transformation. However, such transformations appear to have no physical consequences for renormalized amplitudes [13].

The dependence of the two-loop divergence on duality transformations is closely connected to the well-known similar dependence of the one-loop trace anomaly [15]. One-loop subdivergences in the computation include those dictated by the Gauss-Bonnet term, whose coefficient is the trace anomaly [13]. Duff and van Nieuwenhuizen showed that the trace anomaly changes under duality transformations of p-form fields, suggesting that theories related through such transformations might be quantum-mechanically inequivalent [15]. Others have argued that these effects are gauge artifacts [16–20]. For graviton scattering at two loops in dimensional regularization, quantum equivalence can be restored, but only after combining the bare amplitude and counterterm contributions [13].

The surprising dependence of the two-loop R^3 divergence in gravity on choices of field content outside of four dimensions emphasizes the importance of focusing on the renormalization-scale dependence of renormalized amplitudes as the proper robust quantity for understanding the ultraviolet properties. The divergence itself, of course, never directly affects physical quantities since it can be absorbed into a counterterm. In contrast, the renormalization scale dependence does affect physical quantities because it controls logarithmic parts of the scaling behavior of the theory. While this is well known, what is surprising is that, in contrast to gauge theory, the two-loop divergences of pure gravity are not linked in any straightforward way to the scaling behavior of the theory. An underlying cause is that evanescent operators, such as the Gauss-Bonnet term, contribute to the leading two-loop R^3 divergence of graviton amplitudes [13].

Evanescent operators are well-studied in gauge theory (see e.g. Ref. [21–25]), where they can modify subleading corrections to anomalous dimensions or beta functions. A standard

3

one-loop subdivergence is associated with the one-loop matrix element of a non-evanescent operator; integrating over the remaining loop momentum generates a double pole $1/\epsilon^2$ in the dimensional regulator $\epsilon = (4 - D)/2$. When the operator is evanescent, the matrix element is suppressed in the four-dimensional limit, typically reducing the double pole to a simple pole, but still leaving a contribution to the anomalous dimension. A key property that is special to the two-loop gravity computation is that the divergent evanescent contribution begins at the same order as the first divergence. However, similar effects could appear in other contexts. For example, in the effective field theory of flux tubes with a large length L, there is an evanescent operator which would otherwise contribute to the energy at order $1/L^5$ [26]; presumably it will have to be taken into account in a dimensionally-regularized computation of $(\ln L)/L^7$ corrections to the energy.

In contrast to the divergence, the renormalization-scale dependence does appear to be robust and unaltered by duality transformations or other changes in regularization scheme. Indeed, a simple formula was proposed [13] for the R^3 contribution to this dependence at two loops, which is proportional to the number of four-dimensional bosonic minus fermionic degrees of freedom. Yet in Ref. [13] this simple formula only arose after combining the dimensionally-regularized two-loop amplitude with multiple counterterm contributions. Intermediate steps involved evanescent operators and separate contributions did not respect Hodge duality; nor would they have respected supersymmetry if we had treated fermionic contributions in the same way.

The purpose of the present chapter is to explain the simple renormalization-scale dependence in terms of unitarity cuts in four dimensions. This approach turns a two-loop computation effectively into a one-loop one, it manifestly respects Hodge duality and supersymmetry, and evanescent operators never appear.

This chapter is organized as follows: In Section 3.2 we summarize the previous approach of Ref. [13], along with the the surprisingly simple formula found for the renormalization-scale dependence of the four-graviton amplitude at two loops. Then in Section 1.3 we

derive the formula purely from four-dimensional unitarity cuts. Our conclusions are given in Section 3.8.

1.2   Review of previous approach

Pure gravity is described by the Einstein-Hilbert Lagrangian,

$$\mathcal{L}_{\text{EH}} = -\frac{2}{\kappa^2}\sqrt{-g}R\,, \tag{1.1}$$

where $\kappa^2 = 32\pi G_N = 32\pi/M_P^2$ and the metric signature is $(+---)$. While we are primarily interested in pure gravity, it is insightful to include matter as well, as in Ref. [13], by coupling gravity to n_0 scalars, n_2 two-forms and n_3 three-forms, as well as fermionic fields, $n_{1/2}$ of spin-1/2 and $n_{3/2}$ of spin-3/2.

At one loop, graviton amplitudes do not diverge in four dimensions, because no viable counterterms are available after accounting for field redefinitions and the Gauss–Bonnet (GB) theorem [14]. Divergences do occur if we allow the fields to live outside of four dimensions [10, 11, 15, 27–31]. The Gauss–Bonnet counterterm is given by

$$\mathcal{L}_{\text{GB}} = \frac{1}{(4\pi)^2}\frac{1}{\epsilon}\Big(\frac{53}{90} + \frac{n_0}{360} + \frac{91n_2}{360} - \frac{n_3}{2} + \frac{7n_{1/2}}{1440} - \frac{233n_{3/2}}{1440}\Big) \times \sqrt{-g}(R^2 - 4R_{\mu\nu}^2 + R_{\mu\nu\rho\sigma}^2)\,. \tag{1.2}$$

At one loop, matter self-interactions cannot affect this graviton counterterm. The divergence represented by Eq. (1.2) vanishes for any one-loop amplitude with four-dimensional external gravitons. Amplitudes with four external matter states generically have divergences in four dimensions, starting at one loop. We neglect such divergences in this chapter because they do not affect the two-loop four-graviton divergence.

In the context of dimensional regularization, evanescent operators, whose matrix elements vanish in four dimensions, can contribute to higher-loop divergences. Indeed, the Gauss–

Bonnet term generates subdivergences at two loops, because the momenta and polarizations of internal lines can lie outside of four dimensions [13, 32].

The coefficient in front of Eq. (1.2) has a rather interesting story, because it is proportional to the trace anomaly [10, 11, 15, 27–31]. The connection comes about because the calculations of the ultraviolet divergence and the trace anomaly are essentially identical, except that in the latter calculation we replace one of the four graviton polarization tensors with a trace over indices. As already noted, the trace anomaly has long been known to have the rather curious feature that it is not invariant under duality transformations [15] that relate two classical theories in four dimensions. In more detail, under a Hodge duality transformation, in four dimensions the two-form field is equivalent to a scalar and the three-form field is equivalent to a cosmological-constant contribution:

$$ H_{\mu\nu\rho} \;\leftrightarrow\; \frac{i}{\sqrt{2}}\, \varepsilon_{\mu\nu\rho\alpha}\, \partial^{\alpha}\phi\,, \qquad\qquad H_{\mu\nu\rho\sigma} \;\leftrightarrow\; \frac{2}{\sqrt{3}}\, \varepsilon_{\mu\nu\rho\sigma}\, \frac{\sqrt{\Lambda}}{\kappa}\,. \qquad (1.3) $$

Equation (1.2) shows that the trace anomaly, and hence the associated evanescent divergence, change under duality transformations: The coefficients in front of n_2 and n_0 differ, and the one in front of n_3 is nonzero. Correspondingly, subdivergences in two-loop amplitudes depend on the field representation used.

In contrast to one loop, at two loops pure gravity in four dimensions does diverge in dimensional regularization, as shown by Goroff and Sagnotti [10, 11] and confirmed by van de Ven [12]. In the $\overline{\text{MS}}$ scheme, with $\epsilon = (4 - D)/2$, the divergence is given by

$$ \mathcal{L}_{R^3}^{\text{div}} \;=\; -\frac{209}{1440}\left(\frac{\kappa}{2}\right)^{2}\frac{1}{(4\pi)^4}\frac{1}{\epsilon}\sqrt{-g}\, R^{\alpha\beta}{}_{\gamma\delta}R^{\gamma\delta}{}_{\rho\sigma}R^{\rho\sigma}{}_{\alpha\beta}\,. \qquad (1.4) $$

In this computation, a mass regulator was introduced, in addition to the dimensional regulator, in order to deal with certain infrared singularities. This procedure introduces regulator dependence which is removed by subtracting subdivergences, integral by integral. The sub-
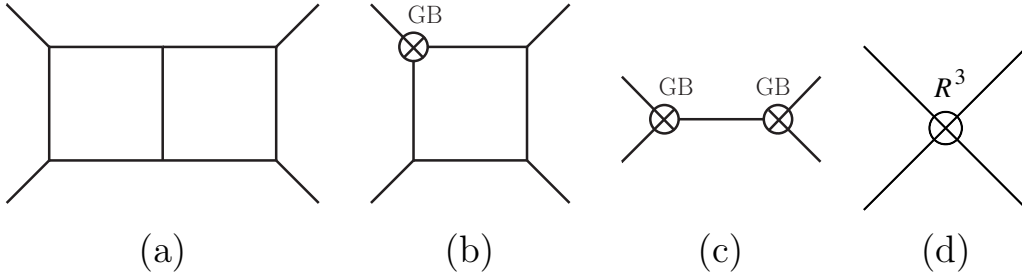
Figure 1.1: Representative four-point diagrams for (a) the bare contribution, and the (b) single-GB-counterterm, (c) double-GB-counterterm, and (d) R^3-counterterm insertions needed to remove all divergences.

divergence subtraction also properly removes the Gauss–Bonnet subdivergences, leaving only the two-loop divergence.

In Ref. [13], the same R^3 divergence (1.4) was extracted from a four-graviton scattering amplitude with all helicities positive, $M_4^{2-\text{loop}}(++++)$. This helicity amplitude is particularly simple to calculate, making it a useful probe of the two-loop ultraviolet structure. It is sensitive to the R^3 operator because the insertion of R^3 into the tree amplitude gives a nonvanishing result. For a single insertion of the Lagrangian term

$$\mathcal{L}_{R^3} \;=\; c_{R^3}(\mu)\sqrt{-g}\, R^{\alpha\beta}{}_{\gamma\delta}R^{\gamma\delta}{}_{\rho\sigma}R^{\rho\sigma}{}_{\alpha\beta}\,, \tag{1.5}$$

the identical-helicity matrix element is [33]

$$M_4(++++) \;=\; -60\,i\,c_{R^3}(\mu)\left(\frac{\kappa}{2}\right)^4 \mathcal{T}^2\, s_{12}s_{23}s_{13}\,, \tag{1.6}$$

where

$$\mathcal{T} = \frac{[12][34]}{\langle 12\rangle\langle 34\rangle}\,, \tag{1.7}$$

and $s_{12} = (k_1 + k_2)^2$, $s_{23} = (k_2 + k_3)^2$ and $s_{13} = (k_1 + k_3)^2$ are the usual Mandelstam invariants. The factor $\mathcal{T}$ is a pure phase constructed from the spinor products $\langle ab\rangle$ and $[ab]$, defined in e.g. Ref. [34].

7

Although no mass regulator was used in Ref. [13], the Gauss–Bonnet operator (1.2) contributes nonvanishing subdivergences, because internal legs of the two-loop amplitude propagate in D dimensions. Fig. 1.1 illustrates the complete set of counterterm contributions required to renormalize the dimensionally-regulated four-graviton amplitude at two loops. Besides the bare amplitude in Fig. 1.1(a), there is the single insertion of the GB operator into a one-loop amplitude in Fig. 1.1(b) and the double-GB-counterterm insertion into a tree amplitude, Fig. 1.1(c). Finally, the two-loop R^3 counterterm insertion is shown in Fig. 1.1(d). All contributions shown are representative ones, out of a much larger number of Feynman diagrams; for example, the bare contribution also includes nonplanar diagrams.

For pure gravity, assembling the contributions from Fig. 1.1(a)–(c), the divergence in the two-loop four-graviton amplitude and associated renormalization-scale dependence is [13]

$$\mathcal{M}_4^{\text{2-loop}}(++++)\Big|_{(a)-(c)} = \left(\frac{\kappa}{2}\right)^6 \frac{i}{(4\pi)^4} s_{12}s_{23}s_{13}\mathcal{T}^2 \left(\frac{209}{24\,\epsilon} - \frac{1}{4}\ln\mu^2\right) + \text{finite}\,. \qquad (1.8)$$

In a minimal subtraction prescription, the effect of the R^3 counterterm in Fig. 1.1(d) is simply to remove the $209/24 \times 1/\epsilon$ term. Including matter fields, the ultraviolet divergence changes under duality transformations [13]. This change might not be surprising, given that the coefficient of the one-loop Gauss–Bonnet subdivergence (1.2) is not invariant under duality transformations [15]. For example, adding n_3 three forms, which do not propagate in four dimensions, changes the coefficient of the infinity in Eq. (1.4) to

$$\frac{209}{1440\epsilon} \quad \to \quad \frac{209}{1440\epsilon} - \frac{1}{8\epsilon}\,n_3\,, \qquad (1.9)$$

while the coefficient of $\ln\mu^2$ is unaltered. Also, the value of the leading infinity depends nontrivially on the details of the regularization procedure, while the coefficient of the $\ln\mu^2$ term does not.

The fact that the two numerical coefficients in Eq. (1.8) are rather different, and that one
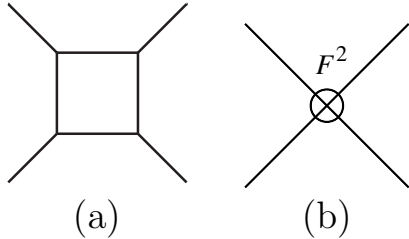
Figure 1.2: Renormalization of on-shell Yang–Mills amplitudes at one loop requires (a) the bare amplitude and (b) an F^2 counterterm, for which representative contributions are shown.

changes under duality transformations but not the other, implies that they are not directly linked. This is rather curious. From the textbook computation of the one-loop beta function in Yang–Mills theory, we are used to the idea that they are linked. In that case, the analog of Fig. 1.1 is Fig. 1.2. To renormalize the on-shell amplitudes in the theory at one loop, we need the bare one-loop amplitude, with a representative diagram shown in Fig. 1.2(a), and a single insertion of the $F^a_{\mu\nu} F^{a\,\mu\nu}$ counterterm into a tree-level amplitude, with a representative diagram shown in Fig. 1.2(b).

Schematically, these two contributions depend on the renormalization scale μ as follows:

$$\frac{C^{(\mathrm{a})}}{\epsilon} (\mu^2)^{\epsilon} + \frac{C^{(\mathrm{b})}}{\epsilon} = \left(C^{(\mathrm{a})} + C^{(\mathrm{b})}\right)\frac{1}{\epsilon} + C^{(\mathrm{a})} \ln \mu^2 + \cdots ,\qquad (1.10)$$

where the $(\mu^2)^{\epsilon}$ factor in the bare amplitude compensates for the dimension of the loop integration measure $d^{4-2\epsilon}\ell$, where ℓ is the loop momentum. In a minimal subtraction scheme, one chooses $C^{(\mathrm{b})} = -C^{(\mathrm{a})}$ to cancel the $1/\epsilon$ pole. Because the counterterm insertion has no factor of $(\mu^2)^{\epsilon}$, the leading divergence $C^{(\mathrm{a})}$ is tied directly to the renormalization-scale dependence of the coupling, i.e. the beta function, independent of the details of the regularization procedure.

What about gravity at two loops? As explained in Ref. [13], the disconnect between the divergences and the renormalization-scale dependence happens because of an interplay between the bare terms and the evanescent subdivergences. The analog of Eq. (1.10) for the

9

divergence and $\ln \mu^2$ dependence of the two-loop gravity amplitude is

$$\frac{C^{(\mathrm{a})}}{\epsilon}(\mu^2)^{2\epsilon}+\frac{C^{(\mathrm{b})}}{\epsilon}(\mu^2)^{\epsilon}+\frac{C^{(\mathrm{c})}}{\epsilon}+\frac{C^{(\mathrm{d})}}{\epsilon}=\left(C^{(\mathrm{a})}+C^{(\mathrm{b})}+C^{(\mathrm{c})}+C^{(\mathrm{d})}\right)\frac{1}{\epsilon}+(2C^{(\mathrm{a})}+C^{(\mathrm{b})})\ln\mu^2+\cdots.$$

(1.11)

The differing powers of μ for each contribution follow from dimensional analysis of the integrals, after accounting for the fact that the counterterm insertions do not carry factors of $(\mu^2)^\epsilon$.

The coefficient of the R^3 counterterm $C^{(\mathrm{d})}$ cancels the two-loop divergence in Eq. (1.11), as a consequence of the renormalization conditions, $C^{(\mathrm{d})}=-C^{(\mathrm{a})}-C^{(\mathrm{b})}-C^{(\mathrm{c})}$. In the amplitude computed in Ref. [13], the value of the coefficient of the two-loop R^3 counterterm depends on duality transformations, while the coefficient in front of the $\ln\mu^2$, namely $2C^{(\mathrm{a})}+C^{(\mathrm{b})}$, does not. The fact that different combinations of coefficients appear in the divergence and in the $\ln\mu^2$ term explains why the two-loop divergence and renormalization-scale dependence do not have to be simply related. As we discuss in the next section, the coefficient of the logarithm can be computed directly in four dimensions, completely avoiding the issue of evanescent operators. On the other hand, the divergence is exposed to the subtleties of evanescent operators and dimensional regularization. More remarkably, as found in a variety of examples [13], the $\ln\mu^2$ coefficient satisfies a simple formula, which we explain in the next section.

The disconnect between the divergence and the renormalization-scale dependence could lead to situations where an explicit divergence is present, yet there is no associated running of a coupling or other physical consequences. As an example, we have computed the divergence in $\mathcal{N}=1$ supergravity with one matter multiplet using the same techniques. It is convenient to include a matter multiplet because for this theory we can construct the two-loop integrand straightforwardly using double-copy techniques [35, 36]. Even though this theory is supersymmetric, the trace anomaly is nonvanishing [37]. Therefore there are subdivergences of the form of Fig. 1.1(b), as well as Fig. 1.1(c). We have computed the four

contributions corresponding to Fig. 1.1. They are given by

$$C^{(a)} = \frac{11}{16}, \qquad C^{(b)} = -\frac{11}{8}, \qquad C^{(c)} = \frac{363}{32}, \qquad C^{(d)} = -\frac{341}{32}, \qquad (1.12)$$

where the normalization corresponds to $C^{(a)} + C^{(b)} + C^{(c)} = 209/24$ for pure gravity; see Eq. (1.8). So the divergence from terms (a)–(c) in Eq. (1.11) is nonzero, but the $\ln \mu^2$ coefficient vanishes, $2C^{(a)} + C^{(b)} = 0$. In fact, it turns out that all logarithms $\ln s_{ij}$ in the amplitude cancel as well. The polynomial terms can be canceled by the same R^3 counterterm but with a finite coefficient (or equivalently, an order ϵ correction to $C^{(d)}$).

The upshot is that for this $\mathcal{N} = 1$ supergravity theory, the divergence and associated trace anomaly has the curious effect of violating the supersymmetry Ward identity [38–40] that requires the identical-helicity amplitude to vanish. The appearance of a divergence is due to the breaking of supersymmetry by the trace anomaly, which induces subdivergences even when supersymmetry implies that no divergences can be present [41, 42]. To restore the supersymmetry Ward identities requires adding an R^3 counterterm to the theory, with both a $1/\epsilon$ and a finite coefficient, which fixes the two-loop amplitude uniquely. This procedure is possible only because the $\ln \mu^2$ coefficient vanishes. That is, in this case there is no loss of predictivity, even though there is a $1/\epsilon$ divergence. If the $\ln \mu^2$ coefficient is nonvanishing, as in the case of pure gravity, then there must be an arbitrary finite constant in the renormalization procedure, associated with fixing the R^3 coupling at different choices of renormalization scale, leading to the usual loss of predictivity of nonrenormalizable theories.

This discussion applies more generally. Suppose there is a hidden symmetry that would enforces finiteness if it can be preserved. Yet if that symmetry is broken by the trace anomaly, or more generally by the regularization procedure, we might conclude that the theory's divergence implies a loss of predictivity. It is therefore always crucial to inspect the renormalization-scale dependence.

In contrast, one might even imagine a regularization prescription that eliminates the $1/\epsilon$

divergence, for example by making the perverse choice $n_3 = 8 \cdot 209/1440$ in Eq. (1.9) for the case of pure gravity. However, since the $\ln \mu^2$ coefficient is nonvanishing in this case, there is still an arbitrariness in the finite R^3 counterterm associated with different choices for μ, and an associated loss of predictivity. The theory is no better than an ultraviolet-divergent theory, even if the $1/\epsilon$ divergence is arranged to cancel.

From now on we focus entirely on the renormalization-scale dependence. For the two-loop graviton identical-helicity scattering amplitude with various matter content, Ref. [13] found the following simple form:

$$\mathcal{M}_4^{\text{2-loop}}(++++)\Big|_{\ln \mu^2} = -\left(\frac{\kappa}{2}\right)^6 \frac{i}{(4\pi)^4} s_{12} s_{23} s_{13} \mathcal{T}^2 \frac{N_b - N_f}{8} \ln \mu^2 , \qquad (1.13)$$

where N_b and N_f are the number of physical four-dimensional bosonic and fermionic states in the theory. Using Eq. (1.6), this result is equivalent to the running of the R^3 coefficient according to

$$\mu \frac{\partial c_{R^3}}{\partial \mu} = \left(\frac{\kappa}{2}\right)^2 \frac{1}{(4\pi)^4} \frac{N_b - N_f}{240} . \qquad (1.14)$$

Because the number of physical four-dimensional states does not change under duality transformations, this equation is automatically independent of such transformations and of the details of the regularization scheme. In fact, the result was only confirmed in Ref. [13] for minimally-coupled scalars, antisymmetric tensors and (non-propagating) three-form fields. The generalization to fermionic contributions was based on the previously-mentioned supersymmetry Ward identities. It is quite remarkable that such a simple formula for the renormalization-scale dependence emerges from the computations carried out in Ref. [13]. How did this happen? We answer this in the next section.

1.3 Renormalization-scale dependence directly from four-dimensional unitarity cuts

In this section we explain the simple form of the renormalization-scale dependence in Eq. (1.13) using four-dimensional unitarity cuts. We show that it holds for any massless theory with minimal couplings to gravity and renormalizable matter interactions. From simple dimensional considerations, contributions to the R^3 operator necessarily involve couplings with the dimension of the gravitational coupling κ, which carries the dimension of inverse mass, $1/M_P$. Renormalizable matter interactions are either dimensionless or carry the dimension of mass, so they can contribute only to lower-dimension operators than R^3 at two loops, and therefore they are not relevant at this order. We will also explain why dilatons and antisymmetric tensors—whose minimal couplings to gravitons have two derivatives, as does pure gravity—also respect Eq. (1.13), as found in the computations of Refs. [13, 43].

Unitarity cuts are not directly sensitive to the $\ln \mu^2$ dependence. However, in a massless theory, simple dimensional analysis relates the coefficient of $\ln \mu^2$ to the coefficients of logarithms of kinematic invariants, $\ln s_{ij}$, because the arguments of all logarithms need to be dimensionless. Because the coefficient of $\ln \mu^2$ is finite, we can evaluate the unitarity cuts in four dimensions (after subtracting a universal infrared divergence). Thus we automatically avoid evanescent operators, such as the Gauss–Bonnet term (1.2). Our approach greatly clarifies the essential physics, showing that duality transformations cannot change the logarithms in the scattering amplitude, because in four dimensions, unlike D dimensions, duality does not change the Lorentz properties or number of physical states. The calculation of the logarithms using unitarity cuts was carried out long ago by Dunbar and Norridge [44]. Recently a similar technique has been applied to two-loop identical-helicity amplitudes in gauge theory by Dunbar, Jehu and Perkins [45, 46]. Here we repeat the two-loop four-graviton calculation, but in a way that completely avoids dimensional regularization and focuses on the consequences and interpretation of the renormalization scale.
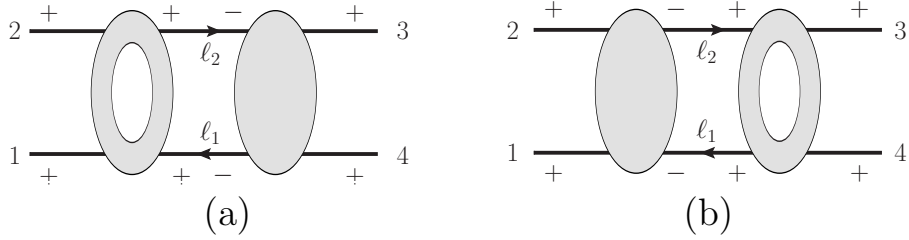
Figure 1.3: The s-channel two-particle cuts (a) and (b) from which we can extract the logarithmic parts of the two-loop four-point identical-helicity four-graviton amplitude. The exposed lines are placed on shell and are in four dimensions.
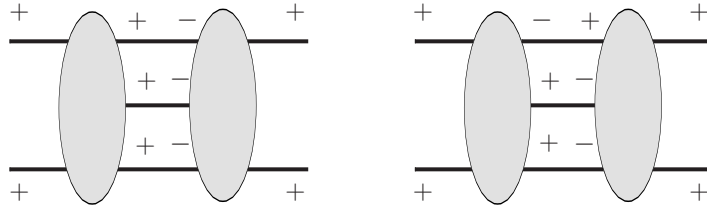
Figure 1.4: Representative contributions to the three-particle cut. This cut generates no new $\ln \mu^2$ contributions to the R^3 operator for the identical-helicity four-graviton amplitude.

We obtain the kinematical logarithms of the all-plus helicity amplitude from the four-dimensional unitarity cuts. At two loops, there are cuts where two particles cross the cut, illustrated in Fig. 1.3, and where three particles cross the cut, shown in Fig. 1.3. In four dimensions, many contributions to these cuts vanish, because the tree amplitude on one side of a cut vanishes.

In pure gravity, all contributions to the three-particle cuts shown in Fig. 1.3 vanish, because they contain a either a tree amplitude with all identical helicities, or one with one leg of opposite helicity. Such five-graviton tree amplitudes vanish. Adding minimally-coupled matter does not alter this conclusion. As already noted, adding matter with renormalizable self couplings cannot affect the coefficient of the R^3 operator. Similarly, dilatons and antisymmetric tensors, with their minimal couplings to each other and to gravity also cannot contribute, because their amplitudes have similar vanishings as the pure gravity case, where a pair of external (pseudo)scalar state should be assigned one plus and one minus helic-

14

ity. All of these vanishings can be understood from the fact that all such amplitudes can be constructed from minimally-coupled gauge theory via the Kawai–Lewellen–Tye (KLT) relations [47–49], which all have the corresponding vanishings. Alternatively, such tree amplitudes can be embedded into $\mathcal{N} = 8$ supergravity, and then the supersymmetry Ward identities [38–40] imply the required vanishings.

The two-particle cut does have nonvanishing contributions; however, the cut lines have to be gravitons, with the helicity configurations displayed in Fig. 1.3. If a massless particle other than a graviton crosses the cut with this helicity configuration, then the tree amplitude entering the cut necessarily vanishes. These vanishings can be understood in various ways. The KLT decomposition offers one such way. Consider the KLT decomposition of the gravitational tree amplitude on the right-hand side of Fig. 1.3(a) into a product of two gauge-theory amplitudes [47–49],

$$M^{\text{tree}}(\ell_1, -\ell_2, 3, 4) = s_{12}\, A^{\text{tree}}(\ell_1, -\ell_2, 3, 4) A^{\text{tree}}(\ell_1, -\ell_2, 4, 3)\,, \tag{1.15}$$

where $M^{\text{tree}}(1, 2, 3, 4)$ is the gravitational tree amplitude and $A^{\text{tree}}(1, 2, 3, 4)$ is a color-ordered Yang–Mills tree amplitude. (In this expression the couplings are stripped off.) If legs 3 and 4 of the gravitational amplitude are positive-helicity gravitons in an all-outgoing convention, then the corresponding legs in the gauge-theory amplitudes are positive-helicity gluons, so that the spins match. For gauge-theory amplitudes where legs 3 and 4 are positive-helicity gluons, the only nonvanishing configuration is where the remaining two legs are negative-helicity gluons. The KLT relations then imply that the only nonvanishing gravity tree amplitude is when the two legs labeled by ℓ_1 and $-\ell_2$ in the unitarity cut are gravitons with negative helicity. Other configurations, corresponding to particles other than negative-helicity gravitons, vanish because at least one of the corresponding gauge-theory amplitudes vanishes.

A consequence of these restrictions is that the one-loop amplitude appearing on the other

side of the two-particle cut must be an all-plus-helicity amplitude with only external gravitons. Such amplitudes are remarkably simple [44]. This simplicity enormously streamlines the calculation of the cut. There are two contributions to the s_{12}-channel cut, shown in Fig. 1.3(a) and (b), depending on whether the loop amplitude is located on the left or right side of the cut. However, they give equal contributions, because Fig. 1.3(b) can be mapped back to Fig. 1.3(a) by relabeling the momenta by $k_i \rightarrow k_{i+2}$, where the indices are modulo 4, and we will see that the cut is invariant under this operation. In addition to the s_{12}-channel cut displayed in Fig. 1.3, there are also cuts in the s_{23} and s_{13} channels, which can be obtained from the s_{12} channel by Bose symmetry, permuting $k_1 \leftrightarrow k_3$ and $k_1 \leftrightarrow k_4$, respectively.

The required one-loop amplitude with four identical-helicity gravitons is [44],

$$M^{\text{1-loop}}(1^+, 2^+, 3^+, 4^+) = -\frac{i}{(4\pi)^2} \frac{N_b - N_f}{240} \left(\frac{\kappa}{2}\right)^4 \mathcal{T}^2 \left(s_{12}^2 + s_{14}^2 + s_{24}^2\right), \tag{1.16}$$

where the permutation-invariant, pure-phase spinor combination $\mathcal{T}$ is defined in Eq. (1.7). The one-loop external graviton amplitude is unaffected by any interactions of the matter fields in a minimally-coupled theory: at one loop with all external gravitons there are no diagrams containing matter self-interactions.

In Yang–Mills theory, Bardeen and Cangemi [50–52] argued that the corresponding identical-helicity amplitude is nonvanishing because of an anomaly in the infinite-dimensional symmetry of the self-dual sector of the theory. Presumably, the same holds in gravity. It is quite interesting that this anomaly-like behavior appears crucial for obtaining a nonvanishing one-loop four-graviton amplitude, which as we will see below leads to a nonvanishing coefficient of the $\ln \mu^2$ term.

We also need the four-graviton tree amplitude. It is easily obtained from the KLT

relation [47–49],

$$
\begin{aligned}
M^{\text{tree}}(1^-, 2^-, 3^+, 4^+) &= -i\left(\frac{\kappa}{2}\right)^2 s_{12} A^{\text{tree}}(1,2,3,4) A^{\text{tree}}(1,2,4,3) \\
&= i\left(\frac{\kappa}{2}\right)^2 s_{12} \frac{\langle 1\,2 \rangle^3}{\langle 2\,3 \rangle \langle 3\,4 \rangle \langle 4\,1 \rangle} \frac{\langle 1\,2 \rangle^3}{\langle 2\,4 \rangle \langle 4\,3 \rangle \langle 3\,1 \rangle} .
\end{aligned}
\tag{1.17}
$$

We now calculate the unitarity cut in Fig. 1.3(a). The cut integrand is given by the relabeled product of Eqs. (1.16) and (1.17),

$$
\begin{aligned}
C_{12} &= \mathcal{N} s_{12} \left(s_{12}^2 + s_{1\ell_1}^2 + s_{2\ell_1}^2\right) \\
&\times \left(\frac{[1\,2]\,[\ell_2\,(-\ell_1)]}{\langle 1\,2 \rangle \langle \ell_2\,(-\ell_1) \rangle}\right)^2 \frac{\langle \ell_1\,(-\ell_2) \rangle^3}{\langle (-\ell_2)\,3 \rangle \langle 3\,4 \rangle \langle 4\,\ell_1 \rangle} \frac{\langle \ell_1\,(-\ell_2) \rangle^3}{\langle (-\ell_2)\,4 \rangle \langle 4\,3 \rangle \langle 3\,\ell_1 \rangle},
\end{aligned}
\tag{1.18}
$$

where the labels follow Fig. 1.3(a) and the normalization factor is

$$
\mathcal{N} = \frac{1}{(4\pi)^2} \frac{N_b - N_f}{240} \left(\frac{\kappa}{2}\right)^6 .
\tag{1.19}
$$

Rearranging the spinor products and using the identity $1/\langle a\,b \rangle = [ba]/(k_a + k_b)^2$ gives

$$
\begin{aligned}
C_{12} &= \mathcal{N} \mathcal{T}^2 s_{12} \left(s_{12}^2 + s_{1\ell_1}^2 + s_{2\ell_1}^2\right) \\
&\times \frac{\langle \ell_1\,\ell_2 \rangle [\ell_2\,3] \langle 3\,4 \rangle [4\,\ell_1] \langle \ell_1\,\ell_2 \rangle [\ell_2\,4] \langle 4\,3 \rangle [3\,\ell_1]}{(\ell_2 - k_3)^2 (\ell_1 + k_4)^2 (\ell_2 - k_4)^2 (\ell_1 + k_3)^2} .
\end{aligned}
\tag{1.20}
$$

The net effect of replacing $-\ell_1$ and $-\ell_2$ with ℓ_1 and ℓ_2 is a factor of $+1$. We can simplify C_{12} further by observing that the numerator forms a trace,

$$
\begin{aligned}
\langle \ell_1\,\ell_2 \rangle [\ell_2\,3] \langle 3\,4 \rangle [4\,\ell_1] \langle \ell_1\,\ell_2 \rangle [\ell_2\,4] \langle 4\,3 \rangle [3\,\ell_1] &= \frac{1}{2} \text{tr}[(1 - \gamma_5)\ell_1\ell_2 k_3 k_4 \ell_1 \ell_2 k_4 k_3] \\
&= (\ell_1 + k_3)^2 (\ell_1 + k_4)^2 s_{34}^2 ,
\end{aligned}
\tag{1.21}
$$

where we used $\ell_2 = \ell_1 + k_3 + k_4$ and the on-shell conditions $\ell_1^2 = \ell_2^2 = 0$ to simplify the trace.

17

Thus, the numerator cancels the (doubled) propagators leaving

$$
\begin{aligned}
C_{12} &= \mathcal{N}\mathcal{T}^2 \, s_{12}^3 \, \frac{s_{12}^2 + s_{1\ell_1}^2 + s_{2\ell_1}^2}{(\ell_2 - k_3)^2(\ell_2 - k_4)^2} \\
&= -\mathcal{N}\mathcal{T}^2 \, s_{12}^2 \, (s_{12}^2 + s_{1\ell_1}^2 + s_{2\ell_1}^2) \left[\frac{1}{(\ell_1 + k_4)^2} + \frac{1}{(\ell_1 + k_3)^2} \right].
\end{aligned}
\tag{1.22}
$$

This expression for the cut actually has an infrared divergence when integrated over phase space. However, this divergence is harmless because infrared singularities of gravity theories are relatively simple [53–56]. The source of the singularity is from exchange of soft virtual gravitons with momentum $\ell_1 + k_3$ or $\ell_1 + k_4$; the soft limit is when $\ell_1 \to -k_4$ or $\ell_1 \to -k_3$, for the first or second term in Eq. (1.22), respectively. To remove the infrared singularity, we simply subtract the soft limit of the integrand, replacing C_{12} by

$$
\tilde{C}_{12} = -\mathcal{N}\mathcal{T}^2 \, s_{12}^2 \, \frac{s_{1\ell_1}^2 + s_{2\ell_1}^2 - s_{14}^2 - s_{24}^2}{(\ell_1 + k_4)^2} + (k_3 \leftrightarrow k_4).
\tag{1.23}
$$

The subtraction terms correspond to cut scalar triangle integrals. Since the triangle integrals that are subtracted converge in the ultraviolet, the subtraction has no effect on the ultraviolet logarithms with which we are concerned here.

The discontinuity is obtained by integrating over the Lorentz-invariant phase space,

$$
I_{12} = \int \mathrm{dLIPS}\, \tilde{C}_{12} = -\mathcal{N}\mathcal{T}^2 \, s_{12}^3 \hat{I}_{12} + (k_3 \leftrightarrow k_4),
\tag{1.24}
$$

where

$$
\hat{I}_{12} = \int \mathrm{dLIPS}\, \frac{(2k_1 \cdot \ell_1)^2 + (2k_2 \cdot \ell_1)^2 - s_{14}^2 - s_{24}^2}{s_{12}\,(2k_4 \cdot \ell_1)}.
\tag{1.25}
$$

We perform the phase-space integration in the center-of-mass frame, parametrizing the ex-

18

ternal momenta as

$$
\begin{aligned}
k_1 &= \frac{\sqrt{s}}{2}(-1,\ \sin\theta\cos\phi,\ \sin\theta\sin\phi,\ \cos\theta)\,, \\
k_2 &= \frac{\sqrt{s}}{2}(-1,\ -\sin\theta\cos\phi,\ -\sin\theta\sin\phi,\ -\cos\theta)\,, \\
k_3 &= \frac{\sqrt{s}}{2}(1,\ 0,\ 0,\ 1)\,, \\
k_4 &= \frac{\sqrt{s}}{2}(1,\ 0,\ 0,\ -1)\,,
\end{aligned}
\tag{1.26}
$$

and the internal momentum as

$$
\ell_1 = \frac{\sqrt{s}}{2}(-1,\ \sin\hat\theta\cos\hat\phi,\ \sin\hat\theta\sin\hat\phi,\ \cos\hat\theta)\,,
\tag{1.27}
$$

while $-\ell_2^0 = \ell_1^0$ and $-\vec{\ell}_2 = -\vec{\ell}_1$. The on-shell conditions enforce the constraints $|\ell_i^0| = |\vec{\ell}_i| = \sqrt{s}/2$, $i = 1, 2$. The standard two-body phase-space measure is

$$
\int \mathrm{dLIPS} = \frac{1}{2}\frac{1}{8\pi}\int_{-1}^{1}\frac{d\cos\hat\theta}{2}\int_{0}^{2\pi}\frac{d\phi}{2\pi}\,.
\tag{1.28}
$$

There is an extra Bose symmetry factor of $1/2$ because two identical-helicity gravitons cross the cut. Substituting the momentum parametrization into Eq. (1.25) gives an expression for $\hat{I}_{12}$ purely in terms of angular variables, which can be integrated easily,

$$
\begin{aligned}
\hat{I}_{12} &= \frac{1}{16\pi}\int_{-1}^{1}\frac{d\cos\hat\theta}{2}\int_{0}^{2\pi}\frac{d\hat\phi}{2\pi}\frac{1}{1-\cos\hat\theta}\Big[\cos^2\theta\,\sin^2\hat\theta - \sin^2\theta\,\sin^2\hat\theta\,\cos^2(\phi-\hat\phi) \\
&\qquad\qquad\qquad\qquad\qquad\qquad - \frac{1}{2}\sin 2\theta\,\sin 2\hat\theta\,\cos(\phi-\hat\phi)\Big] \\
&= \frac{1}{16\pi}\int_{-1}^{1}\frac{d\cos\hat\theta}{2}\frac{1}{1-\cos\hat\theta}\Big[\cos^2\theta\,\sin^2\hat\theta - \frac{1}{2}\sin^2\theta\,\sin^2\hat\theta\Big] \\
&= \frac{1}{16\pi}\Big[\cos^2\theta - \frac{1}{2}\sin^2\theta\Big]\int_{-1}^{1}\frac{d\cos\hat\theta}{2}[1+\cos\hat\theta] \\
&= \frac{2-3\sin^2\theta}{32\pi}\,.
\end{aligned}
\tag{1.29}
$$

Using $s_{13}s_{23} = (s_{12}^2/4) \times \sin^2\theta$, we can re-express the answer in a Lorentz-invariant form:

$$\hat{I}_{12} = \frac{1}{16\pi} \frac{s_{12}^2 - 6s_{13}\, s_{23}}{s_{12}^2}. \tag{1.30}$$

Since this result is invariant under $k_3 \to k_4$, the exchange contribution in Eq. (1.24) just gives a factor of 2.

Putting it all together, we have

$$\tilde{C}_{12} = -\frac{\mathcal{N}\mathcal{T}^2}{8\pi} s_{12}\,(s_{12}^2 - 6s_{13}\, s_{23}) \tag{1.31}$$

$$= 2\pi i \left[\frac{i}{(4\pi)^4} \frac{N_b - N_f}{240} \left(\frac{\kappa}{2}\right)^6 \mathcal{T}^2 s_{12}(s_{12}^2 - 6s_{13}\, s_{23}) \right]. \tag{1.32}$$

We extracted a factor of $2\pi i$ because the analytic continuation of $\ln(-s_{ij}/\mu^2)$ from below the cut $(s_{ij} \to s_{ij} - i\varepsilon)$ to above the cut $(s_{ij} \to s_{ij} + i\varepsilon)$ is

$$\ln\left(\frac{-s_{ij}}{\mu^2}\right) \;\to\; \ln\left(\frac{-s_{ij}}{\mu^2}\right) - 2\pi i. \tag{1.33}$$

Thus, the s_{12}-channel discontinuity we computed is related to the coefficient of $\ln\mu^2$ by

$$M^{2-\text{loop}}\big|_{\ln\mu^2} = \frac{1}{2\pi i} M^{2-\text{loop}}\big|_{\text{disc}} \times \ln\mu^2. \tag{1.34}$$

We also need to multiply by a factor of 2 for the contribution of Fig. 1.3(b), and include the contributions of the other two channels, using

$$s_{12}(s_{12}^2 - 6s_{13}\, s_{23}) + (k_1 \leftrightarrow k_3) + (k_1 \leftrightarrow k_4) = s_{12}^3 + s_{23}^3 + s_{13}^3 - 18 s_{12}s_{23}s_{13} = -15 s_{12}s_{23}s_{13}. \tag{1.35}$$

We obtain

$$M^{2-\text{loop}}(++++)\big|_{\ln\mu^2} = -\left(\frac{\kappa}{2}\right)^6 \frac{i}{(4\pi)^4} s_{12}s_{23}s_{13}\mathcal{T}^2 \frac{N_b - N_f}{8} \ln\mu^2. \tag{1.36}$$

20

Thus, we have derived the simple renormalization-scale dependence of the two-loop four-graviton amplitude [13], but now in a way that avoids reliance on evanescent operators or other subtleties of dimensional regularization. Given that only four-dimensional quantities were used, duality transformations manifestly cannot affect the renormalization-scale dependence.

1.4 Conclusions

In this chapter we explained the simple form of the renormalization-scale dependence of two-loop gravity amplitudes proposed in Ref. [13]. While the two-loop ultraviolet divergence in dimensional regularization changes under duality transformations, and is afflicted by evanescent subdivergences, the renormalization-scale dependence is remarkably simple [13]. In order to explain its simple form, we used four-dimensional unitarity cuts, which effectively converted the two-loop computation into a one-loop one. As in Ref. [13], we studied the identical-helicity amplitude, because it is particularly simple to evaluate, yet is sensitive to the two-loop R^3 ultraviolet divergence. While the renormalization scale $\ln \mu^2$ does not itself have a unitarity cut, on dimensional grounds its coefficient must balance the coefficients of the logarithms of kinematic variables, thus allowing us to extract the $\ln \mu^2$ coefficient directly from the unitarity cuts. This method avoids the need for ultraviolet regularization, as well as all subtleties associated with evanescent operators. A trivial integral over the two-body phase space for intermediate gravitons is all that is required to explain the simple formula (1.36) of Ref. [13].

A rather interesting property of the gravity divergence is that it appears to be tied to an anomaly. In Yang–Mills theory, the nonvanishing of the one-loop identical helicity amplitude has been tied to an anomaly in the conserved currents of self-dual Yang–Mills theory [50–52]. We expect gravity to be similar. Integrability has been used to construct classical self-dual solutions to Einstein's equations [57, 58]. It is natural to conjecture that

a quantum anomaly in the conservation of the associated currents of self-dual gravity [59] could be responsible for the non-vanishing one-loop amplitude (1.16) which underlies the two-loop $\ln \mu^2$ dependence. In any case, not only the two-loop divergence but the nonvanishing of the one- and two-loop identical-helicity amplitudes can be traced to an ϵ/ϵ effect in dimensional regularization, similar to the way that chiral and other anomalies arise. It would be quite enlightening if we could link the pure gravity divergence, or more importantly, the nonvanishing renormalization-scale dependence, more directly to an anomaly.

In this chapter we considered the identical-helicity amplitude, because it is the simplest helicity configuration that is sensitive to the R^3 divergence. It would be interesting to evaluate the other helicity configurations to corroborate our understanding. The other helicity configurations are significantly more complicated, because the three-particle cut no longer vanishes in four dimensions. However, the $(-+++)$ helicity configuration, which also receives contributions from the R^3 operator, should be tractable using four-dimensional unitarity cuts.

Usually in field theory, the first dimensionally-regulated divergence that is encountered is directly related to the renormalization-scale dependence of either a coupling (i.e. the beta function) or the coefficient of an operator (i.e. its anomalous dimension). Pure Einstein gravity at two loops provides an explicit counterexample to this expectation, but it is probably not the only one. As we discussed in Section 3.2, the key feature is that a candidate operator for a first divergence is evanescent, vanishing in four dimensions but not in D dimensions. The different μ dependence associated with the bare and counterterm contributions spoils the textbook relation between the pole in ϵ and the renormalization-scale dependence at the following loop order. Another place this might happen is in the effective field theory of long flux tubes [26]. The key lessons are that ultraviolet divergences in dimensional regularization have to be treated with caution in certain circumstances, and that it is safer to focus on the more physical renormalization-scale dependence of the renormalized theory.

Chapter 2

Curvature-Squared Multiplets, Evanescent Effects and the U(1) Anomaly in $\mathcal{N} = 4$ Supergravity

We evaluate one-loop amplitudes of $\mathcal{N} = 4$ supergravity in D dimensions using the double-copy procedure that expresses gravity integrands in terms of corresponding ones in Yang–Mills theory. We organize the calculation in terms of a set of gauge-invariant tensors, allowing us to identify evanescent contributions. Among the latter, we find the matrix elements of supersymmetric completions of curvature-squared operators. In addition, we find that such evanescent terms and the U(1)-anomalous contributions to one-loop $\mathcal{N} = 4$ amplitudes are tightly intertwined. The appearance of evanescent operators in $\mathcal{N} = 4$ supergravity and their relation to anomalies raises the question of their effect on the known four-loop divergence in this theory. We provide bases of gauge-invariant tensors and corresponding projectors useful for Yang–Mills theories as a by-product of our analysis.

2.1 Introduction and Review

Recent explicit calculations have shown that gravity theories still have perturbative secrets waiting to be revealed. We have learned a number of surprising lessons from these calculations: results in gravity theories can be obtained directly from their Yang–Mills counterparts via a double-copy procedure [36, 60–66]; of a curious disconnect between the leading two-loop divergence of graviton amplitudes [10–12] and the corresponding renormalization-scale dependence [1, 13, 67]; and about the surprisingly tame ultraviolet behavior of certain supergravity theories [4–9]. These lessons augur more surprises to come. In this chapter we investigate the role of evanescent effects in the one-loop four-point amplitude of $\mathcal{N} = 4$ supergravity, along with its relation to the U(1) anomaly in the duality symmetry of this theory [68–70].

Evanescent effects arise from operators whose matrix elements vanish when working strictly in four dimensions, but give rise to nonvanishing contributions in dimensional regularization. Such contributions originate from the cancellation of poles against small deviations in the four-dimensional limit; that is, they are due to ϵ/ϵ effects, where $\epsilon = (4 - D)/2$ is the dimensional regulator. Although such effects might at first appear to be a mere technicality, they turn out to play an important role [13] in understanding ultraviolet divergences of Einstein gravity in the context of dimensional regularization [10–12]. In particular, the Gauss–Bonnet operator is evanescent and appears as a one-loop counterterm whose insertion at two loops contaminates the ultraviolet divergence, but results in no physical consequences in the renormalized amplitude. An important question therefore is whether a supersymmetric version of the Gauss-Bonnet operator appears in the matrix elements of $\mathcal{N} = 4$ supergravity. If such an operator exists it would be important to determine its effects on the known four-loop divergence [71] of the theory.

On the other hand, the $\mathcal{N} = 4$ supergravity theory has an anomaly in its U(1) duality symmetry [68]. The anomaly manifests itself in the failure of certain helicity amplitudes

which vanish at tree level to persist in vanishing at loop level. In the context of dimensional regularization these anomalous amplitudes arise from ϵ/ϵ effects, in much the same way as the usual chiral anomaly arises in the 't Hooft–Veltman scheme [72]. Refs. [69, 71] have suggested that the U(1) duality anomaly plays a key role in the four-loop divergence of the theory [69, 71], although a detailed explanation is still lacking. In contrast to the anomaly terms, it is unlikely that evanescent effects can alter any physical quantity derived from scattering amplitudes [1, 13, 67]. Nevertheless, one may wonder if there any connections between the two phenomena, given that both arise from ϵ/ϵ effects.

In order to investigate these questions we compute the one-loop four-point amplitude of $\mathcal{N} = 4$ supergravity in arbitrary dimensions, using the double-copy procedure based on the duality between color and kinematics [35, 36]. The corresponding helicity amplitudes were previously calculated using various methods [44, 73–77]. Here, we use formal polarizations in order to study evanescent effects, which are hidden when four-dimensional helicity states are used. The conclusion of our study is two-fold: an evanescent contribution of the Gauss–Bonnet type does appear in the pure-graviton amplitude of $\mathcal{N} = 4$ supergravity; and its effects are indeed intertwined with the U(1) duality anomaly.

We argue that the main evanescent contributions to the amplitude correspond to the supersymmetric generalization of the curvature-squared terms. Off-shell forms of curvature-squared operators are known for $\mathcal{N} = 1$ and $\mathcal{N} = 2$ supergravity [78–82]; but explicit forms of a supersymmetric extension of the Gauss-Bonnet curvature-squared operator are not known off shell in $\mathcal{N} = 4$ supergravity.[1] Nonetheless their matrix elements can be computed directly using standard amplitude methods, even without knowing their off-shell forms. In contrast to the nonsupersymmetric case, the coefficients of these matrix elements are finite. This turns out to be a consequence of the same ϵ/ϵ cancellation that generates the anomaly. As we will see, in the context of the double-copy construction there is a single object that has matrix elements that contribute to both the anomaly and evanescent curvature-squared

---

[1]Curvature-squared operators have been studied in the context of conformal supergravity [83–85].

terms.

The double-copy structure implies that we can write the one-loop four-point amplitude of $\mathcal{N} = 4$ supergravity in terms of pure-Yang–Mills theory building blocks, up to an overall factor. We can therefore employ a set of gauge-invariant tensors written in terms of formal gluon polarization vectors to carry out the calculation. We present the results in terms of linearized field strengths, which is natural for connecting to operators in a Lagrangian and making manifest on-shell gauge invariance. In order to explore the evanescent properties we also construct tensors with definite four-dimensional helicity properties. We provide the tensors in a form natural for use in color-ordered Yang–Mills theory, as well as in a fully crossing-symmetric form natural in $\mathcal{N} = 4$ supergravity. Similar gauge-invariant tensors have recently been discussed by Boels and Medina [86].

In the Appendix we give details of the gauge-invariant tensors and describe the construction of projectors for determining the coefficient of the tensors in a given amplitude. These projectors and tensors are useful not only for $\mathcal{N} = 4$ supergravity but can be applied to four-gluon amplitudes at any loop order in any Yang–Mills theory, including quantum chromodynamics (QCD). Because of their more general usefulness we attach a *Mathematica* file, availabe at the arXiv hosting of Ref. [2] that includes the two sets of tensors with different symmetry properties, alongside the corresponding projectors.

This chapter is organized as follows. In Section 2.2 we give the construction of the four-loop four-point amplitude of $\mathcal{N} = 4$ supergravity and describe the gauge-invariant tensors in terms of which the amplitudes are constructed. In Section 2.3 we give the results for the one-loop supergravity amplitudes. Then in Section 2.4 we identify evanescent curvature-squared terms in the amplitude. We show the connection of these terms to the U(1) anomaly in Section 2.5. We give our conclusions in Section 2.6. An appendix describing the gauge-invariant tensors and projectors is included.

2.2 Construction of the One-Loop Amplitude

In this section we construct the one-loop four-point amplitude of $\mathcal{N} = 4$ supergravity. Details of the gauge-invariant tensors used for expressing the results are found in the appendix.

2.2.1 Color-Kinematics Duality and the Double Copy

We apply the double-copy construction of gravity amplitudes based on the duality between color and kinematics [35, 36]. This has previously been discussed in some detail in Ref. [75–77] for the one-loop amplitudes of $\mathcal{N} = 4$ supergravity. In contrast to the earlier construction, we use D-dimensional external states instead of four-dimensional ones, in order to have access to evanescent effects.

Amplitudes of half-maximal supergravity in D dimensions can be obtained through a double copy, where one factor is derived from maximally supersymmetric Yang–Mills theory (MSYM), and the other from pure Yang–Mills (YM) theory. In four dimensions, this gives us amplitudes in $\mathcal{N} = 4$ supergravity in terms of a product of $\mathcal{N} = 4$ and pure Yang–Mills theory. Alternatively, one may also construct $\mathcal{N} = 4$ supergravity amplitudes using two copies of $\mathcal{N} = 2$ super-Yang–Mills (SYM) theory, as shown in Ref. [87]. This latter construction is, however, more complicated, and furthermore includes unwanted matter multiplets. We use the simpler construction.

The double-copy construction starts from the integrands of two Yang–Mills gauge-theory amplitudes, written in terms of purely cubic diagrams. In a Feynman-diagram language, four-point vertices can always be "blown up" into a product of three-point vertices, possibly with the exchange of a fictitious tensor field. The representation of one-loop amplitudes is,

$$\mathcal{A}_m^{\text{1-loop}} = ig^m \int \frac{d^D p}{(2\pi)^D} \sum_{j \in \text{ICD}} \frac{1}{S_j} \frac{n_j c_j}{\prod_{\alpha_j} p_{\alpha_j}^2} \,, \tag{2.1}$$

where the sum runs over the independent cubic diagrams (ICD) labeled by j, while the c_j
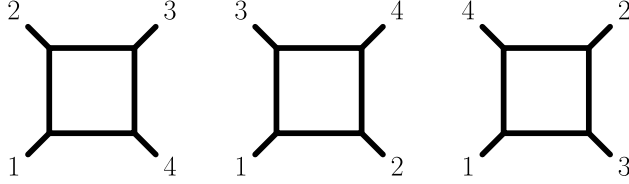
Figure 2.1: Box diagrams of the one-loop four-point amplitude of $\mathcal{N} = 4$ supergravity.

and n_j are the color factors and kinematic numerators associated with each diagram. The factor $1/S_j$ accounts for the usual diagram symmetry factors and the product over α_j runs over the Feynman propagators $1/p_{\alpha_j}^2$ for diagram j. If the kinematic numerators can be arranged to satisfy the same algebraic properties as adjoint representation color factors, that is so that Jacobi relations hold,

$$c_i + c_j + c_k = 0 \;\Rightarrow\; n_i + n_j + n_k = 0 \,, \tag{2.2}$$

along with all anti-symmetry properties, then we can obtain gravity integrands and thence amplitudes by replacing the color factors c_j in Eq. (2.1) by the second Yang–Mills theory's kinematic numerators,

$$c_i \to \tilde{n}_i \,. \tag{2.3}$$

We do this while keeping the original kinematic factors n_j of the first Yang–Mills theory. A similar procedure holds for particles in the fundamental representation [88, 89].

The one-loop four-point amplitude of $\mathcal{N} = 4$ supergravity is easy to construct via the double-copy construction, because the $\mathcal{N} = 4$ MSYM numerators are especially simple [90]. The numerators of triangle and bubble diagrams vanish, and the box integrals illustrated in Fig. 2.1 have kinematic numerators proportional to the tree amplitude,

$$n_{1234} = n_{1342} = n_{1423} = s\, t A_{\mathcal{N}=4}^{\text{tree}}(1, 2, 3, 4) \,, \tag{2.4}$$

where we define the usual Mandelstam invariants,

$$s = (k_1 + k_2)^2, \qquad t = (k_2 + k_3)^2, \qquad u = (k_1 + k_3)^2. \qquad (2.5)$$

These numerators trivially satisfy the dual Jacobi identities in Eq. (3.3). Thus, the $\mathcal{N} = 4$ supergravity one-loop amplitude is

$$M_{\mathcal{N}=4,\mathrm{SG}}^{\text{1-loop}}(1,2,3,4) = istA_{\mathcal{N}=4}^{\text{tree}}(1,2,3,4)\Big(I_{1234}[n_{1234,p}] + I_{1342}[n_{1342,p}] + I_{1423}[n_{1423,p}]\Big), \quad (2.6)$$

where we have stripped the gravitational coupling, and where

$$I_{1234}[n_{1234,p}] \equiv \int \frac{d^D p}{(2\pi)^D} \frac{n_{1234,p}}{p^2(p-k_1)^2(p-k_1-k_2)^2(p+k_4)^2}, \qquad (2.7)$$

is the first box integral in Fig. 2.1 and $n_{1234,p}$ is the pure Yang–Mills kinematic numerator given in Eq. (3.5) of Ref. [43]. We can restore the coupling to the supergravity amplitude via,

$$\mathcal{M}_{\mathcal{N}=4,\mathrm{SG}}^{\text{tree}}(1,2,3,4) = \left(\frac{\kappa}{2}\right)^2 M_{\mathcal{N}=4,\mathrm{SG}}^{\text{tree}}(1,2,3,4), \qquad (2.8)$$

at tree level, and

$$\mathcal{M}_{\mathcal{N}=4,\mathrm{SG}}^{\text{1-loop}}(1,2,3,4) = \left(\frac{\kappa}{2}\right)^4 M_{\mathcal{N}=4,\mathrm{SG}}^{\text{1-loop}}(1,2,3,4), \qquad (2.9)$$

at one loop. The coupling is related to Newton's constant via $\kappa^2 = 32\pi G_N$. An alternate form of Eq. (2.6) is,

$$M_{\mathcal{N}=4,\mathrm{SG}}^{\text{1-loop}}(1,2,3,4) = istA_{\mathcal{N}=4}^{\text{tree}}(1,2,3,4)$$
$$\times \Big(A^{\text{1-loop}}(1,2,3,4) + A^{\text{1-loop}}(1,3,4,2) + A^{\text{1-loop}}(1,4,2,3)\Big), \quad (2.10)$$

where $A^{\text{1-loop}}(1,2,3,4)$ is the color-ordered one-loop amplitude of pure Yang–Mills theory. The difference between Eqs. (2.6) and (2.10) cancels in the permutation sum. The second

form makes gauge invariance manifest, as the building blocks are gauge-invariant color-ordered amplitudes. We use the form in Eq. (2.6) to evaluate the amplitude explicitly.

2.2.2 Gauge-Invariant Building Blocks

The relatively simple double-copy structure of the one-loop four-point $\mathcal{N} = 4$ supergravity amplitude displayed in Eq. (2.10) makes manifest a factorization into the product of an MSYM tree amplitude and a sum over the three distinct permutations of the one-loop color-ordered amplitude of pure Yang–Mills theory. This suggests that we can obtain a convenient organization of the supergravity amplitude by first decomposing the Yang–Mills amplitudes into gauge-invariant contributions. We do so using bases of local on-shell 'gauge-invariant tensors'. By gauge-invariant tensors here we mean polynomials in $(\varepsilon_i \cdot \varepsilon_j), (k_i \cdot \varepsilon_j)$ and $(k_i \cdot k_j)$ that vanish upon replacing ε_i by k_i. These tensors are distinct only if they differ after imposing on-shell conditions. We can build such tensors by starting with tree-level four-point scattering amplitudes for external gluons, for example, or with four-point matrix elements of local gluonic operators, and then multiplying by appropriate factors of s, t, or u to make the quantities local. Boels and Medina [86] have also recently constructed such tensors.

In the Appendix we present two different bases. In the first, we impose definite cyclic symmetry; this yields a basis natural for color-ordered Yang–Mills amplitudes. In the second, we impose definite symmetry under crossing, making them natural for supergravity. Associated with each gauge-invariant tensor is a projector built out of momenta and conjugate polarization vectors. When applied to an integrand, it yields the coefficient of the given tensor. Integrating the coefficient then yields the coefficient of the tensor in the amplitude. This type of projection to a basis of gauge-invariant tensors has been used in Ref. [91]. We stress that the first of these bases is directly useful in gauge-theory calculations. We refer the reader to the Appendix for more details about the bases, their properties, their construction
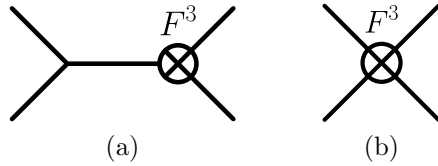
Figure 2.2: Representative diagrams for (a) three- and (b) four-point F^3 insertions.

and the projection techniques. We also make these tensors and projectors available in a ancillary *Mathematica* file, available from the arXiv hosting of Ref. [2].

We apply this projection technique to the integrand in Eq. (2.6). This reduces the numerators to sums of products of inverse propagators and external kinematics. The integrand is then expressed as a sum over tensors, with each coefficient expressed in terms of the scalar box and simpler triangle and bubble integrals that are easy to evaluate (via Feynman parameterization, for example). The scalar box integral is taken from Ref. [92]. As a cross-check we also evaluated the tensor integrals prior to applying the projectors, following the methods of Refs. [93] that express every tensor integral in terms of Schwinger parameters. These integrals are in turn expressed in terms of scalar integrals with shifted dimensions and higher powers of propagators. We use FIRE5 [94, 95] to reduce these integrals to elements of the standard basis of scalar integrals. The integrals are then shifted back to four dimensions using dimension-shifting formulas [93, 96]. Both methods yield identical results.

We introduce linearized field strengths corresponding to each external particle,

$$F_{i\,\mu\nu} \equiv k_{i\,\mu}\varepsilon_{i\,\nu} - k_{i\,\nu}\varepsilon_{i\,\mu}\,, \tag{2.11}$$

in order to organize the results obtained from the projection technique. We express our results using Lorentz-invariant combinations of these linearized field strengths. For four-point scattering in a parity-even theory, the only combinations at the lowest mass dimension

are [5, 97],

$$(F_i F_j F_k F_l) \equiv F_i^{\mu\nu} F_{j\,\nu\rho} F_k^{\rho\sigma} F_{l\,\sigma\mu} \,, \tag{2.12}$$

$$(F_i F_j)(F_k F_l) \equiv F_i^{\mu\nu} F_{j\,\mu\nu} F_k^{\rho\sigma} F_{l\,\rho\sigma} \,. \tag{2.13}$$

These quantities are not symmetrized over the indices i, j, k, and l.

We need only one additional tensor for four-point scattering. This tensor can be expressed as a linear combination of terms of the form $D^2 F^4$. It is, however, more convenient to express this tensor as a matrix element with an insertion of an F^3 operator,

$$F^3 \equiv \frac{1}{3} \operatorname{Tr} F^\mu{}_\nu F^\nu{}_\rho F^\rho{}_\mu \,, \tag{2.14}$$

where the trace is over color. The gauge-invariant tensor is given by

$$T_{F^3} \equiv -ist A_{F^3}^{\text{tree}}(1, 2, 3, 4) \,, \tag{2.15}$$

using the four-point tree-level color-ordered amplitude with a single insertion of the operator (2.14), as depicted in Fig. 2.2. As we see below, after applying the double-copy procedure, this element of our basis is the one giving rise to the curvature-squared matrix elements, as well as some of the anomalous ones.

32

2.3 Result and Mapping to Supergravity

Using the tensors in Eqs. (2.12), (2.13) and (2.15), we can write the supergravity amplitude as follows[2]

$$
\begin{aligned}
M_{\mathcal{N}=4,\text{SG}}^{1\text{-loop}}(1,2,3,4) = {} & c_\Gamma st A_{\mathcal{N}=4}^{\text{tree}}(1,2,3,4) \\
& \times \Bigg[\frac{t_8 F^4}{stu} \left(-\frac{2}{\epsilon^2} \sum_{i<j}^{3} s_{ij} \left(\frac{-s_{ij}}{\mu^2} \right)^{-\epsilon} + L_1(s,t,u) \right) \\
& + \frac{T_{F^3}}{stu} + \left(\frac{4}{3}(F_1 F_2 F_3 F_4) \right) \left(\frac{1}{st} + L_2(s,t,u) \right) \\
& + (F_1 F_2)(F_3 F_4) \left(\frac{1}{s^2} + L_3(s,t,u) \right) + \text{cyclic(2,3,4)} \Bigg],
\end{aligned}
\tag{2.16}
$$

where μ is the usual scale parameter, $s_{12} = s, s_{23} = t, s_{13} = u$; where

$$
c_\Gamma = \frac{\Gamma(1+\epsilon)\Gamma^2(1-\epsilon)}{(4\pi)^{2-\epsilon}\Gamma(1-2\epsilon)},
\tag{2.17}
$$

is the usual one-loop prefactor,

$$
L_1(s,t,u) = -s \ln\left(\frac{-s}{\mu^2}\right) - \frac{(2s^2 + st + 2t^2)}{2u}\left(\ln^2\left(\frac{-s}{-t}\right) + \pi^2\right) + \text{cyclic}(s,t,u),
\tag{2.18}
$$

$$
\begin{aligned}
L_2(s,t,u) = {} & \left[-\frac{2s}{t^2 u}\ln\left(\frac{-s}{-u}\right) + \frac{1}{4u^2}\left(\ln^2\left(\frac{-s}{-t}\right) + \pi^2\right) \right. \\
& \left. + \frac{(s-2t)}{t^3}\left(\ln^2\left(\frac{-s}{-u}\right) + \pi^2\right) \right] + (s \leftrightarrow t),
\end{aligned}
\tag{2.19}
$$

$$
\begin{aligned}
L_3(s,t,u) = {} & \frac{1}{stu}\left(-s\ln\left(\frac{-s}{\mu^2}\right) - t\ln\left(\frac{-t}{\mu^2}\right) - u\ln\left(\frac{-u}{\mu^2}\right) \right) \\
& + \frac{(t-u)}{s^3}\ln\left(\frac{-t}{-u}\right) + \frac{(2s^2 - tu)}{s^4}\left(\ln^2\left(\frac{-t}{-u}\right) + \pi^2\right),
\end{aligned}
\tag{2.20}
$$

---

[2]We write our results in the unphysical region where $s,t,u < 0$; one can analytically continue to the physical region where $s > 0$ and $t,u < 0$ using $\ln(-s) \to \ln(s) - i\pi$.

and where we have used the combination

$$t_8 F^4 = 2(F_1 F_2 F_3 F_4) - \frac{1}{2}(F_1 F_2)(F_3 F_4) + \text{cyclic}(2, 3, 4) , \tag{2.21}$$

familiar from the four-point one-loop type-I superstring amplitude. The rank-8 tensor t_8 arises from the trace over the fermionic zero-modes (see for instance[3] Ref. [98]). The combination in Eq. (2.21) is crossing symmetric and is related to the Yang–Mills tree amplitude via

$$t_8 F^4 = -ist A^{\text{tree}}(1, 2, 3, 4) = -isu A^{\text{tree}}(1, 2, 4, 3) = -itu A^{\text{tree}}(1, 3, 2, 4) . \tag{2.22}$$

The amplitude in Eq. (2.16) is ultraviolet-finite; the poles in ϵ in Eq. (2.16) are infrared ones.

We have carried out a number of checks of the amplitude. A simple check is that the infrared singularity in Eq. (2.16) matches the known form [53, 54, 56],

$$M_{\mathcal{N}=4,\text{SG}}^{\text{1-loop}}\Big|_{\text{IR}} = -M_{\mathcal{N}=4,\text{SG}}^{\text{tree}} \frac{2c_\Gamma}{\epsilon^2} \sum_{i<j}^3 s_{ij} \left(\frac{-s_{ij}}{\mu^2} \right)^{-\epsilon} . \tag{2.23}$$

To see this we express the factors in front of the $1/\epsilon^2$ in Eq. (2.16) in terms of the supergravity tree amplitude,

$$st A_{\mathcal{N}=4}^{\text{tree}}(1, 2, 3, 4) \frac{t_8 F^4}{stu} = -is A_{\mathcal{N}=4}^{\text{tree}}(1, 2, 3, 4) A^{\text{tree}}(1, 2, 4, 3) = M_{\mathcal{N}=4,\text{SG}}^{\text{tree}}(1, 2, 3, 4) , \tag{2.24}$$

where the last step uses the Kawai–Lewellen–Tye (KLT) relation [47] between tree-level gravity and Yang–Mills amplitudes. We have also compared the finite parts of all the amplitudes with external scalars and gravitons to the results in Ref. [44, 69, 75–77] and found agreement. The remaining fermionic amplitudes are related by supersymmetry Ward identities. We have checked that, prior to specializing to $D = 4$, the ultraviolet divergence cancels for $D < 8$,

---

[3]The t_8 tensor used here differs from the one in Ref. [98] by an overall factor of 4.

as expected [5]. In $D = 8$, we match the prediction from the heterotic string (see section 3.A.1 of Ref. [99]) as well as the calculation in Ref. [5]. It may also be possible to compare our D-dimensional expression to the recent $D = 10$ prediction in Ref. [100] obtained from M-theory. However, performing this comparison would be nontrivial as the divergences are quadratic in this dimension and hence depend on the regulator. It would be interesting to study this connection further.

The form in which we presented the amplitude in Eq. (2.16) makes the supersymmetry completely manifest, because it acts only on the MSYM side of the double copy. In addition, this form makes the translation to gravity transparent.

We now show in some detail how this works for the case of external gravitons. In the double-copy construction, amplitudes with four external gravitons can be built from integrands with purely gluonic external states on both sides of the double copy. As discussed in the previous section, it is convenient to use linearized field strengths in Eqs. (2.12) and (2.13) to write the answer. In order to translate to gravity we do this on both sides of the double copy. From this form, we can easily convert the linearized field strengths F in our formulas to a linearized Riemann tensor R using the relation,

$$\frac{2}{\kappa} R_{i\,\mu\nu\rho\sigma} = F_{i\,\mu\nu} F_{i\,\rho\sigma} = (k_{i\,\mu}\varepsilon_{i\,\nu} - k_{i\,\nu}\varepsilon_{i\,\mu})(k_{i\,\rho}\varepsilon_{i\,\sigma} - k_{i\,\sigma}\varepsilon_{i\,\rho}), \qquad (2.25)$$

where the index i refers to the particle label, just as in Eq. (2.11). In this equation the product of Yang–Mills polarization vectors is identified as a graviton polarization tensor via the replacement $\varepsilon_{i\,\mu}\varepsilon_{i\,\nu} \to \varepsilon_{i\,\mu\nu}$. The graviton is related to the metric via $g_{\mu\nu} = \eta_{\mu\nu} + \kappa h_{\mu\nu}$, as in Ref. [5, 97]. The factor of $2/\kappa$ is included in Eq. (2.25) so that $R_{i\,\mu\nu\rho\sigma}$ is given by the linearized Riemann tensor with the field $h_{\mu\nu}$ replaced by a polarization tensor $\varepsilon_{i\,\mu\nu}$.

The contribution from the pure-gluon factor from MSYM is always a factor of $st A^{\text{tree}} = it_8 F^4$. Once we multiply the tensors from both sides of the double-copy we then obtain the

following combinations,

$$t_8 F^4 t_8 F^4 \to t_8 t_8 R^4 \,, \tag{2.26}$$

$$t_8 F^4 (F_i F_j F_k F_l) \to t_8 (R_i R_j R_k R_l) \,, \tag{2.27}$$

$$t_8 F^4 (F_i F_j)(F_k F_l) \to t_8 (R_i R_j)(R_k R_l) \,, \tag{2.28}$$

where

$$(R_i R_j)^{\mu_1 \mu_2 \mu_3 \mu_4} (R_k R_l)^{\ \mu_5 \mu_6 \mu_7 \mu_8} \equiv R_i^{\ \mu_1 \mu_2 \nu \lambda} R_j^{\ \mu_3 \mu_4}{}_{\nu \lambda} R_k^{\ \mu_5 \mu_6 \rho \sigma} R_l^{\ \mu_7 \mu_8}{}_{\rho \sigma} \,, \tag{2.29}$$

$$(R_i R_j R_k R_l)^{\mu_1 \mu_2 \mu_3 \mu_4 \mu_4 \mu_5 \mu_6 \mu_7 \mu_8} \equiv R_i^{\ \mu_1 \mu_2 \nu \lambda} R_j^{\ \mu_3 \mu_4}{}_{\lambda \rho} R_k^{\ \mu_5 \mu_6 \rho \sigma} R_l^{\ \mu_7 \mu_8}{}_{\sigma \nu} \,. \tag{2.30}$$

In ten dimensions Eq. (2.26) is a component of the only $\mathcal{N} = 2$ superinvariant, whereas Eqs. (2.27) and (2.28) are components of the two $\mathcal{N} = 1$ superinvariants [100, 101].

The mapping of the final T_{F^3} tensor to gravity may appear more complicated than for the F^4-class tensors, because the former is generated from a scattering amplitude with an F^3 insertion, as previously illustrated in Fig. 2.2. A relatively simple way to obtain this tensor is to use KLT relations for amplitudes extended to include insertions of this higher-dimensional operator [102, 103]. This extension is in line with expectations from string-theory KLT relations [47, 104, 105], where the operator appears in the low-energy effective action. In Refs. [102, 103] it was established that the KLT relations apply to F^3 operators as,

$$s A^{\mathrm{tree}}(1, 2, 3, 4) \times A_{F^3}^{\mathrm{tree}}(1, 2, 4, 3) = i M_{R^2}^{\mathrm{tree}}(1, 2, 3, 4) \,, \tag{2.31}$$

where all particles are gluons on left-hand side of the equation, and all are gravitons on the right-hand side when the helicities of each pair of gluons align. Direct checks using Feynman diagrams, starting from the Einstein action, confirm that the Gauss–Bonnet insertion into a four-point gravity tree amplitude indeed satisfies Eq. (2.31) [106]. Hence we see that the

36

tensor T_{F^3} maps into the curvature-squared matrix elements in gravity as follows,

$$st A^{\text{tree}}(1,2,3,4) T_{F^3} = -i s u A^{\text{tree}}(1,2,4,3) st A_{F^3}^{\text{tree}}(1,2,3,4) = s t u M_{R^2}^{\text{tree}}(1,2,3,4), \quad (2.32)$$

where we used the crossing symmetry of $st A^{\text{tree}}(1,2,3,4)$ and the KLT relation in Eq. (2.31).

After the complete map to linearized Riemann tensors, the graviton amplitude takes the form,

$$
\begin{aligned}
M_{\mathcal{N}=4,\text{SG}}^{\text{1-loop}} = c_\Gamma \Bigg[& M_{\mathcal{N}=4,\text{SG}}^{\text{tree}} \bigg(-\frac{2}{\epsilon^2} \sum_{i<j}^{3} s_{ij} \Big(\frac{-s_{ij}}{\mu^2} \Big)^{-\epsilon} + L_1(s,t,u) \bigg) \\
& + M_{R^2}^{\text{tree}} + \bigg(\frac{4}{3} t_8(R_1 R_2 R_3 R_4) \Big(\frac{1}{st} + L_2(s,t,u) \Big) \\
& + t_8(R_1 R_2)(R_3 R_4) \Big(\frac{1}{s^2} + L_3(s,t,u) \Big) + \text{cyclic}(2,3,4) \bigg) \Bigg].
\end{aligned}
\quad (2.33)
$$

The same construction works for any supergravity state. For all states in the supergravity multiplet, the same pure Yang–Mills tensors feed into the corresponding supergravity expressions; the differences are solely on the MSYM side of the double copy.

It is remarkable that the coefficient of the curvature-squared matrix element $M_{R^2}^{\text{tree}}$ appearing in Eq. (2.33) is just a simple number. If the theory had a nonvanishing trace anomaly [15, 27, 37, 107], the coefficient of $M_{R^2}^{\text{tree}}$ would have contained a $1/\epsilon$ divergence [10, 11, 13, 30]. In our calculation the divergences are suppressed by an explicit factor of $D-4 = 2\epsilon$, (see, for example, Eq. (2.11) of Ref. [108]) leaving a finite rational contribution. From the perspective of the double copy, this ϵ/ϵ effect also generates the nonvanishing all-plus and single-minus one-loop amplitudes associated with the U(1) duality anomaly [69]. We comment on this below.

2.4 Curvature-Squared Multiplets and Divergences in Supergravity

In the previous section we found curvature-squared contributions to the effective action. In this section we describe these contribution in more detail.

2.4.1 Curvature-Squared Multiplets with Half-Maximal Supersymmetry

In the full superamplitude, we find a term proportional to,

$$sA_{\mathcal{N}=4}^{\text{tree}}(1,2,4,3)A_{F^3}^{\text{tree}}(1,2,3,4)\,, \tag{2.34}$$

which, as described in the previous section, contains the evanescent matrix element of curvature operators. In general dimensions there exist several off-shell curvature-squared operators in gravity theories. The two most important ones are the Gauss–Bonnet density and the square of the Weyl tensor[4], which respectively are given by,

$$E_4 = R_{\mu\nu\rho\sigma}R^{\mu\nu\rho\sigma} - 4R_{\mu\nu}R^{\mu\nu} + R^2\,, \tag{2.35}$$

$$W^2 = W_{\mu\nu\rho\sigma}W^{\mu\nu\rho\sigma} = R_{\mu\nu\rho\sigma}R^{\mu\nu\rho\sigma} - 2R_{\mu\nu}R^{\mu\nu} + \frac{1}{3}R^2\,. \tag{2.36}$$

The difference between the two is,

$$W^2 - E_4 = 2(R_{\mu\nu}R^{\mu\nu} - \frac{1}{3}R^2)\,, \tag{2.37}$$

which vanishes on shell. The single on-shell independent operator is usually chosen to be the Gauss–Bonnet combination (2.35). It is however a total derivative in four dimensions, which

---

[4]There is another interesting curvature-squared operator, the Pontryagin density $^*R_{\mu\nu\rho\sigma}R^{\mu\nu\rho\sigma}$; but it is parity odd and hence it cannot appear in the amplitudes of parity-conserving theories.

implies that all curvature-squared matrix elements are evanescent in this dimension [14]. A consequence of this is the finiteness of pure-graviton amplitudes at one loop [14] in Einstein gravity, as these operators are the only available counterterms. (When matter is added to the theory—even supersymmetric matter multiplets—generic divergences do appear at one loop starting with amplitudes for four matter particles [109, 110].)

Off-shell R^2 supermultiplets were constructed long ago for $\mathcal{N} = 1$ supergravity in four dimensions [78, 79], and more recently for $\mathcal{N} = 2$ supergravity [80–82] using a version of $\mathcal{N} = 2$ superspace. Very recently an $\mathcal{N} = 4$ supersymmetric completion of the Weyl-squared operator has been discussed in Ref. [111] in terms of linearized superfields in four dimensions. However, at the nonlinear level no fully off-shell versions have been constructed to date for any of the curvature-squared multiplets. This is unsurprising in light of the more general unsolved problem of constructing an off-shell $\mathcal{N} = 4$ superspace.

Equation (2.34) also contains matrix elements related by supersymmetry to the one corresponding to curvature-squared operators. These must arise from the $\mathcal{N} = 4$ supersymmetric completion of the curvature operators in Eqs. (2.35) and (2.36). Therefore the existence of such matrix element implies the existence of the corresponding $\mathcal{N} = 4$ curvature-squared multiplets. In particular, these matrix elements should correspond to the single insertion of the operator discussed in Ref. [111] in four dimensions as all curvature-squared operators are equivalent on shell. However, we cannot analyze such matrix elements strictly in four dimensions, because they will vanish identically.

The double-copy construction provides additional information, because it implies that completions of curvature-squared operators with half-maximal supersymmetry should exist in any integer dimension $D \leq 10$ and that their on-shell matrix elements are given by the KLT product of the F^3 operator insertion and ordinary MSYM amplitudes. The restriction to $D \leq 10$ arises because that is the maximum dimension for a super-Yang–Mills theory.

The double-copy perspective also shows that an $\mathcal{N} \geq 5$ supersymmetric completion of curvature-squared operators [112] cannot exist. We have an overall factor of $st A_{\mathcal{N}=4}^{\text{tree}}$ from
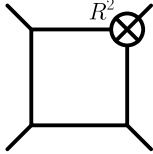
Figure 2.3: Representative diagram for the insertion of the evanescent R^2 counterterm, affecting the two-loop divergence in pure-graviton amplitudes [13].

the MSYM amplitude on the one side of the double copy. On the other side we would have an $\mathcal{N} \geq 1$ super-Yang–Mills amplitude. From the double-copy perspective, in any dimension the R^2 terms correspond to an F^3 operator on this latter side. We would then need a supersymmetric completion of the F^3 operator, to make it compatible with $\mathcal{N} = 1$ supersymmetry. We know, however, that no such completion exists in four dimensions because F^3 matrix element contributes only to all-plus and single-minus helicity configurations; and these are forbidden by a supersymmetric Ward identity [38–40]. This also rules out supersymmetric completions for these theories in any dimension $D > 4$ because on shell there is only a single independent curvature-squared invariant and one can choose the external momenta and states to live in a four-dimensional subspace, and hence the same argument applies.

2.4.2 Possible Effects at Higher Loops

In the context of dimensional regularization, evanescent R^2 contributions such as the ones described here play a crucial role in the two-loop divergences of pure gravity [10–12]. This happens because the evanescent R^2 terms appear at one loop with a divergent coefficient proportional to the trace anomaly. While such terms do not contribute in four dimensions, they do appear at two loops as subdivergences in the dimensionally regulated amplitude, directly affecting the value of the two-loop divergence [13]. One must then subtract a one-loop R^2 counterterm insertion, as illustrated in Fig. 2.3. This evanescent contribution becomes nonvanishing in dimensional regularization where it modifies the two-loop divergence. The net result is a curious disconnect between the coefficient of the dimensionally-regulated two-
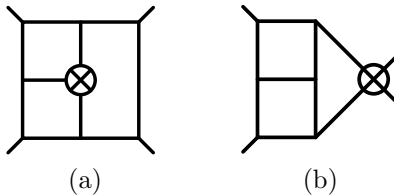
Figure 2.4: Representative diagrams for insertions of the supersymmetric R^2 operator at three loops that could affect the four-loop divergence.

loop R^3 ultraviolet divergence of these theories and the corresponding renormalization-scale dependence. The coefficient of the divergence depends on details of the regularization, while the renormalization scale dependence is simple and robust [1, 13, 67].

As shown in Eq. (2.33), in $\mathcal{N} = 4$ supergravity the R^2 contribution appears with a finite coefficient, so it cannot contribute to possible two-loop divergences. One may nonetheless expect it to modify divergences at yet-higher loops. Explicit calculations reveal no divergences in $\mathcal{N} = 4$ supergravity through three loops [4], but unveil them at four loops [71]. The addition of supersymmetrization of a curvature-squared operator as a local counterterm to the action is not expected to have any physical consequences in the scattering amplitudes, because it is evanescent. The analysis in Ref. [13] shows that it can however affect divergences. It would be interesting to study the effect of such local counterterms on the known four-loop divergence calculated in Ref. [71]. One may wonder whether such a finite counterterm can be used to modify or even remove the four-loop divergence. The answer to this question would require a three-loop computation with insertions of this operator, as illustrated in Fig. 2.4.

2.5   Evanescent Effects and the U(1) Anomaly

We now show that from the vantage point of the double copy that the U(1) anomalous contributions cannot be separated from the evanescent R^2 matrix elements, described in the previous section. We first review the anomaly and its manifestation in one-loop matrix

Pure YM		$\mathcal{N} = 4$ MSYM	$\mathcal{N} = 4$ Supergravity
$\langle g^- g^- g^+ g^+ \rangle$	$\otimes$	$\langle g^- g^- g^+ g^+ \rangle$	$\langle h^{--} h^{--} h^{++} h^{++} \rangle$
$\langle g^- g^+ g^+ g^+ \rangle$	$\otimes$	$\langle g^- g^- g^+ g^+ \rangle$	$\langle h^{--} \phi^{-+} h^{++} h^{++} \rangle$
$\langle g^+ g^+ g^+ g^+ \rangle$	$\otimes$	$\langle g^- g^- g^+ g^+ \rangle$	$\langle \phi^{-+} \phi^{-+} h^{++} h^{++} \rangle$

Table 2.1: Top components of three of the five independent superamplitudes. The other two are obtained from CPT conjugation.

elements [69], before explaining how these effects are intertwined.

In order to describe the anomaly we recall some basic facts about the spectrum of four-dimensional $\mathcal{N} = 4$ supergravity and the associated superamplitudes. We focus here on pure $\mathcal{N} = 4$ supergravity with no matter multiplets. The states of pure $\mathcal{N} = 4$ supergravity fall into two supermultiplets. One contains the positive-helicity graviton and its superpartners [113, 114]:

$$(h^{++}, \psi_a^+, A_{ab}^+, \chi_{abc}^+, \phi^{-+}), \tag{2.38}$$

where h^{++} is the positive-helicity graviton, ψ_a^+ are the four positive-helicity gravitinos, and so forth until the complex scalar ϕ^{-+}. The indices a, b, c are $SU(4)$ R symmetry indices. The other supermultiplet is the CPT conjugate to the one above, containing the negative-helicity graviton h^{--} and the conjugate scalar ϕ^{+-}. Seen through the lens of the double-copy, each multiplet corresponds to the supermultiplet of MSYM multiplied by either a positive- or negative-helicity gluon on the pure Yang–Mills side. For instance the positive-helicity graviton arises from a positive-helicity gluon on both sides of the double copy, and the complex scalars come from negative-helicity gluons on one side and positive-helicity gluons on the other side.

Because not all the states of this theory are in a single supermultiplet, the amplitudes are organized into different sectors not directly related by supersymmetry. For each one of these sectors there is an associated superamplitude. A simple way to understand this organization is via the double-copy construction. The supersymmetry Ward identities imply that the only nonvanishing helicity amplitudes in MSYM are those in the maximally-

helicity-violating (MHV) sector corresponding to amplitudes with two negative-helicity and two positive-helicity gluons $(g^-g^-g^+g^+)$ and their superpartners, which all sit in a single superamplitude. On the pure Yang–Mills side of the double copy, however, there are three distinct types of amplitudes: all-plus $(g^+g^+g^+g^+)$, single-minus $(g^-g^+g^+g^+)$, and two-minus or MHV $(g^-g^-g^+g^+)$, together with their parity conjugates. Hence there are three distinct sectors of supergravity super-amplitudes, inherited from each of the pure-Yang–Mills helicity configurations. In the all-plus and single-minus pure Yang–Mills sectors the gluons do not have the same number of negative or positive helicities as the gluons in the MSYM amplitude. Because of this the corresponding $\mathcal{N}=4$ supergravity superamplitudes do not contain four-graviton amplitudes, but have mixed graviton–scalar amplitudes as their top components, as illustrated in Table 2.1.

Ref. [68] showed that there exists an anomaly in an abelian U(1) subgroup of the SU(1, 1) duality group of $\mathcal{N}=4$ supergravity. This anomaly is manifested in the nonvanishing of the amplitudes,

$$M_{\mathcal{N}=4,\mathrm{SG}}(1_{h^{--}}, 2_{\phi^{-+}}, 3_{h^{++}}, 4_{h^{++}}) = \frac{i}{(4\pi)^2} \frac{\langle 1\,2\rangle^2 \langle 1\,3\rangle^2 [2\,3]^2 [3\,4]^4}{stu},$$

$$M_{\mathcal{N}=4,\mathrm{SG}}(1_{\phi^{-+}}, 2_{\phi^{-+}}, 3_{h^{++}}, 4_{h^{++}}) = \frac{i}{(4\pi)^2} [3\,4]^4, \tag{2.39}$$

as well as those related by supersymmetry [69]. The spinor inner products $\langle a\,b\rangle$ and $[a\,b]$ follow the standard conventions in Ref. [34]. The scalars carry a charge under the U(1) subgroup whereas the gravitons are uncharged and hence these amplitudes violate conservation of this charge. At tree level the charges are conserved because the amplitudes all vanish, but at loop level they do not. This anomaly can be traced back to $\mathcal{O}(\epsilon)$ terms which interfere with a would-be $1/\epsilon$ divergence, leaving behind a rational term. This is similar to the way the chiral anomaly arises in dimensional regularization [72].

As explained above, our calculation reveals evanescent contributions in Eq. (2.34), which are related to the supersymmetric completion of the R^2 operator. Mixed graviton–scalar

$\mathcal{N} = 4$ Supergravity	$-is A_{\mathcal{N}=4}^{\text{tree}}(1,2,4,3) A_{F3}^{\text{tree}}(1,2,3,4)$
$\langle h^{--} h^{--} h^{++} h^{++} \rangle$	0
$\langle h^{--} \phi^{-+} h^{++} h^{++} \rangle$	$-i \frac{\langle 1\,2 \rangle^2 \langle 1\,3 \rangle^2 [2\,3]^2}{stu} \delta^{(8)}(\overline{Q})$
$\langle \phi^{-+} \phi^{-+} h^{++} h^{++} \rangle$	$2i\,\delta^{(8)}(\overline{Q})$

Table 2.2: Top components of the three independent sectors in four dimensions and corresponding superamplitudes.

amplitudes also receive non-evanescent contributions from the same terms. A simple way to see this is by expressing the F^3 matrix element in a basis of gauge-invariant tensors that has definite four-dimensional helicity properties. We give two such bases in the Appendix. In the basis with tensors that have definite crossing-symmetry properties, we find that the F^3 matrix element is given by,

$$T_{F^3} = \frac{2stu}{(s^2 + t^2 + u^2)} H^{(++++)} - H^{(-+++)} + \frac{2(s-t)(s-u)(t-u)}{3(s^2 + t^2 + u^2)^2} H^{\text{ev1}} - \frac{6stu}{(s^2 + t^2 + u^2)^2} H^{\text{ev2}},$$

(2.40)

where the nonlocal denominators all cancel to give a local expression for T_{F^3}. This decomposition explicitly shows that T_{F^3} has nonvanishing contributions to the all-plus and single-minus helicity configurations, with the rest of the tensor being evanescent in four dimensions. This gives some additional insight into the evanescent nature of the R^2 matrix element in gravity. The only nonvanishing amplitudes on the MSYM side of the double copy have an MHV helicity configuration $(--++)$, whereas Eq. (2.40) shows that the F^3 matrix element does not contribute to MHV amplitudes on the pure Yang–Mills side. This implies that the pure-graviton matrix elements vanish in four dimensions. More importantly, we see that this matrix element contributes to the all-plus and single-minus helicities, thus generating anomalous mixed graviton-scalar matrix elements after applying the double-copy construction.

An alternative way to understand the different contributions of this matrix element is to recall that in general dimension, a pair of gluons is mapped via the double copy to a graviton, a dilaton and an antisymmetric tensor. In four dimensions the antisymmetric tensor is dual

to a pseudoscalar that together with the dilaton combines into the complex scalar discussed above. The intertwining of the anomalous and evanescent contributions in Eq. (2.31) therefore follows from the entanglement of the graviton, dilaton and an antisymmetric tensor in the double-copy construction.

From the discussion above, we conclude that the F^3 KLT product in Eq. (2.31) not only gives the evanescent curvature-squared matrix elements, but it necessarily results in an anomalous contribution to the amplitude. It is striking that contributions to both can be traced back to precisely the same term in the double copy. The anomalous contributions arising from T_{F^3} are summarized in Table 2.2. In this table the supermomentum delta function can be expanded as [115]

$$\delta^{(8)}(\overline{Q}) = \delta^{(8)}\Big(\sum_{j=1}^{4} \tilde{\lambda}_j^{\dot{\alpha}} \tilde{\eta}_{ja}\Big) = \prod_{a=1}^{4} \sum_{i<j}^{4} [i\,j]\,\tilde{\eta}_{ia}\tilde{\eta}_{ja}, \tag{2.41}$$

where we take the top component to be the one containing the factor $[3\,4]^4$. Comparing these to the anomalous amplitudes in Eq. (2.39) we see that, while the amplitudes in the single-scalar sector are fully contained in this term, those in the two-scalar sector are off by an overall factor and receive additional contributions that change the overall coefficient.

Finally, it is interesting to note that such anomalous and evanescent effects will not appear in the one-loop amplitudes of $\mathcal{N} \geq 5$ supergravity. The lack of anomalous one-loop amplitudes in $N \geq 5$ supergravity has been recently explained from the vantage point of super-invariants [111]. This, together with the absence of evanescent effects, is understood in the double-copy procedure as a consequence of the vanishing of the one-loop all-plus and single-minus amplitudes in super-Yang–Mills theories.

2.6 Conclusion

In this chapter we identified terms in the dimensionally regulated one-loop four-point amplitude of pure $\mathcal{N} = 4$ supergravity that can be written as insertions of curvature-squared operators into matrix elements. Such terms are evanescent and vanish for four-dimensional external states. We also showed that these evanescent terms are intertwined with contributions generated by the U(1) duality anomaly [68, 69]. These two effects both arise from rational pieces that result from an ϵ/ϵ cancellation, where $\epsilon = (4 - D)/2$ is the dimensional regularization parameter.

Both the anomaly and the evanescent curvature-squared terms may play a central role in the ultraviolet properties of gravity theories. As explained in Ref. [69] the anomaly in $\mathcal{N} = 4$ supergravity gives contributions with a poor ultraviolet behavior. We also know that beyond one loop, evanescent effects contribute to dimensionally regulated ultraviolet divergences in gravity theories [13].

We carried out our analysis using the double-copy construction [35, 36] of $\mathcal{N} = 4$ supergravity [75–77] in terms of the corresponding pure Yang–Mills and $\mathcal{N} = 4$ MSYM amplitudes. The double-copy construction makes the on-shell supersymmetry manifest, because $\mathcal{N} = 4$ supergravity inherits the well-understood on-shell superspace of MSYM theory. By using formal polarization vectors on the pure-Yang–Mills side of the double copy, we were able to evaluate all one-loop four-point amplitudes of $\mathcal{N} = 4$ supergravity simultaneously. In the graviton sector we gave explicit conversion formulas from gauge theory to gravity, using relations between linearized Riemann tensors and Yang–Mills field strengths. The double-copy construction implies that completions of curvature-squared operators with half-maximal supersymmetry should exist in any dimension with $D \leq 10$ and that their on-shell matrix elements are given by the KLT product of the F^3 operator insertion and ordinary MSYM amplitudes.

There are a number of interesting avenues for future research. Although it is is not known

how to write the super-Gauss–Bonnet in an off-shell superspace, this chapter provides all components of four-point matrix elements of single insertions of these operators. For the pure-graviton amplitude the Gauss–Bonnet operator is the correct one for generating these matrix elements. For amplitudes with other external states, one would first need to systematically write down a set of evanescent operators of the same dimension, feed them through a tree-level matrix-element computation and then match them to our evanescent matrix elements. Once the combination of operators leading to our evanescent matrix elements are found, one can try to appropriately package the components into superfields.

We organized the one-loop amplitude in terms of gauge-invariant tensors. These and their associated projectors are described in the appendix and given in the *Mathematica* attachement at the arXiv hosting of Ref. [2]. They are useful, not only for $\mathcal{N} = 4$ supergravity, but for any gauge-theory four-gluon amplitude at any loop order.

In pure gravity the evanescent one-loop curvature-squared terms enter with a coefficient proportional to $1/\epsilon$. Because of this, when inserted as counterterms in a two-loop calculation they affect the leading ultraviolet divergence [13]. In $\mathcal{N} = 4$ supergravity these evanescent terms appear with a finite coefficient. This means that they cannot affect divergences until three loops or higher. Direct calculations show that the three-loop divergences cancel [4] and the first divergence occurs at four loops [71]. It is important to understand the effect of evanescent and anomalous contribution on higher-loop amplitudes, especially to see whether their contributions can account for the four-loop divergence of $\mathcal{N} = 4$ supergravity. A direct study requires a three-loop computation. An important step in this direction would be to analyze the anomalous sector at two loops in $\mathcal{N} = 4$ supergravity and its relation to evanescent effects. In the longer term, understanding the role of anomalies and evanescent effects more generally at higher loops appears to be crucial in order to unravel the ultraviolet properties of supergravity theories.

2.A   Gauge-Invariant Tensors for Yang–Mills Four-Point Amplitudes

In this appendix, we describe two independent sets of Yang–Mills kinematic tensors built out of physical polarization vectors ε_i and on-shell momenta k_i. In both sets, the tensors are constrained to be on-shell gauge invariant, that is vanishing under the substitution $\varepsilon_i \to k_i$ for each external leg independently. The tensors are polynomials in the dot products $k_i \cdot \varepsilon_j$, $\varepsilon_i \cdot \varepsilon_j$, and the Mandelstam invariants s and t. They are thus free of poles by construction. We also organize the tensors to have definite symmetry properties under a relevant symmetry, and to be diagonal in a four-dimensional helicity basis. The tensors are dimension-agnostic, and so the sets are not in general diagonal in a basis of external states outside of four dimensions. Both sets have seven tensors.

In the first set, each tensor represents kinematic parts of a color-ordered amplitude, up to a function of s and t. Such amplitudes are invariant under a cyclic permutation of the external indices, $i \to (i+1) \mod 4$, so we choose the tensors to have definite symmetry properties under the cyclic shift. An arbitrary function can be split up into symmetric and antisymmetric combinations, $f_\pm(s,t) = \frac{1}{2}[f(s,t) \pm f(t,s)]$, so we choose the tensors to be symmetric or antisymmetric. It might seem simpler to choose them to be symmetric; but for some of them, an antisymmetric form is simpler. In an amplitude, such antisymmetric tensors would then appear multiplied by an antisymmetric function of s and t. We present this set in the first subsection.

For the second set, each tensor represents one Yang–Mills copy in a double-copy construction of an $\mathcal{N} = 4$ supergravity amplitude, where the other copy is given by the tree-level tensor. These tensors then suffice to construct the $\mathcal{N} = 4$ supergravity four-point amplitude at one and two loops. These tensors are required to have definite symmetry properties under the full permutation group acting on the external indices. We are interested only in the one-dimensional representations of this group, so again each tensor will either be completely

invariant, or will change sign according to the signature of a permutation. We present this set in the second subsection.

In the third subsection, we describe set of projection operators that can be applied to an expression given in terms of polarization vectors and momenta to obtain the (scalar) coefficients of the different basis tensors.

The referenced *Mathematica* files can be found at the arXiv hosting of Ref. [2].

2.A.1 Tensors with Definite Cyclic Symmetry

We take the first element of the set of tensors with definite cyclic properties to be the tensor of engineering dimension 4 that appears in the tree amplitude,

$$
\begin{aligned}
T^{\text{tree}} = t_8 F^4 = {}& s\,(s+t)\,\epsilon_1{\cdot}\epsilon_4\,\epsilon_2{\cdot}\epsilon_3 - s\,t\,\epsilon_1{\cdot}\epsilon_3\,\epsilon_2{\cdot}\epsilon_4 + t\,(s+t)\,\epsilon_1{\cdot}\epsilon_2\,\epsilon_3{\cdot}\epsilon_4 \\
& - 2\,(s+t)\,\epsilon_1{\cdot}\epsilon_4\,k_1{\cdot}\epsilon_2\,k_1{\cdot}\epsilon_3 - 2\,(s+t)\,\epsilon_1{\cdot}\epsilon_4\,k_1{\cdot}\epsilon_2\,k_2{\cdot}\epsilon_3 \\
& - 2\,s\,\epsilon_1{\cdot}\epsilon_3\,k_1{\cdot}\epsilon_2\,k_2{\cdot}\epsilon_4 - 2\,t\,\epsilon_1{\cdot}\epsilon_2\,k_1{\cdot}\epsilon_3\,k_2{\cdot}\epsilon_4 - 2\,(s+t)\,\epsilon_1{\cdot}\epsilon_2\,k_2{\cdot}\epsilon_3\,k_2{\cdot}\epsilon_4 \\
& - 2\,t\,\epsilon_2{\cdot}\epsilon_4\,k_1{\cdot}\epsilon_3\,k_3{\cdot}\epsilon_1 - 2\,t\,\epsilon_2{\cdot}\epsilon_4\,k_2{\cdot}\epsilon_3\,k_3{\cdot}\epsilon_1 - 2\,s\,\epsilon_2{\cdot}\epsilon_3\,k_2{\cdot}\epsilon_4\,k_3{\cdot}\epsilon_1 \\
& - 2\,(s+t)\,\epsilon_1{\cdot}\epsilon_3\,k_1{\cdot}\epsilon_2\,k_3{\cdot}\epsilon_4 - 2\,(s+t)\,\epsilon_1{\cdot}\epsilon_2\,k_2{\cdot}\epsilon_3\,k_3{\cdot}\epsilon_4 \\
& - 2\,(s+t)\,\epsilon_2{\cdot}\epsilon_3\,k_3{\cdot}\epsilon_1\,k_3{\cdot}\epsilon_4 - 2\,(s+t)\,\epsilon_3{\cdot}\epsilon_4\,k_1{\cdot}\epsilon_2\,k_4{\cdot}\epsilon_1 \\
& - 2\,t\,\epsilon_2{\cdot}\epsilon_4\,k_1{\cdot}\epsilon_3\,k_4{\cdot}\epsilon_1 - 2\,(s+t)\,\epsilon_2{\cdot}\epsilon_4\,k_2{\cdot}\epsilon_3\,k_4{\cdot}\epsilon_1 \\
& - 2\,(s+t)\,\epsilon_2{\cdot}\epsilon_3\,k_3{\cdot}\epsilon_4\,k_4{\cdot}\epsilon_1 - 2\,s\,\epsilon_1{\cdot}\epsilon_4\,k_1{\cdot}\epsilon_3\,k_4{\cdot}\epsilon_2 - 2\,s\,\epsilon_1{\cdot}\epsilon_3\,k_2{\cdot}\epsilon_4\,k_4{\cdot}\epsilon_2 \\
& - 2\,t\,\epsilon_3{\cdot}\epsilon_4\,k_3{\cdot}\epsilon_1\,k_4{\cdot}\epsilon_2 - 2\,s\,\epsilon_1{\cdot}\epsilon_3\,k_3{\cdot}\epsilon_4\,k_4{\cdot}\epsilon_2 - 2\,(s+t)\,\epsilon_3{\cdot}\epsilon_4\,k_4{\cdot}\epsilon_1\,k_4{\cdot}\epsilon_2\,.
\end{aligned} \tag{2.42}
$$

It vanishes, of course, for the $(+\,+\,+\,+)$ and $(-\,+\,+\,+)$ classes of helicities, and is nonvanishing for MHV helicities $(-\,-\,+\,+)$. It is invariant under cyclic shifts of the external legs. We choose the remaining tensors to have definite helicity properties as well. We can give compact expressions for the tensors in terms of the following combinations of

the linearized field-strength tensors defined in Eq. (2.11),

$$F_{st}^4 \equiv (F_1 F_2 F_3 F_4), \qquad F_{tu}^4 \equiv (F_1 F_4 F_2 F_3), \qquad F_{us}^4 \equiv (F_1 F_3 F_4 F_2),$$
$$(F_s^2)^2 \equiv (F_1 F_2)(F_3 F_4), \qquad (F_t^2)^2 \equiv (F_1 F_4)(F_2 F_3), \qquad (F_u^2)^2 \equiv (F_1 F_3)(F_4 F_2), \tag{2.43}$$

along with the T_{F^3} tensor defined in Eq. (2.15). In terms of these quantities, the basis tensors have the following expressions,

$$T^{\text{tree}} = -\frac{1}{2}((F_s^2)^2 + (F_t^2)^2 + (F_u^2)^2) + 2(F_{st}^4 + F_{tu}^4 + F_{us}^4) = t_8 F^4,$$

$$T^{(++++)} = -2 F_{st}^4 + \frac{1}{2}((F_s^2)^2 + (F_t^2)^2 + (F_u^2)^2),$$

$$T^{(-+++)} = -T_{F^3} - (F_{tu}^4 - F_{us}^4)(s-t) + (F_{st}^4 - \frac{1}{4}((F_s^2)^2 + (F_t^2)^2 + (F_u^2)^2))(s+t),$$

$$T^{(--++)} = (F_s^2)^2 - (F_t^2)^2 + 2(F_{tu}^4 - F_{us}^4),$$

$$T^{(-+-+)} = 2 F_{st}^4 - \frac{1}{2}((F_s^2)^2 + (F_t^2)^2 - (F_u^2)^2),$$

$$T^{\text{ev1}} = -(2 F_{st}^4 + \frac{3}{2}((F_s^2)^2 + (F_t^2)^2 + (F_u^2)^2))(s+t) + 2(F_{us}^4(3s+t) + F_{tu}^4(s+3t))$$

$$= -4(F_{tu}^4 s + F_{us}^4 t) - (s+t)(8 F_{st}^4 - 3 T^{\text{tree}}),$$

$$T^{\text{ev2}} = -(2 F_{st}^4 - \frac{1}{2}((F_s^2)^2 + (F_t^2)^2 + (F_u^2)^2))(s-t) + 2(F_{tu}^4 - F_{us}^4)(s+t)$$

$$= 4(F_{tu}^4 s - F_{us}^4 t) - (s-t) T^{\text{tree}}. \tag{2.44}$$

The first tensor is the tree-level tensor given above in Eq. (2.42). The subsequent four tensors each are labeled by the class of four-dimensional helicity configuration on which they are nonvanishing. The final two tensors are nontrivial formal objects, but vanish for all four-dimensional helicities. Outside of four dimensions, they do not vanish, however, as demonstrated, for example, by the nonvanishing value of the sum over states of each tensor multiplied by its conjugate. They represent the kinematic part of evanescent operators in Yang–Mills theory. In a slight abuse of language, we will therefore call them evanescent tensors. Three other gauge-invariant tensors can be constructed, but these do not have the

Tensor	Dimension	Symmetry	Nonvanishing $D=4$ Helicity	$D=4$ Value
T^{tree}	4	$+$	$(--++)$ $(-+-+)$	$\langle 1\,2\rangle^2\,[3\,4]^2$ $\langle 1\,3\rangle^2\,[2\,4]^2$
$T^{(++++)}$	4	$+$	$(++++)$	$[1\,3]^2\,[2\,4]^2$
$T^{(-+++)}$	6	$+$	$(-+++)$	$\langle 1\,2\rangle^2\,[2\,3]^2\,[2\,4]^2$
$T^{(--++)}$	4	$-$	$(--++)$	$\langle 1\,2\rangle^2\,[3\,4]^2$
$T^{(-+-+)}$	4	$+$	$(-+-+)$	$\langle 1\,3\rangle^2\,[2\,4]^2$
T^{ev1}	6	$+$	—	0
T^{ev2}	6	$-$	—	0

Table 2.3: Nonvanishing helicities and values for the color-ordered tensor basis. Each tensor is also nonvanishing on the cyclic permutations and parity conjugates of the indicated helicity states. The evanescent tensors vanish for all four-dimensional helicities but are included in the table.

correct symmetry properties to appear in color-ordered physical amplitudes. The properties of all the tensors, as well as their values in four-dimensional helicity are summarized in Table 2.3. The expressions for the tensors are also given in a companion *Mathematica* file, tensors-ym.m. The notation there is,

$$\text{ee[i,j]} = \varepsilon_i \cdot \varepsilon_j\,, \qquad \text{ke[i,j]} = k_i \cdot \varepsilon_j\,, \qquad \text{dot[i,j]} = k_i \cdot k_j\,. \tag{2.45}$$

The seven tensors in Eq. (2.44) sequentially correspond to $\mathsf{T[[i]]}$ in the file for $i = 1, \ldots, 7$. The spinor-valued expressions for the tensors in four dimensions are also given that file, with the seven values for each four-dimensional helicity configuration recorded in value[*helicity-string*], for example value["++++"]. These expressions employ the notation,

$$\text{spa[i,j]} = \langle i\,j\rangle\,, \qquad \text{spb[i,j]} = [i\,j]\,. \tag{2.46}$$

Conversely, we can express the linearized combinations (2.43) in terms of the color-ordered

tensors,

$$F_{st}^4 = -\frac{T^{\text{ev1}}}{8\,(s+t)} - \frac{(s-t)\,T^{\text{ev2}}}{8\,(s+t)^2} + \frac{1}{4}\,T^{\text{tree}} - \frac{s\,t\,T^{(++++)}}{2\,(s+t)^2}\,,$$

$$F_{tu}^4 = \frac{T^{\text{ev2}}}{4\,(s+t)} + \frac{1}{4}\,T^{\text{tree}} + \frac{t\,T^{(++++)}}{2\,(s+t)}\,,$$

$$F_{us}^4 = -\frac{T^{\text{ev2}}}{4\,(s+t)} + \frac{1}{4}\,T^{\text{tree}} + \frac{s\,T^{(++++)}}{2\,(s+t)}\,,$$

$$(F_s^2)^2 = -\frac{T^{\text{ev1}}}{4\,(s+t)} - \frac{(3\,s+t)\,T^{\text{ev2}}}{4\,(s+t)^2} + \frac{1}{2}\,T^{\text{tree}} + \frac{1}{2}\,T^{(--++)} - \frac{1}{2}\,T^{(-+-+)} + \frac{s^2\,T^{(++++)}}{(s+t)^2}\,,$$

$$(F_t^2)^2 = -\frac{T^{\text{ev1}}}{4\,(s+t)} + \frac{(s+3\,t)\,T^{\text{ev2}}}{4\,(s+t)^2} + \frac{1}{2}\,T^{\text{tree}} - \frac{1}{2}\,T^{(--++)} - \frac{1}{2}\,T^{(-+-+)} + \frac{t^2\,T^{(++++)}}{(s+t)^2}\,,$$

$$(F_u^2)^2 = T^{(-+-+)} + T^{(++++)}\,,$$

$$T_{F^3} = -\frac{(s-t)\,T^{\text{ev2}}}{2\,(s+t)} - T^{(-+++)} - \frac{2\,s\,t\,T^{(++++)}}{s+t}\,.$$

$$(2.47)$$

2.A.2 Tensors with Definite Permutation Symmetry

In this subsection, we present four-gluon kinematic tensors with definite properties under the full permutation group. These are ultimately useful for decomposing $\mathcal{N} = 4$ supergravity amplitudes at one and two loops in a double-copy approach. The tree tensor (2.42) is already fully crossing invariant, so we take it to be the first tensor in this set as well, here calling it H^{tree}. The remaining tensors are either invariant under all permutations of external labels, or are multiplied by the signature of the permutation (± 1). We will call the latter signature-odd.

A signature-odd tensor will be multiplied by a signature-odd polynomial in s and t in any physical amplitude. Any invariant polynomial can also appear as a tensor prefactor in an amplitude, of course. All invariant polynomials can be built out of products of two basic

polynomials,

$$\sigma_2(s,t,u) = s^2 + t^2 + u^2 = 2(s^2 + st + t^2) = -2(st + tu + us)\,,$$
$$\sigma_3(s,t,u) = s^3 + t^3 + u^3 = 3stu\,, \tag{2.48}$$

with a constant prefactor. Any signature-odd polynomial is a product of an invariant polynomial and the basic signature-odd polynomial,

$$\alpha(s,t,u) = -(s-t)(t-u)(u-s) = (s-t)(2s+t)(s+2t)\,. \tag{2.49}$$

This polynomial satisfies the identity

$$2\,\alpha^2 = \sigma_2^3 - 6\,\sigma_3^2\,, \tag{2.50}$$

so that we need not consider powers of α.

We can again express the tensors in terms of the linearized-field strength quantities defined in Eq. (2.43),

$$H^{\text{tree}} = -\frac{1}{2}((F_s^2)^2 + (F_t^2)^2 + (F_u^2)^2) + 2\,(F_{st}^4 + F_{tu}^4 + F_{us}^4) = t_8 F^4\,,$$

$$H^{(++++)} = \frac{3}{2}\,((F_s^2)^2 + (F_t^2)^2 + (F_u^2)^2) - 2\,(F_{st}^4 + F_{tu}^4 + F_{us}^4)\,,$$

$$H^{(-+++)} = -T_{F^3} - \frac{4}{3}\,(F_{tu}^4\,s + F_{us}^4\,t - F_{st}^4\,(s+t))\,,$$

$$H^{\text{MHV1}} = -((F_s^2)^2 + 2\,F_{tu}^4)\,s - ((F_t^2)^2 + 2\,F_{us}^4)\,t + (2\,F_{st}^4 + (F_u^2)^2)\,(s+t)\,,$$

$$H^{\text{MHV2}} = (F_u^2)^2\,(s-t)\,(s+t) + (F_t^2)^2\,t\,(2\,s+t) - (F_s^2)^2\,s\,(s+2\,t)\,,$$

$$H^{\text{ev1}} = 4\,(F_{st}^4\,(s-t)\,(s+t) + F_{us}^4\,t\,(2\,s+t) - F_{tu}^4\,s\,(s+2\,t))\,,$$

$$H^{\text{ev2}} = ((F_s^2)^2 + (F_t^2)^2 + (F_u^2)^2)\,(s^2 + s\,t + t^2) - 4\,(F_{tu}^4\,t\,(s+t) - s\,(F_{st}^4\,t - F_{us}^4\,(s+t)))\,. \tag{2.51}$$

The second and third tensors are again labeled by the four-dimensional helicity class for which they are nonvanishing; the fourth and fifth are both nonvanishing for all MHV

helicities. The last two are again "evanescent", in the sense that they are nonvanishing outside of four dimensions but vanish for all four-dimensional helicity configurations. (As in Section 2.A.1, they do not include factors of $1/\epsilon$ that would be needed to yield a nonvanishing result in four dimensions.)

Tensor	Dimension	Signature	Nonvanishing $D=4$ Helicity	$D=4$ Value
H^{tree}	4	even	$(--++)$	$\langle 1\,2\rangle^2\,[3\,4]^2$
$H^{(++++)}$	4	even	$(++++)$	$[1\,4]^2\,[2\,3]^2 + [1\,3]^2\,[2\,4]^2 + [1\,2]^2\,[3\,4]^2$
$H^{(-+++)}$	6	even	$(-+++)$	$\langle 1\,2\rangle^2\,[2\,3]^2\,[2\,4]^2$
H^{MHV1}	6	even	$(--++)$	$\langle 1\,2\rangle^3\,[1\,2]\,[3\,4]^2$
H^{MHV2}	8	odd	$(--++)$	$(s+2\,t)\,\langle 1\,2\rangle^3\,[1\,2]\,[3\,4]^2$
H^{ev1}	8	odd	—	0
H^{ev2}	8	even	—	0

Table 2.4: Nonvanishing helicities and values for the pregravity tensor basis. Each tensor is also nonvanishing on the permutations and parity conjugates of the indicated helicity states. The evanescent tensors vanish for all four-dimensional helicities but are included in the table.

The expressions for the tensors are also given in a companion *Mathematica* file, tensors-neq4gr.m, with H[[i]], $i = 1, \ldots, 7$ corresponding in order to the tensors in Eq. (2.51). The spinor-valued expressions for the tensors in four dimensions are also given in that file; as in Section 2.A.1, the seven values for each four-dimensional helicity configuration given by value[*helicity-string*]. The notation follows Eqs. (2.45) and (2.46). The properties of the tensors are summarized in Table 2.4.

Because these tensor have definite properties under permutations, we can connect them straightforwardly to matrix elements of corresponding operators after the double copy. A few examples would be,

$$\sigma_2 t_8 F^4 t_8 F^4 \leftrightarrow t_8 t_8 D^4 R^4\,,$$

$$t_8 F^4 (u F_{st}^4 + s F_{tu}^4 + t F_{us}^4) \leftrightarrow t_8 \text{tr}(D^2 R^4)\,, \tag{2.52}$$

$$\sigma_2 t_8 F^4 ((F_s^2)^2 + (F_u^2)^2 + (F_t^2)^2) \leftrightarrow t_8 (\text{tr}(DR)^2)^2\,.$$

2.A.3 Projectors for Basis Tensors

In this subsection, we present a set of projectors that can be used to obtain the scalar co-efficients of the basis tensors for an expression given in terms of polarization vectors and momenta. When applied to an integrated expression for an amplitude, the resulting decomposition will reproduce the original expression; when applied to an integrand, there may be a total-derivative discrepancy that will integrate to zero.

We define an inner product $\odot$ of a polarization vector and its conjugate to be given by the sum over states,

$$\epsilon_i^{*\mu} \odot \epsilon_i^{\nu} = \sum_{\text{states } h} \epsilon_i^{*(h),\mu} \epsilon_i^{(h),\nu} = -g^{\mu\nu} + \frac{k_i^{\mu} q^{\nu} + q^{\mu} k_i^{\nu}}{q \cdot k_i} , \qquad (2.53)$$

where q is a null reference vector not collinear to any external momentum. (It is similar to a lightcone-gauge vector.) In four dimensions, the state sum becomes,

$$\sum_{\text{states } h} \epsilon_i^{*(h),\mu} \epsilon_i^{(h),\nu} = \sum_{h=\pm} \epsilon_i^{*(h),\mu} \epsilon_i^{(h),\nu} = \sum_{h=\pm} \epsilon_i^{(-h),\mu} \epsilon_i^{(h),\nu} , \qquad (2.54)$$

where the sum is over vector helicities.

In all dimensions, the projector onto the jth tensor is then given by,

$$P_j = c_{ji} T_i^* , \qquad (2.55)$$

where the matrix c is the inverse of the (symmetric) inner product matrix m, whose elements are given by,

$$m_{ij} = T_i^* \odot T_j . \qquad (2.56)$$

The coefficient of T_j in an expression X is given by $P_j \odot X$.

Each basis has a corresponding set of projectors; the projectors for the cyclicly-organized basis described in Section 2.A.1 are given alongside the tensors and helicity values in tensors-

ym.m, where the projector P_j onto T_j is given by P[[j]]. The expressions make use of the following notation in addition to that in Eq. (2.45),

$$\mathsf{cc[i,j]} = \varepsilon_i^* \cdot \varepsilon_j^* \,, \qquad \mathsf{kc[i,j]} = k_i \cdot \varepsilon_j^* \,, \qquad \mathsf{chi} = t/s \,, \qquad \mathsf{d} = D \,. \qquad (2.57)$$

In four dimensions, m has rank 5, as expected from the nature of T_5 and T_6. In six dimensions, it has rank 7, showing indirectly that there are some helicities with non-vanishing values for these two tensors. The corresponding projectors for the basis of Section 2.A.2 organized under the full crossing symmetry are given in tensors-neq4gr.m. The projector matrix again has rank 5 in four dimensions, and rank 7 in six dimensions.

Chapter 3

Ultraviolet Properties of $\mathcal{N} = 8$ Supergravity at Five Loops

We use the recently developed generalized double-copy construction to obtain an improved representation of the five-loop four-point integrand of $\mathcal{N} = 8$ supergravity whose leading ultraviolet behavior we analyze using state-of-the-art loop-integral expansion and reduction methods. We find that the five-loop critical dimension where ultraviolet divergences first occur is $D_c = 24/5$, corresponding to a $D^8 R^4$ counterterm. This ultraviolet behavior stands in contrast to the cases of four-dimensional $\mathcal{N} = 4$ supergravity at three loops and $\mathcal{N} = 5$ supergravity at four loops whose improved ultraviolet behavior demonstrates enhanced cancellations beyond implications from standard-symmetry considerations. We express this $D_c = 24/5$ divergence in terms of two relatively simple positive-definite integrals reminiscent of vacuum integrals, excluding any additional ultraviolet cancellations at this loop-order. We note nontrivial relations between the integrals describing this leading ultraviolet behavior and integrals describing lower-loop behavior. This observation suggests not only a path towards greatly simplifying future calculations at higher loops, but may even allow us to directly investigate ultraviolet behavior in terms of simplified integrals, avoiding the construction of complete integrands.

3.1 Introduction

Since the discovery of supergravity theories [116, 117], a complete understanding of their ultraviolet properties has remained elusive. Despite tremendous progress over the years, many properties of gravitational perturbation theory remain unknown. Power counting arguments, driven by the dimensionality of Newton's constant, suggest that all point-like theories of gravity should develop an ultraviolet divergence at a sufficiently high loop order. However, if a point-like theory were ultraviolet finite, it would imply the existence of an undiscovered symmetry or structure that should likely have a fundamental impact on our understanding of quantum gravity. Explicit calculations in recent years have revealed the existence of hidden properties, not readily apparent in Lagrangian formulations. One might wonder whether these tame the ultraviolet behavior of point-like gravity theories. For example, all-loop-order unitarity cuts exhibit remarkable infrared and ultraviolet cancellations [118–120] whose consequences remain to be fully explored. Indeed, we know of examples in $\mathcal{N} = 4$ [113, 121, 122] and $\mathcal{N} = 5$ [123] supergravity theories that display "enhanced cancellations" [4–9, 108], where quantum corrections exclude counterterms thought to be consistent with all known symmetries. In addition, there are indications that anomalies in known symmetries of supergravity theories play a role in the appearance of ultraviolet divergences [2, 68–71, 111, 124]. Restoration of these symmetries in S-matrix elements by finite local counterterms may lead to the cancellation of known divergences. In this chapter, we take a step forward by presenting a detailed analysis of the ultraviolet behavior of the five-loop four-point scattering amplitude in the maximally supersymmetric theory, $\mathcal{N} = 8$ supergravity[1] [125–127], and observe properties that should help us determine its four-dimensional ultraviolet behavior at even higher loops.

Its many symmetries suggest that, among the point-like theories of gravity, the maximally

---

[1]Strictly speaking the maximally supersymmetric theory is only recognized as $\mathcal{N} = 8$ supergravity in four dimensions. While we concern ourselves with mainly higher dimensions, in this chapter we take the liberty to apply the four-dimensional nomenclature.

supersymmetric theory has the softest ultraviolet behavior. These symmetry properties also make it technically easier to explore and understand its structure. Over the years there have been many studies and predictions for the ultraviolet behavior of $\mathcal{N} = 8$ supergravity [90, 128–138]. The current consensus, based on standard symmetry considerations, is that $\mathcal{N} = 8$ supergravity in four dimensions is ultraviolet finite up to at least seven loops [139–144]. Through four loops, direct computation using modern scattering amplitude methods prove that the critical dimension of $\mathcal{N} = 8$ supergravity where divergences first occur is [61, 145–148]

$$D_c = \frac{6}{L} + 4\,, \qquad (2 \leq L \leq 4) \tag{3.1}$$

where L is the number of loops. This matches the formula [145, 149] for $\mathcal{N} = 4$ super-Yang–Mills theory [150, 151] which is known to be an ultraviolet finite theory in $D = 4$ [152–155]. At one loop the critical dimension, for both $\mathcal{N} = 4$ super-Yang–Mills theory and $\mathcal{N} = 8$ supergravity [90], is $D_c = 8$. We define the theories in dimensions $D > 4$ via dimensional reduction of $\mathcal{N} = 1$ supergravity in $D = 11$ and $\mathcal{N} = 1$ super-Yang–Mills theory in $D = 10$ [90].

In this chapter we address the longstanding question of whether Eq. (3.1) holds for $\mathcal{N} = 8$ supergravity at five loops. Symmetry arguments [142, 143] suggest $D^8 R^4$ as a valid counterterm and that the critical dimension for the five-loop divergence should be $D_c = 24/5$ instead of that suggested by Eq. (3.1), $D_c = 26/5$. (See also Refs. [139–141, 144].) Such arguments, however, cannot ascertain whether quantum corrections actually generate an allowed divergence. Indeed, explicit three-loop calculations in $\mathcal{N} = 4$ supergravity and four-loop calculations in $\mathcal{N} = 5$ supergravity reveal that while counterterms are allowed by all known symmetry considerations, none actually exist [4, 6]. These enhanced cancellations are nontrivial and only manifest upon applying Lorentz invariance and a reparametrization invariance to the loop integrals [108]. This implies that the only definitive way to settle the five-loop question is to directly calculate the coefficient of the potential $D^8 R^4$ counterterm

in $D = 24/5$, as we do here. This counterterm is of interest because it is the one that would contribute at seven loops if $\mathcal{N} = 8$ supergravity were to diverge in $D = 4$.

Our direct evaluation of the critical dimension of the $\mathcal{N} = 8$ supergravity theory at five loops proves unequivocally that it first diverges in $D_c = 24/5$ and no enhanced cancellations are observed. The fate of $\mathcal{N} = 8$ supergravity in four-dimensions remains to be determined. Even with the powerful advances exploited in this current calculation, direct analysis at seven loops would seem out of reach. Fortunately the results of our current analysis, when combined with earlier work at lower loops [4, 6, 9, 61, 71, 146–148], reveal highly nontrivial constraints on the subloops of integrals describing the leading ultraviolet behavior through five loops. These patterns suggest not only new efficient techniques to directly determine the ultraviolet behavior at ever higher loops, but potentially undiscovered principles governing the ultraviolet consistency. In this work we will describe these observed constraints, leaving their detailed study for the future.

The results of this chapter are the culmination of many advances in understanding and computing gauge and gravity scattering amplitudes at high-loop orders. The unitarity method [156–160] has been central to this progress because of the way that it allows on-shell simplifications to be exploited in the construction of new higher-loop amplitudes. We use its incarnation in the maximal-cut organization [160] to systematically build complete integrands [60, 161].

The unitarity method combines naturally with double-copy ideas, including the field-theoretic version of the string-theory Kawai, Lewellen and Tye (KLT) relations between gauge and gravity tree amplitudes [47] and the related Bern, Carrasco and Johansson (BCJ) color-kinematics duality and double-copy construction [35, 36]. The double-copy relationship reduces the problem of constructing gravity integrands to that of calculating much simpler gauge-theory ones. For our calculation, a generalization [60] of the double-copy procedure has proven invaluable [161].

The analysis in Ref. [161] finds the first representation of an integrand for the five-loop

four-point amplitude of $\mathcal{N} = 8$ supergravity. The high power counting of that representation obstructs the necessary integral reductions needed to extract its ultraviolet behavior. Here we use similar generalized double-copy methods [60] to construct an improved integrand that enormously simplifies the integration. The key is starting with an improved gauge-theory integrand, which we build by constraining a manifest-power-counting ansatz via the method of maximal cuts. The needed unitarity cuts are easily obtained from the gauge-theory integrand of Ref. [162].

The earlier representation of the supergravity integrand, given in Ref. [161], is superficially (though not actually) quartically divergent in the dimension of interest. The new representation shifts these apparent quartic divergences to contributions that only mildly complicate the extraction of the underlying logarithmic divergences. Our construction proceeds as before except for small differences related to avoiding certain spurious singularities. The complete gauge and supergravity integrands can be found in plain-text ancillary files at the arXiv hosting of Ref. [3].

Recent advances in loop integration methods proved essential for solving the challenges posed by the calculation of ultraviolet divergences at five loops. Related issues appeared in the five-loop QCD beta function calculation, which was completed recently [163–165]. For supergravity, higher-rank-tensors related to the nature of the graviton greatly increase the number of terms while the absence of subdivergences dramatically simplifies the calculation. At high-loop orders the primary method for reducing loop integrals to a basis relies on integration-by-parts (IBP) identities [95, 166–174]. The complexity of such IBP systems tends to increase prohibitively with the loop order and the number of different integral types. Ideas from algebraic geometry provide a path to mitigating this problem by organizing them in a way compatible with unitarity methods [175–189]. We also simplify the problem by organizing the IBP identities in terms of an SL(5) symmetry of the five-loop integrals [108].

The final expression for the leading ultraviolet behavior is incredibly compact, and exposes, in conjunction with previous results [4, 6, 9, 61, 71, 146–148], simple and striking

patterns. Indeed, analysis of this leading ultraviolet behavior indicates the existence of potentially more powerful methods for making progress at higher loops.

This chapter is organized as follows. In Section 3.2, we review the generalized double-copy construction, as well as the underlying ideas including BCJ duality and the method of maximal cuts. We also summarize properties of the previously constructed five-loop four-point integrand of Ref. [161]. In Section 3.3, we construct new $\mathcal{N} = 4$ super-Yang–Mills and $\mathcal{N} = 8$ supergravity integrands with improved power-counting properties. Then, in Section 3.4 describe our procedure for expanding the integrands for large loop momenta, resulting in integrals with no external momenta, which we refer to as vacuum integrals. In Section 3.5, as a warm up to the complete integral reduction described in Section 3.6, we simplify the integration-by-parts system of integrals by assuming that the only contributing integrals after expanding in large loop momenta are those with maximal cuts. The results for the five-loop ultraviolet properties are given in these sections. In Section 3.7, by collecting known results for the leading ultraviolet behavior in terms of vacuum integrals we observe and comment on the intriguing and nontrivial consistency for such integrals between higher and lower loops. We present our conclusions in Section 3.8.

3.2 Review

The only known practical means for constructing higher-loop gravity integrands is the double-copy procedure that recycles gauge-theory results into gravity ones. Whenever gauge-theory integrands are available in forms that manifest the BCJ duality between color and kinematics [35, 36], the corresponding (super)gravity integrands are obtained by replacing color factors with the kinematic numerators of the same or of another gauge theory. Experience shows that it is sometimes difficult to find such representations of gauge-theory integrands. In some cases this can be overcome by increasing the power count of individual terms [190], or by introducing nonlocalities in integral coefficients [191]. Another possibility is to find

an integrand where BCJ duality holds on every cut, but does not hold with cut conditions removed [192]. Unfortunately, these ideas have not, as yet, led to a BCJ representation of the five-loop four-point integrand of $\mathcal{N} = 4$ super-Yang–Mills theory.

To avoid this difficulty, a generalized version of the BCJ double-copy construction has been developed. Although relying on the existence of BCJ duality at tree level, the generalized double-copy construction does not use any explicit representation of tree- or loop-level amplitudes that satisfies BCJ duality. It instead gives an algorithmic procedure which converts generic gauge-theory integrands into gravity ones [60]. This is used in Ref. [161] to construct an integrand for the five-loop four-point amplitude of $\mathcal{N} = 8$ supergravity.

In this section we give an overview of the ingredients and methods used in the construction of the five-loop integrand. We begin with a brief review of BCJ duality and the maximal-cut method which underlies and organizes the construction, and then proceed to reviewing the generalized double copy and associated formulae. We then summarize features of the previously constructed integrand [161] for the five-loop four-point amplitude of $\mathcal{N} = 8$ supergravity. In Section 3.3 we use the generalized double copy to find a greatly improved integrand for extracting ultraviolet properties, which we do in subsequent sections.

3.2.1 BCJ duality and the double copy

The BCJ duality [35, 36] between color and kinematics is a property of on-shell scattering amplitudes which has so far been difficult to discern in a Lagrangian formulation of Yang-Mills field theories [193, 194]. Nevertheless various tree-level proofs exist [195–200].

The first step to construct a duality-satisfying representation of amplitudes is to organize them in terms of graphs with only cubic (trivalent) vertices. This process works for any tree-level amplitude in any D-dimensional gauge theory coupled to matter fields. For the adjoint
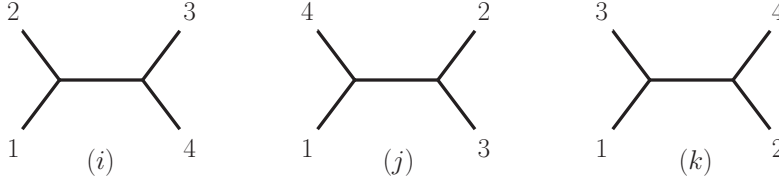
Figure 3.1: The three four-point diagrams participating in either color or numerator Jacobi identities.

representation case, an m-point tree-level amplitude may be written as

$$\mathcal{A}_m^{\text{tree}} = g^{m-2} \sum_j \frac{c_j n_j}{\prod_{\alpha_j} p_{\alpha_j}^2} \,, \tag{3.2}$$

where the sum is over the $(2m-5)!!$ distinct tree-level graphs with only cubic vertices. Such graphs are the only ones needed because the contribution of any diagram with quartic or higher-point vertices can be assigned to a graph with only cubic vertices by multiplying and dividing by appropriate propagators. The nontrivial kinematic information is contained in the kinematic numerators n_j; they generically depend on momenta, polarization, and spinors. The color factors c_j are obtained by dressing every vertex in graph j with the group theory structure constant, $\tilde{f}^{abc} = i\sqrt{2} f^{abc} = \text{Tr}([T^a, T^b]T^c)$, where the Hermitian generators of the gauge group are normalized via $\text{Tr}(T^a T^b) = \delta^{ab}$. The denominator is given by the product of the Feynman propagators of each graph j.

The kinematic numerators of an amplitude in a BCJ representation obey the same algebraic relations as the color factors [35, 36, 61, 201–204]. The key property is the requirement that all Jacobi identities obeyed by color factors are also obeyed by the kinematic numerators,

$$c_i + c_j + c_k = 0 \;\; \Rightarrow \;\; n_i + n_j + n_k = 0 \,, \tag{3.3}$$

where i, j, and k refer to three graphs which are identical except for one internal edge. Fig. 3.1 shows three basic diagrams participating in the Jacobi identity for color or numerator

64

factors. They can be embedded in a higher-point diagram. Furthermore, the kinematic numerators should obey the same antisymmetry under graph vertex flips as the color factors. A duality-satisfying representation of an amplitude can be obtained from a generic one through generalized gauge transformations—shifts of the kinematic numerators,

$$n_i \to n_i + \Delta_i \,, \tag{3.4}$$

which are constrained not to change the amplitude. When the duality is manifest, the kinematic Jacobi relations (3.3) express all kinematic numerators in terms of a small set of "master" numerators. While there is a fairly large freedom in choosing them, only the numerators of certain graphs can form such a basis.

Once gauge-theory tree amplitudes have been arranged into a form where the duality is manifest [35, 36], we obtain corresponding gravity amplitudes simply by replacing the color factors of one gauge-theory amplitude with the kinematic numerators of another gauge-theory amplitude,

$$c_i \;\to\; \tilde{n}_i \,, \tag{3.5}$$

as well as readjusting the coupling constants. This replacement gives the double-copy form of a gravity tree amplitude,

$$\mathcal{M}_m^{\text{tree}} = i \left(\frac{\kappa}{2}\right)^{m-2} \sum_j \frac{\tilde{n}_j n_j}{\prod_{\alpha_j} p_{\alpha_j}^2} \,, \tag{3.6}$$

where κ is the gravitational coupling and $\tilde{n}_j$ and n_j are the kinematic numerator factors of the two gauge theories. The gravity amplitudes obtained in this way depend on the specific input gauge theories. As discussed in Refs. [36, 193], Eq. (3.6) holds provided that at least one of the two amplitudes satisfies the duality (3.3) manifestly. The other may be in an arbitrary representation.

An earlier related version of the double-copy relation valid at tree level is the KLT

relations between gauge and gravity amplitudes [47]. Their general form in terms of a basis of gauge-theory amplitudes is,

$$\mathcal{M}_m^{\text{tree}} = i \left(\frac{\kappa}{2} \right)^{m-2} \sum_{\tau, \rho \in \mathcal{S}_{m-3}} K(\tau|\rho) \tilde{A}_m^{\text{tree}} \left(1, \rho_2, \ldots, \rho_{m-2}, m, (m-1) \right)$$

$$\times A_m^{\text{tree}} \left(1, \tau_2, \ldots, \tau_{m-2}, (m-1), m \right) . \tag{3.7}$$

Here the A_m^{tree} are color-ordered tree amplitudes with the indicated ordering of legs and the sum runs over $(m-3)!$ permutations of external legs. The KLT kernel K is a matrix with indices corresponding to the elements of the two orderings of the relevant partial amplitudes. It is also sometimes referred to as the momentum kernel. Compact representations of the KLT kernel are found in Refs. [49, 195–200, 205].

At loop-level, the duality between color and kinematics (3.3) remains a conjecture [36], although evidence continues to accumulate [43, 61, 120, 190–192, 206–211]. As at tree level, loop-level amplitudes in a gauge theory coupled to matter fields in the adjoint representation can be expressed as a sum over diagrams with only cubic (trivalent) vertices:

$$\mathcal{A}_m^{L\text{-loop}} = i^L g^{m-2+2L} \sum_{\mathcal{S}_m} \sum_j \int \prod_{l=1}^{L} \frac{d^D p_l}{(2\pi)^D} \frac{1}{S_j} \frac{c_j n_j}{\prod_{\alpha_j} p_{\alpha_j}^2} . \tag{3.8}$$

The first sum runs over the set $\mathcal{S}_m$ of $m!$ permutations of the external legs. The second sum runs over the distinct L-loop m-point graphs with only cubic vertices; as at tree level, by multiplying and dividing by propagators it is trivial to absorb numerators of contact diagrams that contain higher-than-three-point vertices into numerators of diagrams with only cubic vertices. The symmetry factor S_j counts the number of automorphisms of the labeled graph j from both the permutation sum and from any internal automorphism symmetries. This symmetry factor is not included in the kinematic numerator.

The generalization of BCJ duality to loop-level amplitudes amounts to demanding that all diagram numerators obey the same algebraic relations as the color factors [36]. The Jacobi

identities are implemented by embedding the three diagrams in Fig. 3.1 into loop diagrams in all possible ways and demanding that identities of the type in Eq. (3.3) hold for the loop-level numerators as well. In principle, given any representation of an amplitude, one may attempt to construct a duality-satisfying one by modifying the kinematic numerators through generalized gauge transformations (3.4); however, a more systematic approach is to start with an ansatz exhibiting certain desired properties and impose the kinematic Jacobi relations. As at tree level, when the duality is manifest all kinematic numerators are expressed in terms of those of a small number of "master diagrams" [61, 191].

Just like with tree numerators, once gauge-theory numerator factors which satisfy the duality are available, replacing the color factors by the corresponding numerator factors (3.5) yields the double-copy form of gravity loop integrands,

$$\mathcal{M}_m^{L\text{-loop}} = i^{L+1} \left(\frac{\kappa}{2}\right)^{m-2+2L} \sum_{\mathcal{S}_m} \sum_j \int \prod_{l=1}^{L} \frac{d^D p_l}{(2\pi)^D} \frac{1}{S_j} \frac{\tilde{n}_j n_j}{\prod_{\alpha_j} p_{\alpha_j}^2}, \qquad (3.9)$$

where $\tilde{n}_j$ and n_j are gauge-theory numerator factors. The theories to which the gravity amplitudes belong are dictated by the choice of input gauge theories.

Thus, the double-copy construction reduces the problem of constructing loop integrands in gravitational theories to the problem of finding BCJ representations of gauge-theory amplitudes.[2] Apart from offering a simple means for obtaining loop-level scattering amplitudes in a multitude of (super)gravity theories, the double-copy construction has also been applied to the construction of black-hole and other classical solutions [62, 63, 212–215] including those potentially relevant to gravitational-wave observations [64–66, 216–218], corrections to gravitational potentials [219–221], and the relation between symmetries of supergravity and gauge theory [87, 222–231]. The duality underlying the double copy has also been identified in a wider class of quantum field and string theories [205, 232–247], including those with

---

[2]Through four loops, there exist BCJ representations of $\mathcal{N} = 4$ super-Yang–Mills amplitudes that exhibit the same graph-by-graph power counting as the complete amplitude, *i.e.* all ultraviolet cancellations are manifest. It is an interesting open problem whether this feature will continue at higher loops.
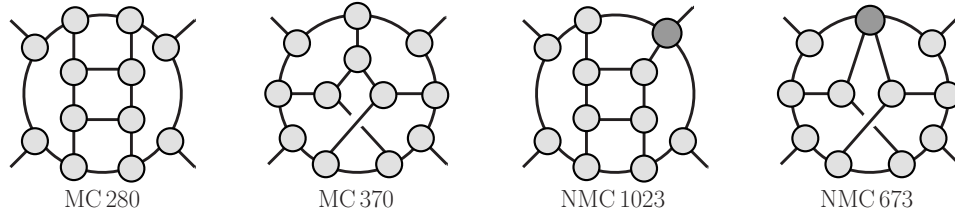
Figure 3.2: Sample maximal and next-to-maximal cuts. The exposed lines connecting the blobs are taken to be on shell delta-functions.

fundamental representation matter [88, 89]. For recent reviews, see Ref. [201–204].

When it turns out to be difficult to find a duality-satisfying representation of a gauge-theory amplitude, as in the case for the five-loop four-point amplitude of $\mathcal{N} = 8$ supergravity, an alternative method is available. We use the generalized double-copy procedure [60] that relies only on the existence of duality-consistent properties at tree-level. This type of approach may also potentially aid applications of BCJ duality to problems in classical gravity.

3.2.2 Method of maximal cuts

The generalized double-copy construction of Refs. [60, 161] relies on the interplay between the method of maximal cuts [160] and tree-level BCJ duality. The maximal-cut method is a refinement of the generalized-unitarity method [156–159], designed to construct the integrand from the simplest set of generalized unitarity cuts. In the generalized double-copy approach we apply the maximal-cut method in a constructive way, assigning missing contributions to new higher-vertex contact diagrams as necessary.

In both gauge and gravity theories, the method of maximal cuts [160] constructs multiloop integrands from generalized-unitarity cuts that decompose loop integrands into products of tree amplitudes,

$$\mathcal{C}^{\mathrm{N}^k\mathrm{MC}} = \sum_{\text{states}} \mathcal{A}^{\text{tree}}_{m(1)} \cdots \mathcal{A}^{\text{tree}}_{m(p)} \,, \qquad\qquad k \equiv \sum_{i=1}^{p} m(i) - 3p \,, \qquad (3.10)$$
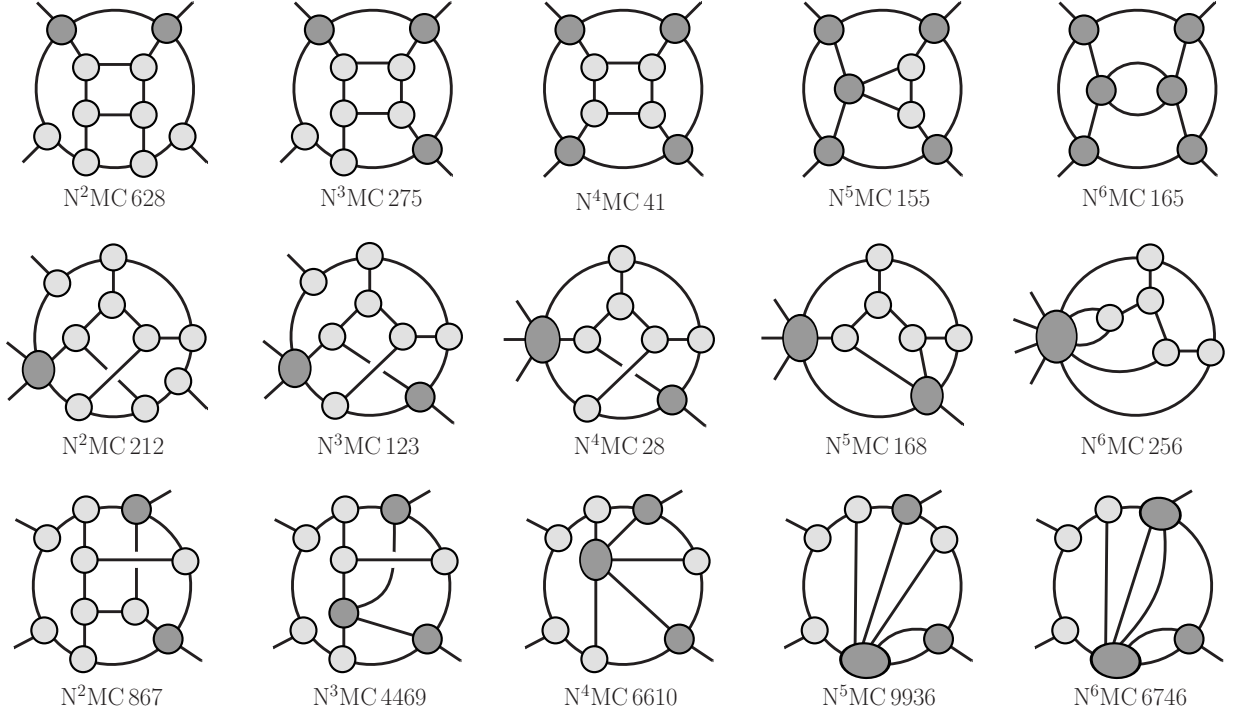
Figure 3.3: Sample N^kMCs used in the construction of five-loop four-point amplitudes. The exposed lines connecting the blobs are taken to be on-shell delta-functions.

where the $\mathcal{A}^{\text{tree}}_{m(i)}$ are tree-level $m(i)$-multiplicity amplitudes corresponding to the blobs illustrated for various five-loop examples in Figs. 3.2 and 3.3. We organize these cuts according to levels that correspond to the number k of internal propagators that remain off shell.

When constructing gauge-theory amplitudes, we use tree amplitudes directly as in Eq. (3.10). For $\mathcal{N} = 4$ super-Yang–Mills it is very helpful to use a four-dimensional on-shell superspace [248] to organize the state sums [249, 250]. Some care is needed to ensure that the obtained expressions are valid in D dimensions, either by exploiting cuts whose supersums are valid in $D \leq 10$ dimensions [149, 162] or using six-dimensional helicity [251–253]. Once we have one version of a gauge-theory integrand, we can avoid re-evaluating the state sums to find new representations, simply by using the cuts of the previously constructed integrand instead of Eq. (3.10) to construct target expressions. In the same spirit, for $\mathcal{N} = 8$ supergravity we can always bypass Eq. (3.10) by making use of the KLT tree relations (3.7). The state sums also factorize allowing us to express the $\mathcal{N} = 8$ supergravity cuts directly in terms

of color-order $\mathcal{N} = 4$ super-Yang–Mills cuts. (See Section 2 of Ref. [161] for further details).

Figs. 3.2 and 3.3 give examples of cuts used in the construction of the integrands of five-loop four-point amplitudes. At the maximal-cut (MC) level, e.g. the first two diagrams of Fig. 3.2, the maximum number of internal lines are placed on shell and all tree amplitudes appearing in Eq. (3.10) are three-point amplitudes. At the next-to-maximal-cut (NMC) level, e.g. the third and fourth diagrams of Fig. 3.2, all except one internal line are placed on shell shell; all tree amplitudes are three-point amplitudes except one which is a four-point amplitude. Similarly, for an N2, two internal lines are kept off shell and so forth, as illustrated in Fig. 3.3.

In the method of maximal cuts, integrands for loop amplitudes are obtained by first finding an integrand whose maximal cuts reproduce the direct calculation of maximal cuts in terms of sums of products of three-point tree-level amplitudes. This candidate integrand is then corrected by adding to it contact terms such that all NMCs are correctly reproduced and systematically proceeding through the next^k-maximal cuts (Nks), until no further corrections are necessary. The level where this happens is determined by the power counting of the theory and by choices made at earlier levels. For example, for five-loop amplitudes in $\mathcal{N} = 4$ super-Yang–Mills theory, cuts through the N3 level are needed, though as we describe in the next section, it is useful to skip certain ill-defined cuts at the N2 and N3 level and then recover the missing information by including instead certain N4 level cuts. For the four-point $\mathcal{N} = 8$ supergravity amplitude at the same loop order, cuts through the N6 level are necessary. In general, it is important to evaluate more cuts than the spanning set (necessary for constructing the amplitude) to gain nontrivial crosschecks of the results. For example, in Ref. [161] all N7 cuts and many N8 cuts were checked, confirming the construction.

To make contact with color/kinematics-satisfying representations of gauge-theory amplitudes it is convenient to absorb all contact terms into diagrams with only cubic vertices [4, 6, 9, 61, 71, 146–148, 190, 192]. For problems of the complexity of the five-loop supergravity integrand, however, it can be more efficient to assign each new contribution of an

Figure 3.4: New contribution found via the method of maximal cuts can be assigned to contact terms. The labels (X:Y) correspond to the labeling of Ref. [161] and refer to the level and contact diagram number.

Nk to a contact diagram instead of to parent diagrams, consisting of ones with only cubic vertices. These new contributions are, by construction, contact terms—they contain only the propagators of the graph with higher-point vertices—because any contribution that can resolve these vertices into propagator terms is already accounted for at earlier levels. In this organization each new contact diagram can be determined independently of other contact diagrams at the same level and depends only on choices made at previous levels. More explicitly, as illustrated in Fig. 3.4, a new contribution arising from an Nk is assigned to a contact diagram obtained from that cut by replacing the blobs representing tree-level amplitudes by vertices with the same multiplicity. The contact terms should be taken off shell by removing the cut conditions in a manner that reflects the diagram symmetry. Off-shell continuation necessarily introduces an ambiguity since it is always possible to include terms proportional to the inverse propagators that vanish by the cut condition; such ambiguities can be absorbed into contact terms at the next cut level.

3.2.3 Generalized double-copy construction

Whenever gauge-theory amplitudes are available in a form that obeys the duality between color and kinematics, the BCJ double-copy construction provides a straightforward method of obtaining the corresponding (super)gravity amplitudes. If a duality-satisfying representation is expected to exist but is nonetheless unavailable, the generalized double-copy construction supplies the additional information necessary for finding the corresponding

(super)gravity amplitude. Below we briefly summarize this procedure. A more thorough discussion can be found in Ref. [161].

The starting point of the construction is a "naive double copy" of two (possibly distinct) gauge-theory amplitudes written in terms of cubic diagrams obtained by applying the double-copy substitution (3.5) to these amplitudes despite none of them manifesting the BCJ duality between color and kinematics. While the resulting expression is not a (super)gravity amplitude, it nonetheless reproduces the maximal and next-to-maximal cuts of the desired (super)gravity amplitude as the three- and four-point tree-level amplitudes entering these cuts obey the duality between color and kinematics. Contact term corrections are necessary to satisfy the Nk with $k \geq 2$; the method of maximal cuts can be used to determine them. For N2 and N3 at five loops, whose associated contact terms are the most complicated [156–159, 162], it is advantageous to obtain these corrections using formulas that express the cuts in terms of violations of the BCJ relations (3.3).

The existence of BCJ representations at tree level implies that representations should exist for all cuts of gauge-theory amplitudes that decompose the loop integrand into products of tree amplitudes to any loop order. This further suggests that the corresponding cuts of the gravity amplitude can be expressed in double-copy form,

$$\mathcal{C}_{\text{GR}} = \sum_{i_1,\ldots,i_q} \frac{n^{\text{BCJ}}_{i_1,i_2,\ldots i_q} \tilde{n}^{\text{BCJ}}_{i_1,i_2,\ldots i_q}}{D^{(1)}_{i_1} \ldots D^{(q)}_{i_q}}, \tag{3.11}$$

where the n^{BCJ} and $\tilde{n}^{\text{BCJ}}$ are the BCJ numerators associated with each of the two copies. In this expression the cut conditions are understood as being imposed on the numerators. Each sum runs over the diagrams of each blob and $D^{(m)}_{i_m}$ are the product of the uncut propagators associated to each diagram of blob m. This notation is illustrated in Fig. 3.5 for an N2. In this figure, each of the two four-point blobs is expanded into three diagrams, giving a total of nine diagrams. For example, the indices $i_1 = 1$ and $i_2 = 1$ refers to the five-loop diagram produced by taking the first diagram from each blob and connecting it to the remaining parts

$$(0 \colon 366) \to n_{1,1} \qquad (0 \colon 342) \to n_{1,2} \qquad (0 \colon 307) \to n_{1,3}$$

$$(0 \colon 298) \to n_{2,1} \qquad (0 \colon 346) \to n_{2,2} \qquad (0 \colon 366) \to n_{2,3}$$

$$(0 \colon 346) \to n_{3,1} \qquad (0 \colon 286) \to n_{3,2} \qquad (0 \colon 342) \to n_{3,3}$$

$\text{N}^2\text{MC}\,867$
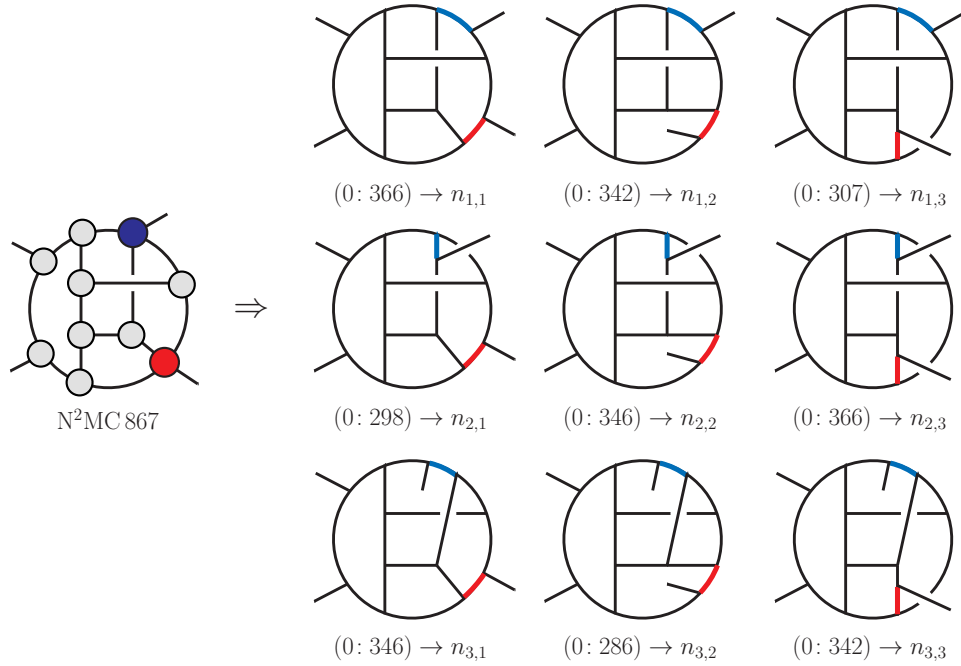
Figure 3.5: An example illustrating the notation in Eq. (3.11). Expanding each of the two four-point blob gives a total of nine diagrams. The label N2 867 refer to 867th diagram of the 2nd level cuts, and the $n_{i,j}$ correspond to labels used in the cut. The shaded thick (blue and red) lines are the propagators around which BCJ discrepancy functions are defined.

of the five-loop diagram. The denominators in Eq. (3.11) correspond to the thick (colored) lines in the diagrams.

The BCJ numerators in Eq. (3.11) are related [36, 193] to those of an arbitrary representation by a generalized gauge transformation (3.4); the shift parameters follow the same labeling scheme as the numerators themselves,

$$n_{i_1,i_2,\ldots i_q} \;\; = \;\; n^{\text{BCJ}}_{i_1,i_2,\ldots i_q} + \Delta_{i_1,i_2,\ldots i_q} \,. \tag{3.12}$$

The shifts $\Delta_{i_1,i_2,\ldots i_q}$ are constrained to leave the corresponding cuts of the gauge-theory amplitude unchanged. Using such transformations we can reorganize a gravity cut in terms of cuts of a naive double copy and an additional contribution,

$$\mathcal{C}_{\text{GR}} = \sum_{i_1,\ldots,i_q} \frac{n_{i_1,i_2,\ldots i_q}\tilde{n}_{i_1,i_2,\ldots i_q}}{D^{(1)}_{i_1} \ldots D^{(q)}_{i_q}} + \mathcal{E}_{\text{GR}}\left(\Delta\right) \,, \tag{3.13}$$

where the cut conditions are imposed on the numerators. Rather than expressing the correction $\mathcal{E}_{\text{GR}}$ in terms of the generalized-gauge-shift parameters, it is useful to re-express the correction terms as bilinears in the violations of the kinematic Jacobi relations (3.3) by the generic gauge-theory amplitude numerators. These violations are known as BCJ discrepancy functions.

As an example, the cut in Fig. 3.5 is composed of two four-point tree amplitudes and the rest are three-point amplitudes. For any cut of this structure, two four-point trees connected to any number of three-point trees, the correction has a simple expression,

$$\mathcal{E}^{4\times 4}_{\text{GR}} = -\frac{1}{d^{(1,1)}_1 d^{(2,1)}_1}\left(J_{\bullet,1}\tilde{J}_{1,\bullet} + J_{1,\bullet}\tilde{J}_{\bullet,1}\right), \tag{3.14}$$

where $d_i^{(b,p)}$ is the pth propagator of the ith diagram inside the bth blob and

$$J_{\bullet,i_2} \equiv \sum_{i_1=1}^{3} n_{i_1 i_2}\,, \qquad J_{i_1,\bullet} \equiv \sum_{i_2=1}^{3} n_{i_1 i_2}\,, \qquad \tilde{J}_{\bullet,i_2} \equiv \sum_{i_1=1}^{3} \tilde{n}_{i_1 i_2}\,, \qquad \tilde{J}_{i_1,\bullet} \equiv \sum_{i_2=1}^{3} \tilde{n}_{i_1 i_2}\,. \quad (3.15)$$

are BCJ discrepancy functions. Notably, these discrepancy functions vanish whenever the numerators involved satisfy the BCJ relations, even if the representation as a whole does not satisfy them. Such expressions are not unique and can be rearranged using various relations between Js [60, 161, 254, 255]. For example, an alternative version, equivalent to Eq. (3.14), is

$$\mathcal{E}_{\mathrm{GR}}^{4\times4} = -\frac{1}{9} \sum_{i_1,i_2=1}^{3} \frac{1}{d_{i_1}^{(1,1)} d_{i_2}^{(2,1)}} \left(J_{\bullet,i_2} \tilde{J}_{i_1,\bullet} + J_{i_1,\bullet} \tilde{J}_{\bullet,i_2} \right). \quad (3.16)$$

Similarly, a cut with a single five-point tree amplitude and the rest three-point tree amplitudes is given by

$$\mathcal{C}_{\mathrm{GR}}^{5} = \sum_{i=1}^{15} \frac{n_i \tilde{n}_i}{d_i^{(1)} d_i^{(2)}} + \mathcal{E}_{\mathrm{GR}}^{5} \qquad \text{with} \qquad \mathcal{E}_{\mathrm{GR}}^{5} = -\frac{1}{6} \sum_{i=1}^{15} \frac{J_{\{i,1\}} \tilde{J}_{\{i,2\}} + J_{\{i,2\}} \tilde{J}_{\{i,1\}}}{d_i^{(1,1)} d_i^{(1,2)}}\,, \quad (3.17)$$

where $J_{\{i,1\}}$ and $J_{\{i,2\}}$ are BCJ discrepancy functions associated with the first and second propagator of the ith diagram. (See Ref. [161] for further details.)

As the cut level k increases the formulas relating the amplitudes' cuts with the cuts of the naive double copy become more intricate, but the basic building blocks remain the BCJ discrepancy functions. The formulas often enormously simplify the computation of the contact term corrections and are especially helpful at five loops at the N2 and N3 level, where calculating the contact terms via the maximal-cut method can be rather involved. Beyond this level the contact terms become much simpler due to a restricted dependence on loop momenta and are better dealt with using the method of maximal cuts and KLT relations [47], as described in Ref. [161].
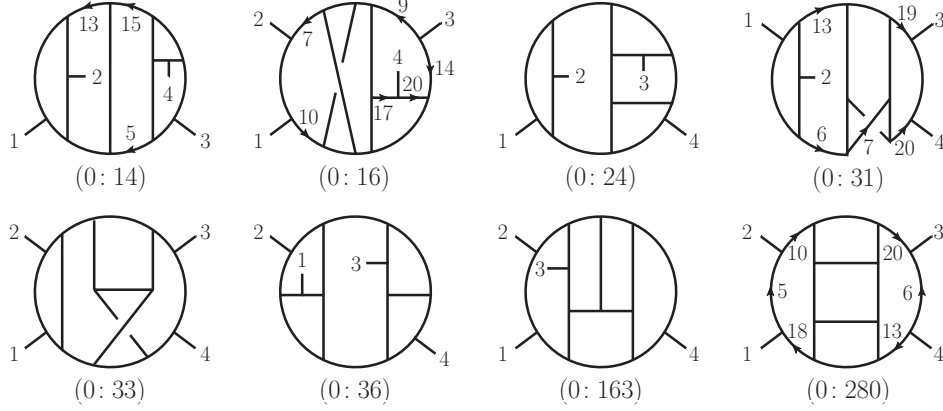
Figure 3.6: Sample graphs for the five-loop four-point $\mathcal{N} = 4$ super-Yang–Mills amplitude. The graph labels correspond to the ones in Ref. [161] and here.

3.2.4 Previously Constructed Five-Loop Four-Point Integrands

Five-loop four-point integrands have previously been constructed for $\mathcal{N} = 4$ super-Yang–Mills [162] and $\mathcal{N} = 8$ supergravity [161]. Here we review some of their properties which serve as motivation for the construction in Section 3.3 of new $\mathcal{N} = 4$ super-Yang–Mills and $\mathcal{N} = 8$ supergravity integrands with better manifest ultraviolet properties.

The five-loop four-point integrand of $\mathcal{N} = 8$ supergravity constructed in Ref. [161] is obtained through the generalized double-copy procedure, starting from a slightly modified form of the corresponding $\mathcal{N} = 4$ super-Yang–Mills integrand of Ref. [162]. This modified super-Yang–Mills representation is given explicitly in an ancillary file of Ref. [161].

All representations of the five-loop four-point $\mathcal{N} = 4$ super-Yang–Mills amplitude that we use contain solely diagrams with only cubic (trivalent) vertices, so can be written using Eq. (3.8) as

$$\mathcal{A}_4^{(5)} = i g^{12} s t A_4^{\text{tree}} \sum_{\mathcal{S}_4} \sum_{i=1}^{N_D} \int \prod_{j=5}^{9} \frac{d^D \ell_j}{(2\pi)^D} \frac{1}{S_i} \frac{c_i \, N_i}{\prod_{m_i=5}^{20} \ell_{m_i}^2} \,, \tag{3.18}$$

where we have explicitly extracted an overall crossing symmetric prefactor of $s t A_4^{\text{tree}}$ from the kinematic numerators when compared to Eq. (3.8). The gauge coupling is g, the color-ordered D-dimensional tree amplitude is $A_4^{\text{tree}} \equiv A_4^{\text{tree}}(1, 2, 3, 4)$, and $s = (k_1 + k_2)^2$ and

$t = (k_2 + k_3)^2$ are the standard Mandelstam invariants. We denote external momenta by k_i with $i = 1, \ldots, 4$ and the five independent loop momenta by ℓ_j with $j = 5, \ldots, 9$. The remaining momenta ℓ_j with $10 \leq j \leq 20$ of internal lines are linear combinations of the five independent loop momenta and external momenta. As always, the color factors c_i of all graphs are obtained by dressing every three-vertex in the graph with a factor of $\tilde{f}^{abc}$.

The number N_D of diagrams that we include depends on the particular representation we choose. The form given in Ref. [162] has 416 diagrams, while the one used in Ref. [161] has 410 diagrams. Some sample graphs from this list of 410 diagrams are shown in Fig. 3.6.

It is useful to inspect some of the numerators associated with the sample diagrams. Choosing as examples diagrams 14, 16, 31 and 280 from the 410 diagram representation of Ref. [161], we have the $\mathcal{N} = 4$ super-Yang–Mills numerators

$$N_{14} = s\left(s^2 s_{3,5} - \frac{5}{2}\ell_5^2 \ell_{13}^2 \ell_{15}^2\right),$$
$$N_{16} = -s\left(s^3 + s^2\tau_{3,15} - \frac{3}{2}s\ell_7^2\ell_{10}^2 + \frac{3}{2}\ell_7^2\ell_{10}^2(\tau_{1,15} + \tau_{2,15} + \tau_{4,15} + \ell_9^2 - \ell_{14}^2 - \ell_{17}^2 + \ell_{20}^2)\right),$$
$$N_{31} = s\left(s\left(-s^2 - \ell_{13}^2\ell_{20}^2 + s(\tau_{6,19} + \ell_{13}^2 + \frac{1}{2}\ell_{20}^2) + \ell_6^2(\ell_{20}^2 - \ell_{19}^2)\right) - \frac{1}{2}\ell_6^2\ell_7^2\ell_{19}^2\right),$$
$$N_{280} = s^4 + s^3(\tau_{10,13} + \tau_{18,20}) + \frac{1}{2}s^2(\tau_{10,13}^2 + \tau_{18,20}^2) + 2t(\ell_5^2 + \ell_6^2)(\ell_{13}^2\ell_{18}^2 + \ell_{10}^2\ell_{20}^2), \quad (3.19)$$

where s and t are the usual Mandelstam invariants and

$$s_{i,j} = (\ell_i + \ell_j)^2, \qquad\qquad \tau_{i,j} = 2\ell_i \cdot \ell_j. \qquad\qquad (3.20)$$

The corresponding naive double-copy numerators are obtained by simply squaring these expressions.

The $\mathcal{N} = 8$ integrand found in Ref. [161] suffers from poor graph-by-graph power counting, which obstructs the extraction of its leading ultraviolet behavior. Many of its diagrams in the naive double-copy part contain spurious quartic power divergences in $D = 24/5$, which are equivalent to logarithmic divergences in $D = 4$. As discussed in [139–144], such

divergences are spurious and should cancel out. The difficulties raised by the spurious power counting are two fold. First, we will see in Section 3.4 that their presence causes a rapid growth in the number of terms in the series expansion of the integrand necessary to isolate the potential logarithmic divergence in $D = 24/5$. Second, this expansion yields graphs with propagators raised to a high power, which leads to an IBP system with billions of integrals.

There are two distinct ways to overcome these difficulties. The first is to construct a new super-Yang–Mills integrand which improves the power counting of the naive double copy. This in turn minimizes the number of integrals and equations in the full IBP system. We will give the construction of this new representation of the $\mathcal{N} = 4$ super-Yang–Mills integrand as well as of the $\mathcal{N} = 8$ supergravity integrand that follows from it in the next section. This represents a complete solution. Still it is useful to have a separate check. Our second resolution is to make simplifying assumptions on the type of integrals that can contribute to the final result after applying IBP integral identities. This approach will be discussed in Section 3.5 and will allow us to integrate the more complicated integrand of Ref. [161]. The agreement between the results of these two approaches represents a highly non-trivial confirmation of both the integrands and the integration procedure.

3.3   Improved integrands

In this section we describe the construction of a new form of the five-loop four-point integrand for $\mathcal{N} = 4$ super-Yang–Mills theory and then use it to construct an improved $\mathcal{N} = 8$ supergravity integrand. The $\mathcal{N} = 8$ integrand we obtain still exhibits power divergences in $D = 24/5$ but, as we shall see, their structure is such that they do not lead to a dramatic increase in the number of integrals needed for the extraction of the leading logarithmic ultraviolet behavior of the amplitude. In Section 3.6 we extract the ultraviolet properties using this improved $\mathcal{N} = 8$ five-loop integrand without making any assumptions on the final form of the large-loop momentum integrals.
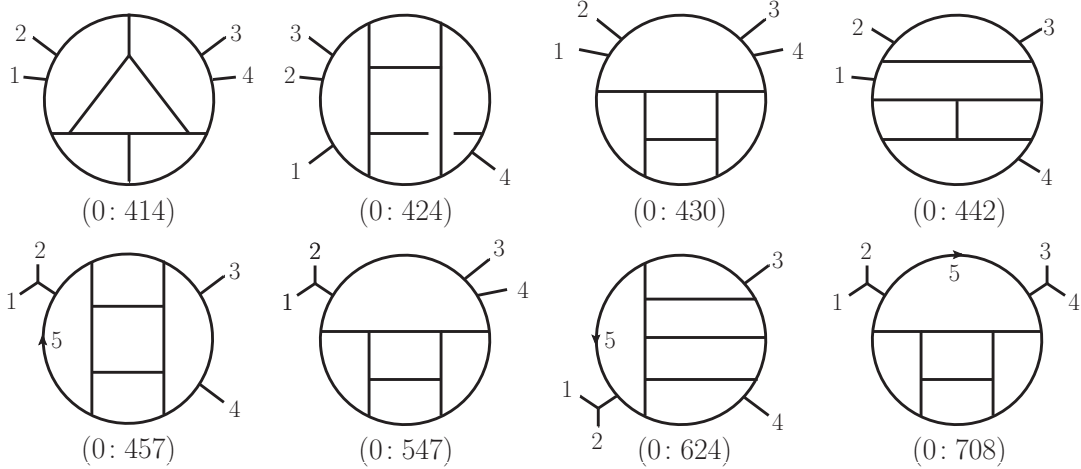
Figure 3.7: Some of the additional graphs for the improved representation of the integrand of the five-loop four-point $\mathcal{N} = 4$ super-Yang–Mills amplitude. These graphs were not needed in earlier constructions [161, 162]. The labeling scheme is to the contact level and then the diagram number corresponding to the labels of the ancillary files of Ref. [3].

3.3.1 Construction of improved $\mathcal{N} = 4$ super-Yang–Mills integrand

The key power-counting requirement we demand of every term of the improved Yang–Mills representation is that its naive double copy, as described in Section 3.2, has no worse than a logarithmic divergence in $D = 24/5$. This translates to a representation with no more than four powers of loop momenta in the kinematic numerator of any one-particle-irreducible diagram. These conditions require us to introduce new diagrams of the type illustrated in Fig. 3.7. These graphs are characterized by the vanishing of their maximal cuts. For these diagrams, this implies that the poles due to the propagators independent of loop momenta (to which we will refer to as "dangling trees") are spurious. It also turns out that their numerators have fewer than four powers of loop momenta. Such dangling tree diagrams are crucial for obtaining ultraviolet-improved supergravity expressions via the generalized double-copy procedure. The general pattern is that, to improve the double-copy expression, the terms with the highest power counting in the super-Yang–Mills integrand should come from diagrams with dangling trees. Due to the reduced number of possible loop-momentum

79

factors in their kinematic numerators, the squaring of the numerator (naive double copy) of such diagrams keeps the superficial power counting under control.

To construct such a representation of the five-loop four-point $\mathcal{N} = 4$ super-Yang–Mills integrand we apply the maximal-cut method to an ansatz that has the desired power counting properties. Inspired by the structure of the lower-loop amplitudes [36, 61, 145, 256] we further simplify the ansatz and improve the power-counting properties of the naive double copy by imposing the following constraints:

- Each numerator is a polynomial of degree eight in momenta, of which no more than four can be loop momenta.

- Every term in every numerator contains at least one factor of an external kinematic invariant, s or t.

- No diagram contains a one-loop tadpole, bubble or triangle subdiagram. Also, two-point two- and three-loop subdiagrams, and three-point two-loop subdiagrams, are excluded.

- For each one-loop n-gon the maximum power of the corresponding loop momentum is $n - 4$. In particular, this means that numerators do not depend on the loop momenta of any box subdiagrams.

- Diagram numerators respect the diagram symmetries.

- The external state dependence is included via an overall factor of the tree amplitude.

Such simplifying conditions can always be imposed as long as the system of equations resulting from matching the cuts of the ansatz with those of the amplitude still has solutions. The conditions above turn out to be incompatible with a representation where BCJ duality holds globally on the fully off-shell integrand. They are nevertheless compatible with all two-term kinematic Jacobi relations (meaning where one of the three numerators of the Jacobi relation (3.3) vanishes by the above constraints), which we impose *a posteriori*:

- The solution to cut conditions is such that the ansatz obeys all two-term kinematic Jacobi relations.

Similarly with the earlier representation of the five-loop four-point $\mathcal{N} = 4$ super-Yang–Mills amplitude, we organize the integrand in terms of diagrams with only cubic vertices; the numerators have the structure shown in Eq. (3.18). In the present case we have 752 diagrams. The first 410 diagrams are the same as for the previous integrand [161], some of which are displayed in Fig. 3.6. There are an additional 342 diagrams, a few of which are displayed in Fig. 3.7. In addition to the dangling tree graphs discussed above, this includes other diagrams such the ones on the first line of Fig. 3.7.

For each diagram we write down an ansatz for the N_i which is a polynomial of fourth degree in the independent kinematic invariants, subject to the constraints above. Each independent term is assigned an arbitrary parameter. This ansatz is valid for all external states, as encoded in the overall tree-level amplitude factor in Eq. (3.18). This simple dependence on external states is expected only for the four-point amplitudes.[3] The most general ansatz that obeys the first four constraints above has $535,146$ terms; requiring that each numerator respects the graph's symmetries and also imposing the maximal cuts of the amplitude reduces this to a more managable size.

The parameters of the ansatz are determined via the method of maximal cuts. Rather than constructing unitarity cuts directly from their definition as products of tree-level amplitudes, it is far more convenient to use the previously constructed versions [161, 162] of the amplitude integrand as input. This approach circumvents the need for supersymmetric state sums [249, 250] (which become nontrivial at high-loop orders and in arbitrary dimensions) and recycles the simplifications which have already been carried out for the construction of that integrand. Moreover, it makes full use of the D-dimensional validity of that integrand, which is confirmed in Ref. [162].

---

[3] For higher-point amplitudes the necessary ansatz is more involved [191] and it will not exhibit a clean separation between external state data and loop kinematics.
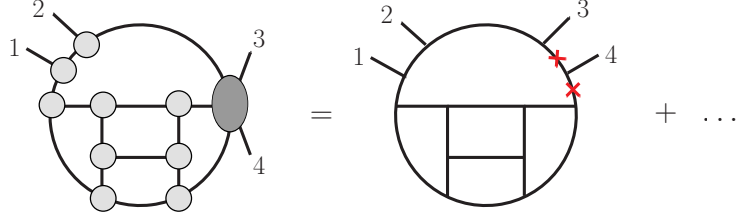
Figure 3.8: This cut is not considered as it contains a singular diagram; instead we recover the missing information from higher level cuts. The shaded (red) "×" mark complete propagators (not replaced by delta functions), the other exposed propagators are all placed on shell (replaced by delta functions).

The maximal cuts impose simple constraints on the free parameters; it is convenient to replace them in the ansatz. Next, NMC conditions are solved; as their solution is quite involved, it is impractical to plug it back directly into the ansatz. To proceed, we introduce the notion of a presolution of a given Nk as the solution of all constraints imposed by all lower-level cuts which overlap with the given cut. The advantage of using presolutions is that they account for a large part of the lower-level cut constraints on the parameters entering the given cut without the complications ensuing from simultaneously solving all the lower-level cut conditions and replacing the solution in the ansatz. Thus, instead of simultaneously solving all the NMC cut constraints and evaluating the ansatz on the solution before proceeding to the N2 cuts, we construct all the N2 presolutions and then solve each of them simultaneously with the N2 cut condition. We proceed recursively in this way through all relevant cut levels. The integrand of the amplitude is then found by simultaneously resolving all the new constraints on the parameters of the ansatz derived at each level. While this is equivalent to adding contact terms, the ansatz approach effectively distributes them in the diagrams of the ansatz and prevents the appearance of any terms with artificially high power count.

In carrying out this application of the method of maximal cuts we encounter a technical complication with diagrams with four-loop bubble subdiagrams, three of which are illustrated in Fig. 3.7: $(0:430)$, $(0:547)$ and $(0:708)$. The main difficulty stems from the fact that both
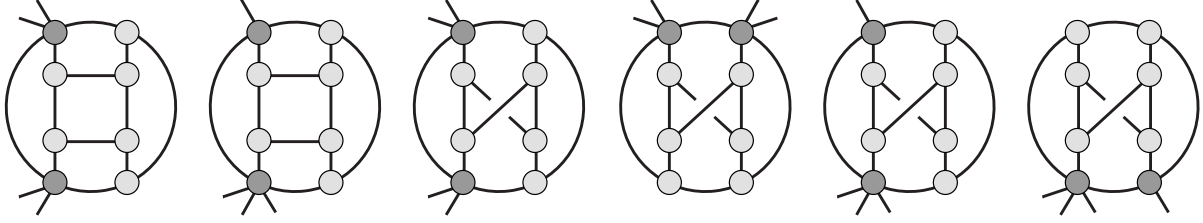
Figure 3.9: The list of additional N^{4}MCs that are needed to fix the diagrams with doubled propagators.

propagators connecting the bubble to the rest of the diagram carry the same momentum so the diagram effectively exhibits a doubled propagator. While such double propagators are spurious and can in principle be algebraically eliminated since the representations of Refs. [161, 162] does not have them, they nevertheless make difficult the evaluation of the cuts. It moreover turns out that, with our strict power counting requirements, there is no solution that explicitly eliminates the double poles from all diagrams, even though they cancel in all cuts. Such graphs cause certain cuts to be ill-defined without an additional prescription. Indeed, if only one of the two equal-momentum propagators is cut the tree amplitude containing the second one becomes singular unless a specific order of limits is taken. This phenomenon is illustrated in Fig. 3.8; by replacing the propagator on one side of the bubble subdiagram with an on-shell delta-function, the propagator on the other side, marked by a shaded (red) "×", becomes singular.

One can devise a prescription that realizes the expected cancellation of such 1/0 terms among themselves. It is, however, more convenient to simply skip the singular cuts altogether and recover the missing information from higher-level cuts that overlap with the skipped ones (*i.e.* cuts in which the doubled propagator is not cut). In the absence of doubled propagators, cuts through N3 level contain all the information necessary for the construction of the amplitude, as seen in [161], because the power counting of the theory implies that numerators can have at most three inverse propagators and thus there can be at most N^3 contact terms. In our case, to recover cut constraints absent due to the unevaluated singular

cuts we must include certain N4 cuts; the complete list is shown in Fig. 3.9. All other N4 as well as some N5 cuts serve as consistency checks of our construction.

Our new representation for the five-loop four-point integrand is given in an ancillary file at the arXiv hosting of Ref. [3]. Generalized gauge invariance implies that there is no unique form of the integrand; indeed, the global solution of the cut conditions and of the two-term Jacobi relations leaves 10607 free parameters. They "move" terms between diagrams without affecting any of the unitarity cuts. These parameters should not affect any observable; in particular, they should drop out of the gravity amplitude (after nontrivial algebra) resulting from the generalized double-copy construction based on this amplitude. To simplify the expressions we set them to zero.

It is instructive to see how the power counting of the new representation differs from that of the previous one [161]. Setting the free parameters to zero, the counterparts of the numerators N_{14}, N_{16}, N_{31} and N_{280} shown for the previous representation in Eq. (3.19) are

$$
\begin{aligned}
N_{14} &= \frac{1}{2} s^3 \left(\tau_{3,5} - \tau_{4,5} - s \right) , \\
N_{16} &= N_{14} , \\
N_{31} &= \frac{1}{2} s^3 \left(\tau_{1,5} + \tau_{1,6} + \tau_{2,5} + \tau_{2,6} + 2\tau_{3,6} + 2\tau_{5,6} - s \right) , \\
N_{280} &= s^4 + 2s^3 u - u\tau_{2,5}\tau_{3,5}\ell_6^2 + s\tau_{3,5}^2\ell_6^2 + \cdots + 8u^2\ell_5^2\ell_6^2 ,
\end{aligned}
\tag{3.21}
$$

where in N_{280} we have kept only a few terms, since it is somewhat lengthy. The complete list of kinematic numerators is contained in the ancillary file at the arXiv hosting of Ref. [3].

Compared to the super-Yang–Mills numerators in Eq. (3.19), the maximum number of powers of loop momenta dropped from six to one in the first three numerators and to four powers in N_{280}. Consequently, the naive double-copy numerators have only up to eight powers of loop momenta. The naive double-copy numerators also inherit the property that every term carries at least two powers of s or t, a property that all contact term corrections

share by construction.

Similarly, the additional diagrams in Fig. 3.7 are also very well-behaved at large loop momenta. An illustrative sample of the additional numerators is

$$
\begin{aligned}
N_{547} &= \frac{3}{2} s \ell_5^2 (t\tau_{1,5} - u\tau_{2,5} - 3s\tau_{3,5} - 6u\tau_{3,5}) \,, \\
N_{624} &= -\frac{61}{10} s^3 (u - t + \tau_{1,5} - \tau_{2,5}) \,, \\
N_{708} &= 6s^2 (t - u) \ell_5^2 \,,
\end{aligned}
\tag{3.22}
$$

where the labels correspond to those in Fig. 3.7.

The naive double copy of all 752 diagrams gives diagrams that are completely ultraviolet finite in $D = 22/5$. In $D = 24/5$ it exhibits no power divergences, in contrast to the double copy of the earlier representation of the super-Yang–Mills amplitude. As we will see below, the contact term corrections needed to obtain the $\mathcal{N} = 8$ supergravity amplitude will lead to contributions that individually have power divergences but, as we will discuss in Section 3.4, it is such that it that does not increase the number of integrals that must be evaluated. Furthermore, as we note in Section 3.6, in $D = 22/5$ the contact term contributions all cancel after IBP reduction, leaving a completely ultraviolet finite result.

To confirm our construction, we have performed the standard checks of verifying cuts beyond those needed for the construction, such as all non-singular cuts at the N4 and N5 levels. We have confirmed that our improved $\mathcal{N} = 4$ super-Yang–Mills integrand generates exactly the same ultraviolet divergence in the critical dimension $D_c = 26/5$ as obtained in Ref. [161] using the earlier representation of the amplitude. To carry out this check we followed the same procedure explained in that paper for extracting the ultraviolet divergence, using the same integral identities.
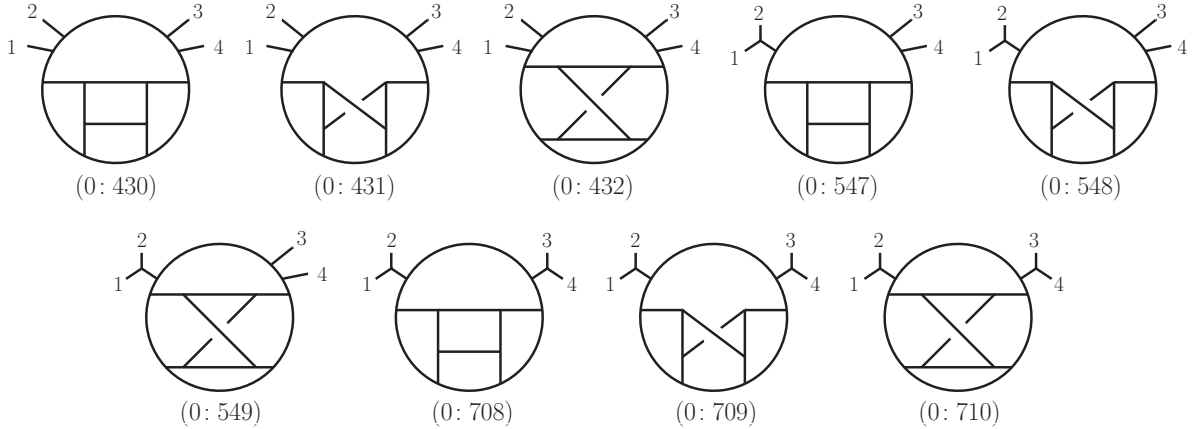
85

Figure 3.10: The diagrams whose numerators were set to zero, to simplify the supergravity construction by avoiding doubled propagators.

3.3.2 Improved $\mathcal{N} = 8$ supergravity integrand

Armed with the new five-loop four-point integrand of $\mathcal{N} = 4$ super-Yang–Mills theory we now proceed to the construction of the corresponding improved integrand of $\mathcal{N} = 8$ supergravity, following the generalized double-copy construction [60] outlined in Section 3.2. Our construction essentially follows the same steps as in Ref. [161], so we will not repeat the details. We obtain a set of contact terms, organized according to levels, which correct the naive double copy to an integrand for the $\mathcal{N} = 8$ supergravity amplitude. As a consequence of the improved term-by-term ultraviolet behavior of the gauge-theory amplitude, the individual terms of the resulting supergravity integrand are also better behaved at large loop momenta.

The difference with the construction in Ref. [161] is related to the existence of the diagrams with doubled propagators in the super-Yang–Mills amplitude, such as $(0\colon 430)$, $(0\colon 547)$ and $(0\colon 708)$ of Fig. 3.7. Unlike the gauge-theory construction, here we can avoid needing to identify and skip cuts with ill-defined values. To this end we notice that, since the maximal cuts of these diagrams vanish, they contribute only contact terms even in the naive double copy. We may therefore simply set to zero these diagrams in the naive double copy and re-

Level	No. diagrams	No. nonvanishing diagrams
0	752	649
1	2,781	0
2	9,007	1,306
3	17,479	2,457
4	22,931	2,470
5	20,657	1,335
6	13,071	256
total	86,678	8,473

Table 3.1: The number of diagrams at each contact-diagram level as well as the number of diagrams at each level with nonvanishing numerators.

cover their contributions directly as contact terms at the relevant level. For the same reason we can also set to zero in the naive double copy other diagrams with vanishing maximal cuts. The consistency of this reasoning is checked throughout the calculation by the absence of ill-defined cuts as well as by the locality of all contact term numerators. Had the latter not be the case it would imply the violation of some lower-level cuts. This in turn would have meant that some term we set to zero contributed more than merely contact terms to the amplitude. The net effect is that we can build the complete integrand by using cuts through the N6 level, just as in the previous construction [161], and there is no need to go beyond this, except to verify the completeness of the result.

As discussed in Section 3.2, the cuts of the supergravity amplitude can be computed in terms of the BCJ discrepancy functions of the full gauge-theory amplitude rather than from the discrepancy functions of the amplitude with the doubled-propagator diagrams set to zero. It turns out that the cuts touching the doubled-propagator diagrams are sufficiently simple to be efficiently evaluated using KLT relations on the cuts. The completeness of the construction is guaranteed by verifying all (generalized) unitarity cuts.

The complete amplitude is given by a sum over the 752 diagrams of the naive double

copy and the 85,926 contact term diagrams,

$$\mathcal{M}_4^{\text{5-loop}} = i\left(\frac{\kappa}{2}\right)^{12} stu M_4^{\text{tree}} \sum_{k=0}^{6} \sum_{\mathcal{S}_4} \sum_{i=1}^{T_k} \int \prod_{j=5}^{9} \frac{d^D \ell_j}{(2\pi)^D} \frac{1}{S_i} \frac{\mathcal{N}_i^{(k)}}{\prod_{m_i=5}^{20-k} \ell_{m_i}^2}, \qquad (3.23)$$

where M_4^{tree} is the four-point $\mathcal{N} = 8$ supergravity tree amplitude and $u = -s - t$. Here T_k is the total number of diagrams at level k; they are given in Table 3.1. The diagram count at each level differs somewhat from the earlier construction [161] because here we include all the daughter diagrams that arise collapsing propagators of any of the 752 parent diagrams of the naive double copy instead of those obtained only from the first 410 diagrams. The parent-level diagrams are obtained from the improved representation of the $\mathcal{N} = 4$ super-Yang–Mills four-point amplitude through the double-copy substitution (3.5) and setting to zero the numerators of the diagrams shown in Fig. 3.10. The contact terms are generated using the procedures summarized above. We collect the results for all diagrams, numerators $\mathcal{N}_i^{(k)}$ and symmetry factors, S_i, at each level in the plain-text MATHEMATICA-readable ancillary files, found at the arXiv hosting of Ref.[3].

A striking property of the supergravity contact terms, which is obvious from Table 3.1, is that most of them vanish. The precise number of vanishing diagrams depends on the particular starting point used in the naive double copy and on details of the off-shell continuation of the contact terms at each level. As for the previously-constructed integrand in Ref. [161], this is a consequence of the many kinematic Jacobi identities that hold for the super-Yang–Mills amplitude used in our construction. This effect is even more clear here, where the $\mathcal{N} = 4$ super-Yang–Mills integrand obeys all the two-term kinematic Jacobi relations. While this integrand does not support a solution for all three-term Jacobi relations, it may be possible to further reduce the number of supergravity contact terms by imposing a judiciously-chosen subset of these relations.
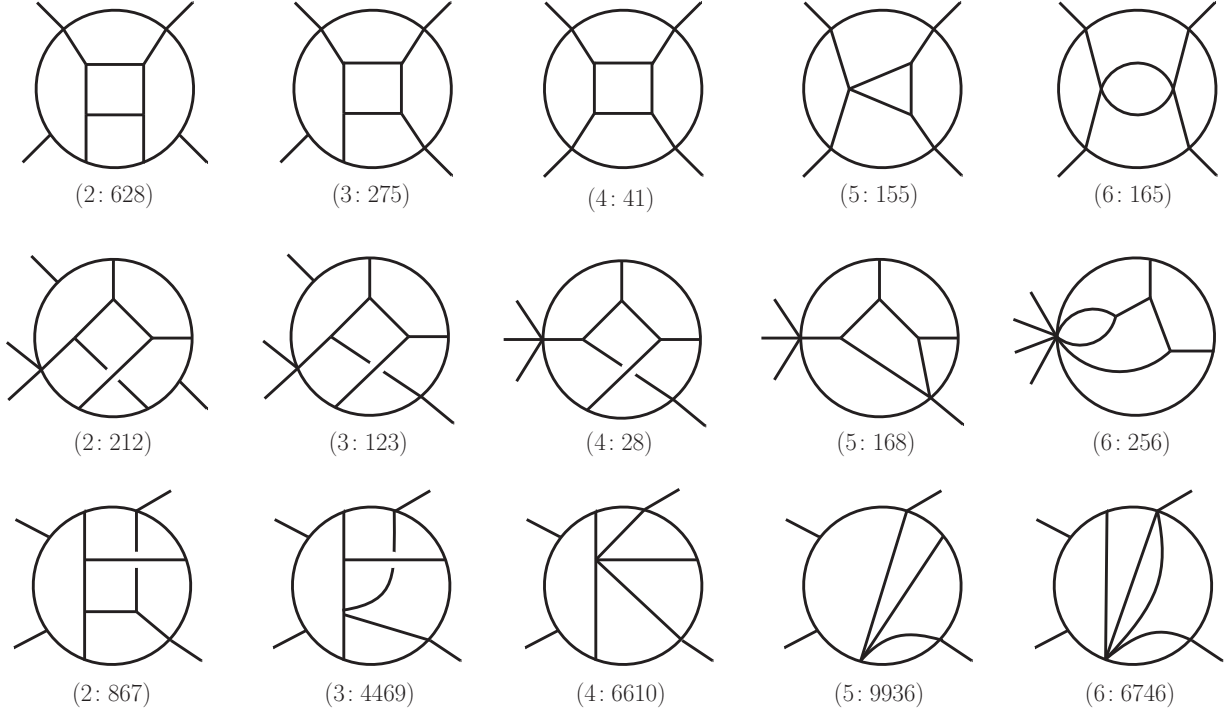
Figure 3.11: Sample contact term diagrams corresponding to the cuts in Fig. 3.3. The labels (X: Y) refer to the level and contact diagram number. The final four diagrams have vanishing numerator; the first eleven are nonvanishing.

3.4 Ultraviolet vacuum integral expansion

In previous sections we reviewed the integrand of the five-loop four-point amplitude of $\mathcal{N} = 8$ supergravity found in Ref. [161] and constructed a new one, with certain improved power-counting properties. In this section we expand these integrands in the ultraviolet, *i.e.* for external momenta small compared to the loop momenta, and point out key features of the new integrand. This expansion generates integrals reminiscent of vacuum integrals with no external momenta; we call such integrals "vacuum integrals" as well. While we are interested in the logarithmic divergence in $D = 24/5$, both integrands also exhibit spurious quadratic and quartic divergences in this dimension. Finiteness of the five-loop amplitude in $D < 24/5$ guarantees that they should cancel out. However, the graph-by-graph presence of spurious singularities both in the naive double-copy part and in the contact terms of the integrand of

89

Ref. [161] leads to a rapid increase in the number of terms when extracting the logarithmic divergence. By construction, the new integrand can have power divergences only through its contact terms. Moreover, their structure is such that the number of different integrals which appear in the ultraviolet expansion is substantially decreased compared to the earlier integrand.

3.4.1 Vacuum expansion of integrands

The basic challenge is to extract logarithmic divergences underneath spurious power divergences. To do so we follow the standard method of series expanding the integrand in the ultraviolet region [257–259], where the external momenta are much smaller than loop momenta, which are commensurate. This strategy was applied to various supergravity calculations in Refs. [4, 6, 9, 71]. The different orders in this expansion are expressed as vacuum integrals with different degrees of ultraviolet divergence. In dimensional regularization, only logarithmically divergent vacuum integrals can result in a pole. Logarithmically-divergent terms in lower dimensions are power divergent in higher dimensions. Thus, by integrating all logarithmically-divergent terms in $D < 24/5$, we are checking that power divergences cancel in $D = 24/5$. Indeed, as we explain in Section 3.6, we explicitly verify that in $D = 22/5$ all the divergences cancel. This also proves that any power divergences in $D = 24/5$ are artifacts of our representations. While we do not have representation of the integrand that exhibits only logarithmic divergences in this dimension, the naive double-copy contributions in our new representation were constructed to have this property.

Dimensional analysis shows that the local term[4] in the effective action that corresponds to a logarithmic divergence in $D = 24/5$ at five loops has the generic structure $D^8 R^4$. Its momentum space form has 16 momentum factors; of them, eight correspond to the $(stA^{\text{tree}})^2 = stuM_4^{\text{tree}}$ prefactor of the amplitude. Thus, the logarithmically-divergent part of

---

[4]This is the same term that may appear at seven loops in $D = 4$, though the appearance of the former of course does not immediately imply the presence of the latter.

each integral has eight factors of external momenta. Because every term in every supergravity numerator $\mathcal{N}$ has at least two powers of s or t, we need to expand the integrand to at most fourth order in small external momenta.

The dependence of the numerator polynomial on external momenta determines the order to which each term must be expanded. It is therefore useful to decompose each numerator into expressions $\mathcal{N}^{(m)}$ with fixed number m of external momenta (and $16 - m$ powers of loop momentum)

$$\mathcal{N} = \mathcal{N}^{(4)} + \mathcal{N}^{(5)} + \mathcal{N}^{(6)} + \cdots + \mathcal{N}^{(16)} . \tag{3.24}$$

There is freedom in this decomposition, including that induced by the choice of independent loop momenta. Terms with more than eight powers of external momenta in the numerator are ultraviolet finite in $D = 24/5$ and can therefore be ignored. For terms $\mathcal{N}^{(8)}$ with exactly eight powers of external momentum in the numerator we need only the leading terms in the expansion of the propagators as higher-order terms are finite. It suffices therefore to set to zero all external momenta in propagators, $e.g.$ for the $\mathcal{N}^{(8)}$ terms in the diagram shown in Fig. 3.12(a)

$$\frac{\mathcal{N}^{(8)}}{(\ell_5^2)^3 \, (\ell_6^2)^3 \, \ell_7^2 \, \ell_8^2 \, \ell_9^2 (\ell_5 + \ell_7)^2 (\ell_5 - \ell_9)^2 (\ell_5 + \ell_6 + \ell_7)^2 (-\ell_5 - \ell_6 + \ell_9)^2}$$
$$\times \frac{1}{(\ell_5 + \ell_6 + \ell_8 - \ell_9)^2 (\ell_5 + \ell_6 + \ell_8)^2 (\ell_5 + \ell_6 + \ell_7 + \ell_8)^2} . \tag{3.25}$$

The leading divergence of terms with $4 \leq m \leq 7$ is power-like. The extraction of the logarithmic divergence underneath requires that propagators be expanded to $(8 - m)$-th order in the momenta k_i:

$$\frac{\mathcal{N}^{(m)}}{\prod_{i=1}^I d_i} \to \frac{\mathcal{N}^{(m)}}{(8-m)!} \sum_{i_1,\ldots,i_{8-m}=1}^3 k_{i_1}^{\mu_1} \ldots k_{i_{8-m}}^{\mu_{8-m}} \left(\frac{\partial}{\partial k_{i_1}^{\mu_1}} \cdots \frac{\partial}{\partial k_{i_{8-m}}^{\mu_{8-m}}} \frac{1}{\prod_{i=1}^I d_i} \bigg|_{k_j=0} \right) , \tag{3.26}$$

where I is the number of internal lines of the diagram and d_i the corresponding inverse

propagators. The action of derivatives leads to propagators raised to higher powers—*i.e.* to repeated propagators—which we denote by dots, one for each additional power. Up to four further dots appear when derivatives act four times and external momenta are set to zero. Examples, with numerators suppressed, are included in diagrams (b) and (c) of Fig. 3.12. The increase in the number of classes of vacuum integrals (as specified by the number of dots) leads in turn to an increase in the complexity of the IBP system necessary to reduce them to master integrals. The expansion also leads to higher-rank tensor vacuum integrals, which appear as integrals with numerators containing scalar products of loop and external momenta. We discuss dealing with such integrals below.

It is instructive to contrast, from the standpoint of the vacuum expansion, the old and new four-point five-loop $\mathcal{N} = 8$ supergravity integrands; we will choose the level-0 diagrams 14, 16, 31, 280 shown in Fig. 3.6 as illustrative examples. The numerators of these diagrams are, respectively, the naive double copies (*i.e.* squares) of the numerator factors of the old representation of the $\mathcal{N} = 4$ super–Yang–Mills amplitude, given in Eq. (3.19), and the new representation, given in Eq. (3.21). In the old representation, $\mathcal{N}_{0:14}^{(4)}$, $\mathcal{N}_{0:16}^{(4)}$, $\mathcal{N}_{0:31}^{(4)}$, $\mathcal{N}_{0:280}^{(4)}$ are all nonvanishing and, for these terms, the logarithmic divergence is given by Eq. (3.26) with $m = 4$. The resulting vacuum diagrams exhibit up to eight dots. [5] In the improved representation constructed in Section 3.3, the first nonvanishing terms in the decomposition of supergravity numerators are $\mathcal{N}_{0:14}^{(8)}$, $\mathcal{N}_{0:16}^{(8)}$, $\mathcal{N}_{0:31}^{(8)}$, $\mathcal{N}_{0:280}^{(8)}$. Thus, no expansion of propagators is needed and the leading term obtained by setting to zero external momenta in the propagators gives the logarithmic divergence in $D = 24/5$. The corresponding vacuum integrals have four dots.

Because of the complexity of the expressions, essentially all combinations of repeated propagators—up to the maximally-allowed number of dots—and numerators can appear either in the expansion itself or as part of the IBP system. Thus, a clear requirement to

---

[5]The leading term in the small momentum expansion is quartically divergent and corresponds to a logarithmic divergence in $D = 4$ which should cancel on general grounds when all contributions are collected.
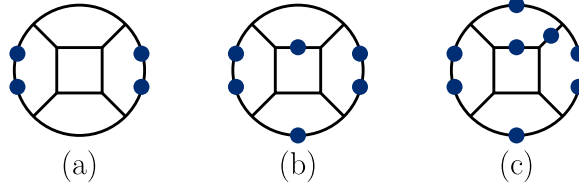
Figure 3.12: After series expanding one encounters vacuum diagrams with up to 8 additional propagators, as well as numerators which are suppressed here. Each (blue) dot corresponds to a repeated propagator. Diagram (a), (b) and (c) are examples with four, six and eight higher-power propagators.

simplify the integration is to reduce the maximal number of dots. As discussed above, we would naively expect up to eight dots from the expansion of the naive double copy (level-0) diagrams in the representation of Ref. [161]. It turns out however that, upon reduction of tensor integrals, all seven- and eight-dot vacuum integrals drop out diagram by diagram. This is a consequence of the structure of the representation of the gauge-theory amplitude. As will be seen in Section 3.6, the IBP system does not close unless it includes integrals with an extra dot compared to the desired ones. Thus, for the old representation we need vacuum integrals with up to seven dots. There are 1,292,541,186 different such vacuum integrals of which 16,871,430 are distinct integrals. It is nontrivial to construct and solve the relevant complete IBP system.

For the improved representation of Section 3.3, every term in the numerators of level-0 diagrams has at least eight external momenta; thus, the leading term corresponds already to logarithmic divergences in $D = 24/5$. No further expansions of propagators is necessary, implying that the integration of level-0 diagrams in the vacuum expansion requires vacuum integrals with at most four dots and an IBP system relating integrals with up to five dots. This is an enormous simplification over the earlier integrand.

Although simpler, the contact diagrams of the new representation of the four-point five-loop $\mathcal{N} = 8$ integrand contain nonvanishing $\mathcal{N}^{(4)}$ numerator components and thus up to quartic power divergences. Extraction of their logarithmic divergences requires therefore an expansion to fourth order. One might therefore expect vacuum graphs with up to eight dots,

93

which would ruin the simplification of the naive double-copy terms. It turns out however that $\mathcal{N}^{(m)}$ with $m \leq 7$ are nonzero only in contact terms in which at least $(8 - m)$ external lines are attached with four- or higher-point vertex. In the absence of any expansion, the vacuum limit of these graphs has only at most $(m - 4)$ dots; expanding to $(8 - m)$-th order (3.26) to extract the logarithmic divergence yields therefore at most four dots. To illustrate this phenomenon, consider the toy example

$$\frac{2\ell_5 \cdot k_1}{\ell_5^2(\ell_5 + k_1)^2} = \frac{1}{\ell_5^2} - \frac{1}{(\ell_5 + k_1)^2} \, , \tag{3.27}$$

which we embed in a term that is logarithmically divergent, *i.e.* the numerator on the left-hand side is part of the numerator component $\mathcal{N}^{(8)}$ of some graph. As discussed before, such terms require no expansion and yield vacuum graphs with four dots. The terms on the right-hand side mimic the way contact terms are constructed by canceling propagators. Because each numerator on the right-hand side is missing a power of external momentum compared to the left-hand side, it is now of $\mathcal{N}^{(7)}$ type and we need to series expand the denominator to first order in external momenta (which may be either k_1 or the other external momenta of the graph). This series expansion produces exactly one doubled propagator. This however it does not increase the number of repeated propagators compared to the left-hand side because in going from the left- to right-hand side we lost a repeated propagator when setting the external momentum k_1 to zero. The net effect is that the total number of dots in any vacuum graphs arising from the expansion of the contact diagrams does not increase beyond the four that arise from naive double-copy diagrams.

Closing the IBP system by including the diagrams with an additional repeated propagator, we obtain 845,323 independent integrals. We will discuss the construction of this system and its solution in section 3.6.

A further important simplification is that since we are working near a fractional dimension, $D = 24/5 - 2\epsilon$, which in any case is below the critical dimensions at lower-loop orders, no
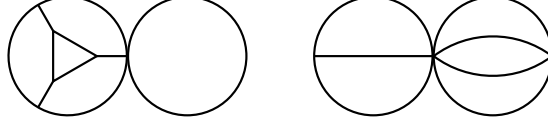
Figure 3.13: Sample factorized vacuum integrals that do not contribute because of the absence of subdivergences.

subdivergences are possible. Only genuine five-loop vacuum integrals, which do not factorize into lower-loop integrals, can contribute to the logarithmic ultraviolet divergence. Factorized integrals, such as those shown in Fig. 3.13, are finite in this dimension and can be ignored.

The result of the expansion in external momenta is a collection of vacuum tensor integrals, in which the numerator factors are polynomials in Mandelstam invariants of external momenta, inverse propagators and scalar products of loop and external momenta. For each integral the numerator is separately homogeneous in the loop and external momentum dependence. These integrals can be further reduced by making use of Lorentz invariance—specifically, that any vacuum tensor integral is a linear combination of products of metric tensors—to separate the dependence on external momenta from that on loop momenta. More precisely, under integration we can replace a two-tensor which is dotted into external momentum by

$$\ell_i^\mu \ell_j^\nu \;\to\; \frac{1}{D}\,\eta^{\mu\nu}\,\ell_i \cdot \ell_j\,, \tag{3.28}$$

and a four-tensor by

$$\ell_i^\mu \ell_j^\nu \ell_k^\rho \ell_l^\sigma \;\mapsto\; \frac{1}{D(D-1)(D+2)}\left(A\,\eta^{\mu\nu}\,\eta^{\rho\sigma} + B\,\eta^{\mu\rho}\,\eta^{\nu\sigma} + C\,\eta^{\mu\sigma}\,\eta^{\nu\rho}\right), \tag{3.29}$$

where

$$A = (D+1)\ell_i \cdot \ell_j\,\ell_k \cdot \ell_l - \ell_i \cdot \ell_k\,\ell_j \cdot \ell_l - \ell_i \cdot \ell_l\,\ell_j \cdot \ell_k\,,$$

$$B = -\ell_i \cdot \ell_j\,\ell_k \cdot \ell_l + (D+1)\ell_i \cdot \ell_k\,\ell_j \cdot \ell_l - \ell_i \cdot \ell_l\,\ell_j \cdot \ell_k\,,$$

$$C = -\ell_i \cdot \ell_j\,\ell_k \cdot \ell_l - \ell_i \cdot \ell_k\,\ell_j \cdot \ell_l + (D+1)\ell_i \cdot \ell_l\,\ell_j \cdot \ell_k\,. \tag{3.30}$$

95

Since in both cases the highest divergence is quartic, the expansion in small external momenta is to at most fourth order. Thus, there can be at most four scalar products of loop and external momenta and consequently reduction formulas of tensor integrals of rank six or higher are not necessary.

3.4.2 Labeling the vacuum diagrams

After applying Lorentz invariance to reduce the expanded integrals to a collection of scalar vacuum integrals, with possible numerators and repeated propagators, we need to organize them into a standard form and eliminate further redundancies. The relevant graph topologies are shown in Fig. 3.14. A particularly good labeling scheme has been devised by Luthe [260]. Straightforward counting shows that every vacuum integrand in Fig. 3.14 has 15 independent Lorentz dot products between loop momenta. Depending on the integral, these dot products are either inverse propagators or irreducible numerators i.e. quadratic combinations of loop momenta that are linearly independent of the propagators. Remarkably, a global labeling scheme for momenta can be found for vacuum integrals at five loops. We define, following Ref. [260],

$$q_1 = \ell_1, \quad q_2 = \ell_2, \quad q_3 = \ell_3, \quad q_4 = \ell_4, \quad q_5 = \ell_5, \quad q_6 = \ell_1 - \ell_3, \quad q_7 = \ell_1 - \ell_4,$$

$$q_8 = \ell_1 - \ell_5, \quad q_9 = \ell_2 - \ell_3, \quad q_{10} = \ell_2 - \ell_4, \quad q_{11} = \ell_2 - \ell_5, \quad q_{12} = \ell_3 - \ell_5,$$

$$q_{13} = \ell_4 - \ell_5, \quad q_{14} = \ell_1 + \ell_2 - \ell_4, \quad q_{15} = \ell_3 - \ell_4 \,. \tag{3.31}$$

For example, the labeling of the four parent vacuum integrals—vacuum integrals with only cubic vertices—in this scheme is shown in Fig. 3.15, where the propagator labeled with i corresponds to q_i^2. The irreducible numerators are q_i^2 for the three i labels missing from that diagram. For daughter diagrams, i.e. the 44 diagrams in Fig. 3.14 with fewer than 12 distinct propagators, the number of irreducible numerators is larger, so that the total
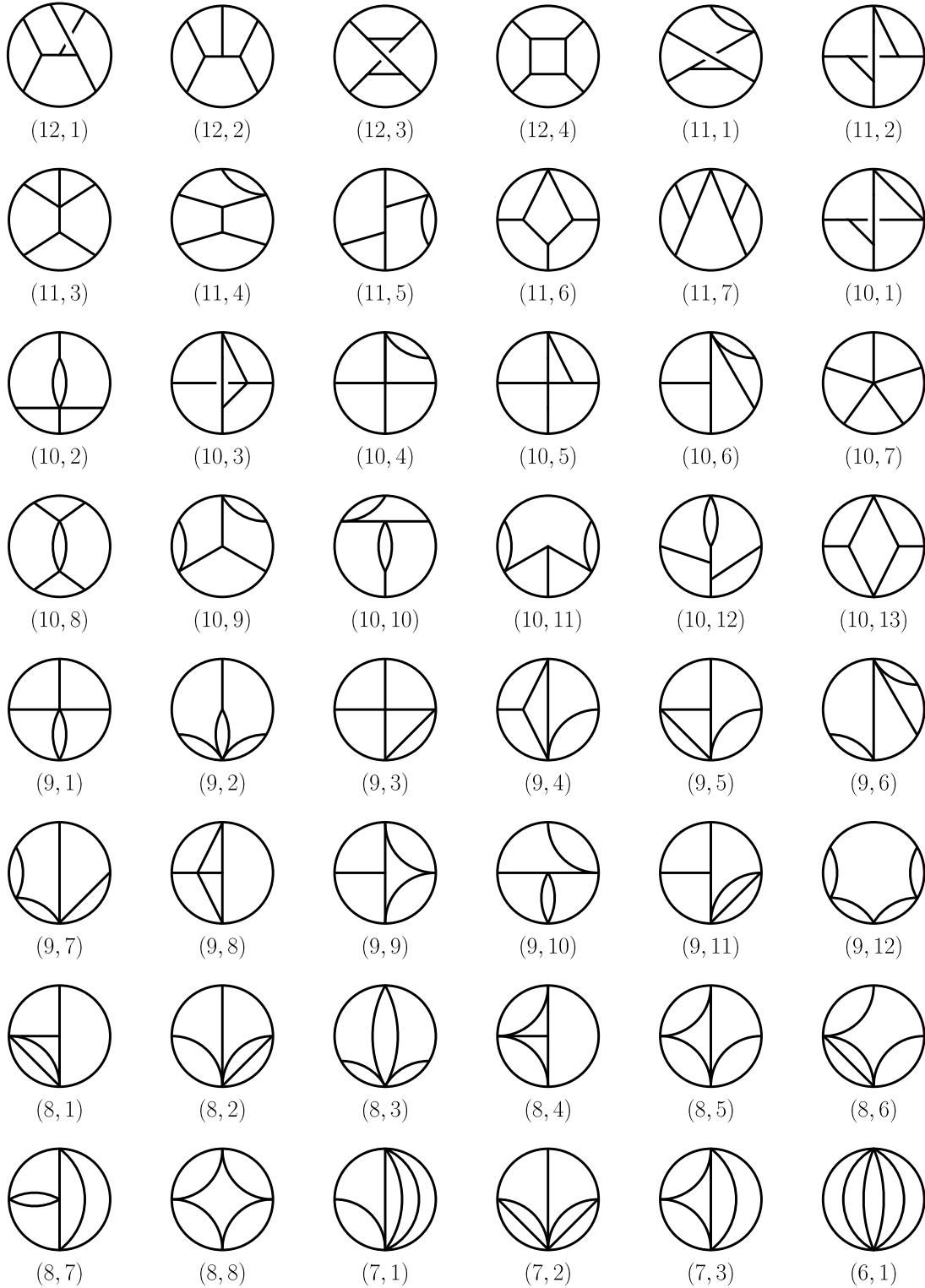
Figure 3.14: All 48 independent vacuum propagator structures, that do not factorize into products of lower-loop diagrams. The first number in the diagram label is the number of propagators and the second is the diagram number at that level.
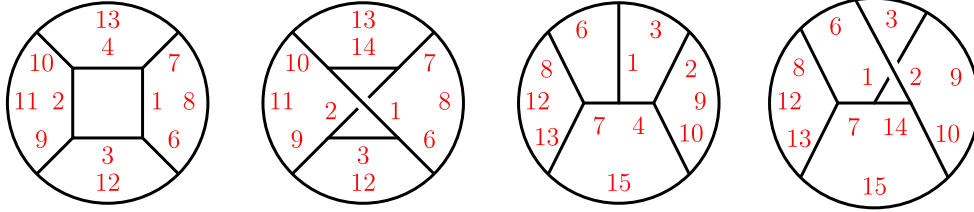
97

Figure 3.15: The parent vacuum integrals—vacuum integrals with only cubic vertices—with 12 distinct propagators and their labels.

number of independent Lorentz dot products between loop momenta remains the same. For each daughter diagram there are several possible labelings, inherited from its parents. We pick a standard one and map to it all other occurrences of the diagram.

After applying momentum conservation we can rewrite any term in the integrand of a vacuum integral using the 15 invariants. With this labeling scheme we can specify each integral by a list of the indices representing the exponent of each of the 15 q_i^2,

$$\frac{1}{(q_1^2)^{a_1}(q_2^2)^{a_2}(q_3^2)^{a_3}\cdots(q_{14}^2)^{a_{14}}(q_{15}^2)^{a_{15}}} \Leftrightarrow F(a_1, a_2, a_3, \ldots, a_{14}, a_{15}), \qquad (3.32)$$

where a negative power indicates an irreducible numerator rather than a propagator denominator. This description is agnostic to whether the integral is planar or nonplanar, or which diagram the integral is a daughter of. Along with the symmetry relations presented next, it elegantly control the large redundancies introduced by the vacuum expansion.

In terms of these Fs, the four diagrams in Fig. 3.15 with no irreducible numerators and no repeated propagators are

$$F(1,1,1,1,0,1,1,1,1,1,1,1,1,0,0), \qquad F(1,1,1,0,0,1,1,1,1,1,1,1,1,1,0),$$

$$F(1,1,1,1,0,1,1,1,1,1,0,1,1,0,1), \qquad F(1,1,1,0,0,1,1,1,1,1,0,1,1,1,1). \qquad (3.33)$$
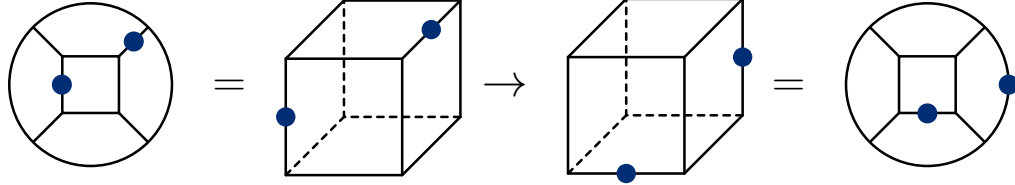
Figure 3.16: Moving dots via symmetry in diagram $(12, 4)$ corresponding to the cube.

3.4.3 Symmetry relations among vacuum integrals

In order to efficiently express all integrals in terms of a basis it is useful to first eliminate redundant integrals that are identical under relabelings. Fig. 3.16 shows an example of using graph symmetries to rearrange into a canonical format dots that might appear in diagram $(12, 4)$, the cube. In terms of the Fs, this symmetry maps

$$F(1, 2, 1, 1, 0, 1, 2, 1, 1, 1, 1, 1, 1, 0, 0) \rightarrow F(1, 1, 2, 1, 0, 1, 1, 2, 1, 1, 1, 1, 1, 0, 0). \qquad (3.34)$$

When irreducible numerators are present, the situation is a bit more complex because we also need to map the numerators according to the symmetry transformation. This can generate many contributions when we re-express the numerators back in terms of the basis q_i^2 monomials. A simple example we encounter is

$$F(1, 1, 1, -1, 0, 3, 2, 0, 0, 0, 0, 2, 2, 1, 0) \rightarrow F(3, 1, 1, 0, 0, 0, 0, 2, 1, 1, 0, 2, 0, 1, 0)$$
$$- F(3, 1, 2, -1, 0, 0, 0, 2, 1, 1, 0, 2, 0, 1, 0) + F(3, 1, 2, 0, 0, 0, 0, 2, 1, 1, 0, 2, 0, 1, -1). \qquad (3.35)$$

The vast majority of these numerator relabeling relations often involve iterating the process many times, generating relations between hundreds of different integrals.

Graph isomorphism is not sufficient to remove all the trivial redundancy, since certain non-isomorphic graphs can represent the same Feynman integral. Such relations typically involve "sliding" a bubble subdiagram along the propagators that connect it to the rest of the graph. In addition to a different graph structure, these transformations can change
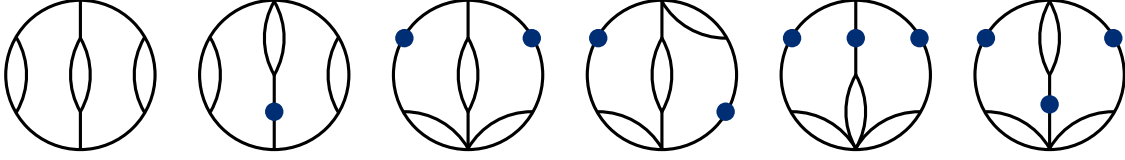
99

Figure 3.17: Example of non-isomorphic graphs that all correspond to the same Feynman integral.

$$(\ell_1 \cdot \ell_2) \quad\rightarrow\quad -(\ell_1 \cdot \ell_3)$$
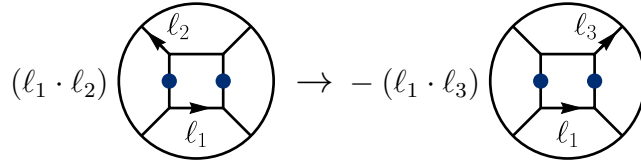
Figure 3.18: Numerator relations from residual automorphisms that keep the dot positions invariant.

the number of dots, as illustrated in the example in Fig. 3.17. We implement these non-isomorphism graph relations via a graph transformation that swaps bubble subdiagrams and propagators, corresponding to the swaps which map the diagrams in e.g. Fig. 3.17 into each other. We will refer to this as "enhanced graph isomorphisms". This method efficiently identifies equivalent five-loop vacuum integrals not related by graph isomorphisms.

A less efficient alternative, which we use in parts of the calculation as a consistency check, is to compute the Symanzik polynomials and bring them to a canonical form [261, 262]. This uses analytic properties of Feynman integrals without resorting to their graph representation.

Implementing the isomorphism and non-isomorphism relations, we map all integrals to a set of canonical ones. There are 3,079,716 scalar vacuum integrals with up to five dots and unit numerator, which map onto 94,670 canonical configurations, as demonstrated in Fig. 3.16.

In the presence of momentum-dependent numerator factors there also exist symmetry relations due to automorphisms that preserve both the graph structure and the position of the dots but change the numerator. This is distinct from relations of the type in Eq. (3.35)

100

which do not relate canonical integrals, but are used to move dots to canonical positions. An example of one particularly simple such relation is given in Fig. 3.18. Transformations of this type generate linear relations between canonical integrals, which are similar to IBP relations. Because of this, it is convenient to include and analyze them together with the IBP relations in Section 3.6.

3.5   Simplified ultraviolet integration

In this section we discuss the large-loop-momentum integration of the original form [161] of the five-loop four-point $\mathcal{N} = 8$ supergravity integrand. Although, an assumption will be required, this will not only provide a strong cross check of the complete result obtained in the next section, but will also point to more powerful ways of extracting the ultraviolet properties of supergravity theories, especially when combined with the observations of Section 3.7. As explained in the previous section, after series expanding and simplifying the original form of the integrand we encounter vacuum integrals with up to six dots, or repeated propagators, and irreducible numerators. Together with the additional dot needed to close the system, this causes a rather unwieldy IBP system. We will see here that the problem can be enormously simplified by targeting parent vacuum integrals—vacuum integrals with only cubic vertices or, equivalently, vacuum integrals that have maximal cuts, or also as vacuum integrals with the maximum number of distinct propagators. The relevant parent vacuum integrals are shown in Fig. 3.15. We solve the integration-by-parts system on the maximal cuts of the vacuum integrals, using modern algebraic geometry methods that combine unitarity cuts with IBP reduction for Feynman integrals [175–188, 263–266].

Besides enormously simplifying reduction to a set of master integrals by focusing on the vacuum integrals with maximal cuts, targeting parent vacuum integrals also has the added benefit of allowing us to immediately drop large classes of contact terms from the integrand, including all contact terms obtained from the N5 and N6 levels, even before expanding into

vacuum diagrams. Any term where a propagator is completely canceled in the vacuum graph can be dropped.

In manipulating the vacuum integrals, there are two important issues that must be addressed. The first one is the separation of the infrared and ultraviolet divergences. This is an important ingredient in various studies of ultraviolet properties, such as the analysis of $\mathcal{N} = 4$, $\mathcal{N} = 5$ and $\mathcal{N} = 8$ supergravity at three and four loops [4, 6, 71, 146–148], and the computation the five-loop beta function in QCD [163–165]. Although there are no physical infrared singularities in $D > 4$, our procedure of series expanding around small external momenta introduces spurious ones. We will show in detail in the next section that in an infrared-regularized setup for integrals with no ultraviolet subdivergences, terms in the IBP system that are proportional to the infrared regulator involve only ultraviolet-finite integrals. Thus, since we are interested only in the ultraviolet poles, we can effectively reduce the vacuum integrals without explicitly introducing an infrared regulator. For the rest of this section, when we discuss linear relations between integrals, it should be understood that we actually mean linear relations between the ultraviolet poles of the integrals.

A second issue is that the vacuum expansion of our integrand contains propagators with raised powers, which is in contradiction with the naive unitarity cut procedure of replacing propagators by on-shell delta functions. Fortunately, two solutions to this problem are available in the literature. One option [181, 267, 268] is to define the cut as the contour integral around propagator poles; this effectively identifies the cut as the residue of the propagator pole even for higher-order poles. Another, proposed in Ref. [189], is to use dimension shifting [93, 96] such that all propagators appear only once at the cost of shifting the integration dimension and raising the power of numerators, before imposing the maximal-cut conditions to discard integrals with canceled propagators. Here we will use the second strategy.

Starting with the integrand of Ref. [161], the end result of dimension shifting procedure is a set of vacuum integrals in $D = -36/5 - 2\epsilon$ with a total 30 powers of the irreducible

numerators. For example, for the crossed-cube vacuum diagram shown in the second diagram of Fig. 3.15, we have integrals of the form

$$\int \prod_{k=1}^{5} \frac{d^D \ell_k}{(2\pi)^D} \frac{(q_4^2)^{A_4} (q_5^2)^{A_5} (q_{15}^2)^{A_{15}}}{q_1^2 q_2^2 q_3^2 \widehat{q_4^2} \widehat{q_5^2} q_6^2 q_7^8 q_8^2 q_9^2 q_{10}^2 q_{11}^2 q_{12}^2 q_{13}^2 q_{14}^2 \widehat{q_{15}^2}}, \tag{3.36}$$

where $D = -36/5 - 2\epsilon$ and the "hats" in the denominator mean to skip those propagators. The q_i are the uniform momenta defined in Eq. (3.31). Here the three irreducible numerators are q_4^2, q_5^2 and q_{15}^2; these cannot be written as the linear combinations of the 12 propagator denominators, as explained in the previous section. To obtain a logarithmic divergence in the shifted dimension $-36/5$, we need 30 powers of numerator factors

$$A_4 + A_5 + A_{15} = 30, \qquad \text{with } A_4 \geq 0, A_5 \geq 0, A_{15} \geq 0. \tag{3.37}$$

In total there are 496 different combinations of A_j that satisfy Eq. (3.37). With the new integrand of Section 3.3 the power counting is greatly improved so we need only shift to $D = -16/5 - 2\epsilon$ with 20 powers of numerators. This gives 231 integrals to evaluate.

Consider the cross-cube diagram shown in the second diagram in Fig. 3.15. The IBP identities relating the 496 integrals are of the form

$$\int \prod_k \frac{d^D \ell_k}{(2\pi)^D} \frac{\partial}{\partial \ell_i^\mu} \frac{v_i^\mu}{\prod_j d_j} = 0, \tag{3.38}$$

where v_i^μ has polynomial dependence on external and internal momenta and the d_j are the various propagators. We refer to

$$v_i^\mu \frac{\partial}{\partial \ell_i^\mu}, \tag{3.39}$$

as the IBP-generating vector, while the rest of Eq. (3.38),

$$\int \prod_k \frac{d^D \ell_k}{(2\pi)^D} \frac{1}{\prod_j d_j}, \tag{3.40}$$

103

is referred to as the seed integral. Integration by parts as above re-introduces auxiliary integrals with propagators raised to higher powers, since the derivatives can act on the propagator denominators. Lowering again the propagator powers through dimension shifting leads still to new integrals because, while of the same topology at the starting ones, they are now in a different dimension.

To eliminate these auxiliary integrals Gluza, Kadja and Kosower [175] formulated IBP relations without doubled propagators, using special IBP-generating vectors that satisfy

$$v_i^\mu \frac{\partial}{\partial \ell_i^\mu} d_j = f_j \, d_j \,, \tag{3.41}$$

for *all* values of j with f_j restricted to be polynomials (in external and loop momenta). This cancels any squared propagator generated by derivatives, and does not introduce spurious new denominators since f_j are polynomials. Since the original publication, strategies for solving Eq. (3.41) have been explored in Refs. [175, 183–188, 265, 266]. We use the strategy in Ref. [265, 266] to obtain a complete set of vectors v_i^μ using computational algebraic geometry algorithms implemented in SINGULAR [269]. They in turn give the complete set of IBP relations among the 496 cross cube integrals discussed above (3.36), (3.37) and implies that all of them are expressed in terms of a single integral—the second diagram in Fig. 3.15. A similar analysis solves the analogous problem for the 496 integrals of cube topology and expresses them in terms of the integral corresponding to the first graph in Fig. 3.15. The IBP systems restricted to integrals with maximal cuts for the parent topologies with internal triangles, corresponding to the third and fourth graph in Fig. 3.15, sets all integrals to zero, implying that they are all reducible to integrals that do not have maximal cuts.

As a cross-check for the crossed-cube topology, we have also analytically solved for the integrals in closed form by contour integration [263, 264] using the Baikov representations [270–273], without making use of integral relations of the type (3.38). We refer the reader to Ref. [161] for the details of the analogous computation in $D = 22/5$. In that case, all parent

vacuum diagrams cancel, as expected.

By inverting the dimension shifting relations we can re-express the final result in terms of parent master integral in the original dimension $D = 24/5 - 2\epsilon$. The final result for the leading ultraviolet behavior is remarkably simple:

$$\mathcal{M}_4^{(5)}\Big|_{\text{leading}}^{\text{parent-level}} = -\frac{629}{25}\left(\frac{\kappa}{2}\right)^{12}(s^2 + t^2 + u^2)^2 stu M_4^{\text{tree}}\left(\frac{1}{3}\boxplus + \boxtimes\right). \quad (3.42)$$

We obtain identical result, whether we start from the integrand of Ref. [161] or the improved one in Section 3.3. This provides a highly nontrivial check on the cut construction and the integral reduction procedure. Most importantly, as we show in the next section, the result in Eq. (3.42) is complete, even though we kept only the parent master integrals, which have no canceled propagators. As we shall see in Section 3.7, this seems unlikely to be accidental.

3.6 Full ultraviolet integration

In this section, we extract the ultraviolet divergence of the five-loop four-point $\mathcal{N} = 8$ supergravity amplitude without making any assumptions on the class of vacuum integrals that contribute. To keep the IBP system under control, we use the improved representation of the integrand found in Section 3.3, expanded at large loop momentum, as described in Section 3.4. We organize the IBP relations using and $\mathrm{SL}(L)$ reparametrization symmetry of L loop momenta [108]. We also incorporate the integral relations resulting from graph automorphisms that change kinematic numerator factors, a simple example of which is shown in Fig. 3.18.

3.6.1 IBP for ultraviolet poles modulo finite integrals

Since standard IBP reduction is usually performed for full integrals in dimensional regularization, there is a large amount of unnecessary computation for our purpose of extracting
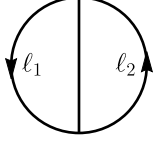
Figure 3.19: Two-loop example illustrating $\text{SL}(L)$ symmetry.

only the ultraviolet poles.[6] We now review setting up a simplified IBP system that only gives linear relations between the leading ultraviolet poles of different vacuum integrals [108].

As a warm up, consider the toy example of two-loop vacuum integrals in $D = 5 - 2\epsilon$ shown in Fig. 3.19. This example will mimic the supergravity situation because there are no (one-loop) subdivergences due to the properties of dimensional regularization. We define such two-loop integrals as

$$V_{A,B,C} = \int \frac{d^D \ell_1}{(2\pi)^D} \frac{d^D \ell_2}{(2\pi)^D} \frac{1}{[(\ell_1)^2 - m^2]^A [(\ell_2)^2 - m^2]^B [(\ell_1 - \ell_2)^2 - m^2]^C} \, , \tag{3.43}$$

where we require $A+B+C = 5$ since we are interested in logarithmically divergent integrals. In this case, there are no irreducible numerators.

Consider GL(2) transformations of the loop momenta $\Delta\ell_i \equiv \Omega_{ij}\ell_j$, which generate IBP relations of the form,

$$0 = \int \frac{d^D \ell_1}{(2\pi)^D} \frac{d^D \ell_2}{(2\pi)^D} \frac{\partial}{\partial \ell_i^\mu} \frac{\Omega_{ij}\ell_j^\mu}{[(\ell_1)^2 - m^2]^A [(\ell_2)^2 - m^2]^B [(\ell_1 - \ell_2)^2 - m^2]^C} \, , \tag{3.44}$$

where $D = 5 - 2\epsilon$. We first look at the SL(2) subalgebra which excludes the trace part of the GL(2) generators. For example, the SL(2) generator

$$\Omega_{ij} = \begin{pmatrix} 1 & 0 \\ 0 & -1 \end{pmatrix} \, , \tag{3.45}$$

---

[6]We have already performed expansion in the ultraviolet region to produce vacuum integrals, but even the (infrared-regulated) vacuum integrals contain finite parts that are not of interest to us here.

produces the IBP relation

$$0 = \int \frac{d^D \ell_1}{(2\pi)^D} \frac{d^D \ell_2}{(2\pi)^D} \left(\ell_1^\mu \frac{\partial}{\partial \ell_1^\mu} - \ell_2^\mu \frac{\partial}{\partial \ell_2^\mu} \right) \frac{1}{(\ell_1^2 - m^2)^A (\ell_2^2 - m^2)^B \left[(\ell_1 - \ell_2)^2 - m^2 \right]^C}$$

$$= (-2A + 2B) V_{A,B,C} - 2C \, V_{A-1,B,C+1} + 2C V_{A,B-1,C+1}$$

$$+ m^2 \left(-2A \, V_{A+1,B,C} + 2B \, V_{A,B+1,C} \right) , \tag{3.46}$$

where we used $A + B + C = 5$. The second-to-last line of the above equation contains integrals that are logarithmically divergent in the ultraviolet, while the last line contains integrals that are ultraviolet finite by power counting—as indicated by simple considerations of dimensional analysis, since the last line is proportional to m^2. Absence of subdivergences implies that *overall* power counting is sufficient for showing whether an integral is ultraviolet finite. Therefore, for the purpose of extracting ultraviolet divergences, we can disregard the last line of the above equations, and instead work with an IBP system *modulo finite integrals*. Since the generators of the SL(2) subalgebra are traceless, the IBP relations we generate have no explicit dependence on the dimension D.

Inspecting Eq. (3.46) we see that, setting $m = 0$ from the beginning removes the last line of that equation while preserving the relation between integrals exhibiting ultraviolet poles. Thus, even though setting $m = 0$ turns these vacuum integrals into scaleless integrals that vanish in dimensional regularization, the SL(2) subalgebra nonetheless generates the correct IBP relations between between ultraviolet poles. In contrast, including the trace generator,

$$\Omega_{ij} = \begin{pmatrix} 1 & 0 \\ 0 & 1 \end{pmatrix} , \tag{3.47}$$

which extends SL(2) to GL(2), requires nonvanishing m. Indeed, this generator produces

the IBP relations

$$0 = \int \frac{d^D \ell_1}{(2\pi)^D} \frac{d^D \ell_2}{(2\pi)^D} \frac{\partial}{\partial \ell_i^\mu} \frac{\ell_i^\mu}{[(\ell_1)^2 - m^2]^A [(\ell_2)^2 - m^2]^B [(\ell_1 - \ell_2)^2 - m^2]^C}$$

$$= -4\epsilon V_{A,B,C} - 10m^2 (V_{A+1,B,C} + V_{A,B+1,C} + V_{A,B,C+1}) \,. \tag{3.48}$$

If we set $m = 0$, the above relations imply that $V_{A,B,C} = 0$. The factor (-4ϵ) is expected because the diagonal transformation probes the scaling weight of the integral, which would be exactly zero in $D = 5$. As long as the IBP relations corresponding to the trace part of GL(2) are omitted, the IBP system no longer sets to zero massless vacuum integrals and correctly reflects the ultraviolet poles of these integrals without contamination from IR poles.

The above argument straightfowardly carries over to the five-loop vacuum integrals in $D = 24/5 - 2\epsilon$, since no subdivergences exist in this dimension. The resulting IBP system only involves logarithmically divergent vacuum integrals, and does not include any finite integrals or power-divergent integrals (which do not produce poles in dimensional regularization). This enormously reduces the size of the linear system to be solved.

A useful property of the SL(L)-generated IBP system is that, even though each vacuum integral depends on the dimension D implicitly, the relations between them do not contain any explicit dependence on D [108]. This fact appears to help explain the observations in Section 3.7.

3.6.2   The IBP system at five loops

The complete set of integral topologies—suppressing dots or numerators—that we need to consider for the reduction of the vacuum integrals of the five-loop four-point $\mathcal{N} = 8$ supergravity amplitude is shown in Fig. 3.14. This list does not include any diagram that factorizes, such as those illustrated in Fig. 3.13. It also removes integrals related to kept ones by identities between integrals not isomorphic to each other, such as those illustrated

in Fig. 3.17.

By acting with the SL(5) generators on all logarithmically divergent canonical integrals with up to four dots, we find IBP relations between vacuum integrals with up to five dots, the additional dot following from acting with derivatives on propagators. While such integrals do not appear in the expansion of the integrand in $D = 24/5$, they are necessary for finding the relations between integrals with four dots. We also include relations between integrals generated by graph automorphisms which transform nontrivially the numerator factors, as illustrated in Fig. 3.18. In these relations, all the integrals are mapped to canonical integrals using enhanced graph isomorphisms as described in Section 3.4.3. Because of their similarity with the IBP relations it is convenient to solve them simultaneously. The solution to this system of equations expresses all needed vacuum integrals in terms of master integrals.

As a warm up to setting up and solving the IBP system for the supergravity problem in $D = 24/5$, we solved the much simpler cases of $\mathcal{N} = 8$ supergravity in $D = 22/5$ and $\mathcal{N} = 4$ super-Yang–Mills theory in $D = 26/5$. The integrals which appear in both these simpler cases have at most two dots and thus, the IBP system contains integrals with up to three dots. In the case of $\mathcal{N} = 8$ supergravity in $D = 22/5$, the three-dot system has 44,428 different integrals, and about 1.7×10^5 linear relations generated. The simpler numerator factors of $\mathcal{N} = 4$ super-Yang–Mills make this case much simpler, containing only 5,975 distinct integrals and about 9,900 linear relations between them. The solution of the latter system expresses all the two-dot vacuum integrals, divergent in $D = 26/5$, in terms of the 16 master vacuum integrals displayed in Fig. 3.6.2.

For the main problem of $\mathcal{N} = 8$ supergravity in $D = 24/5$ with the improved integrand obtained in Section 3.3, we have to reduce integrals with up to four dots. There are 141,592 distinct integrals of this type. The relevant five-dot system has 3,687,534 integrals of which 845,323 are distinct. The SL(5) transformations generate about 2.8×10^6 IBP relations, while numerator-changing isomorphisms generate about 9×10^5 further relations. This system is straightforward to solve using sparse Gaussian elimination and finite-field
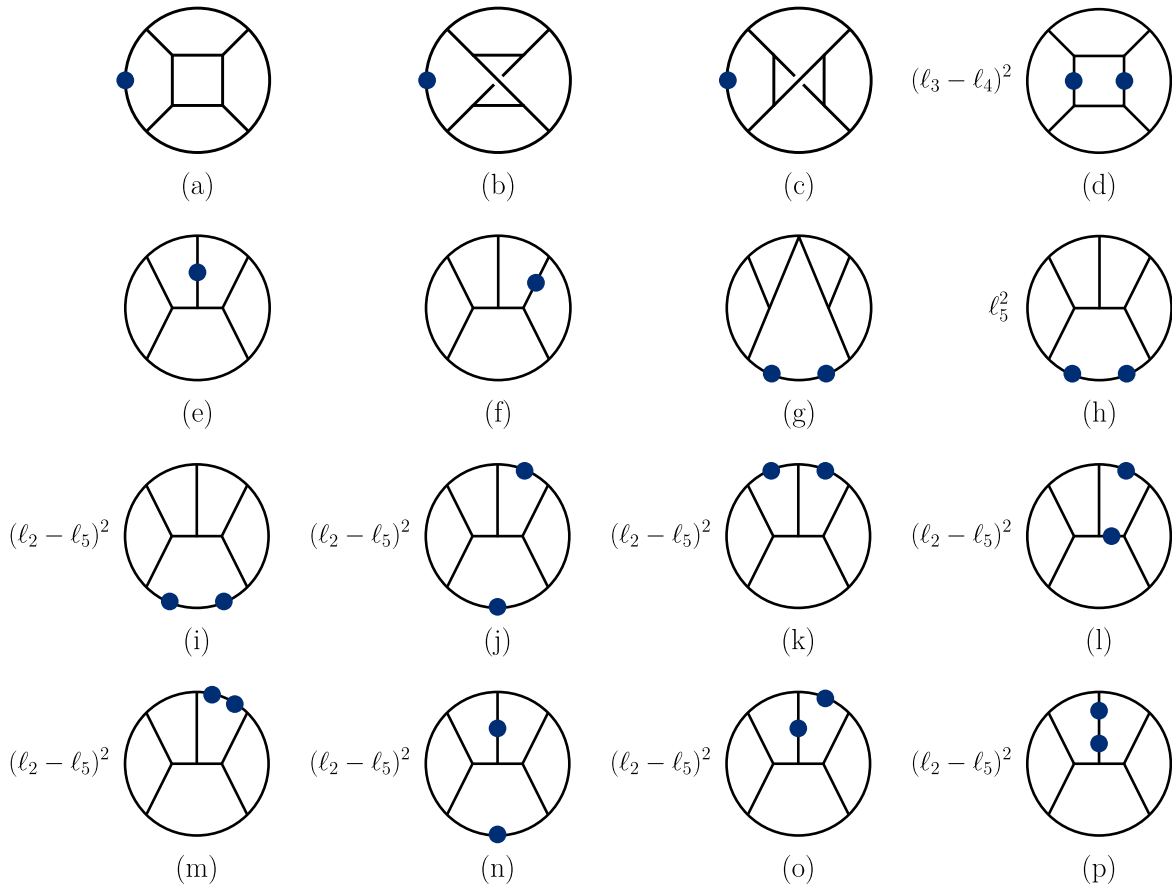
109

Figure 3.20: The sixteen master integrals to which any five-loop vacuum integrals in $\mathcal{N} = 4$ super-Yang–Mills with up to two dots can be reduced. The dots represent repeated propagators. The labels of the diagrams match those of Fig. 3.15.
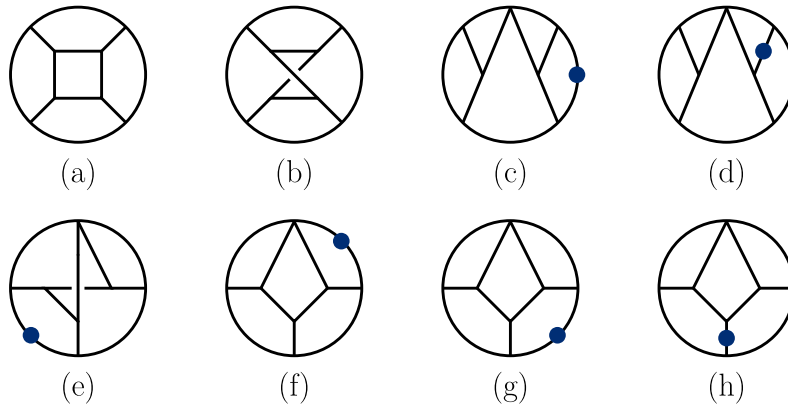

Figure 3.21: The eight master integrals to which any five-loop vacuum integrals in $\mathcal{N} = 8$ supergravity with up to four dots can be reduced. The dots represent repeated propagators.

methods [274, 275]; we used the linear system solver LINBOX [276], and confirmed the solution with FINRED[7] [277]. The result is that all vacuum integrals for the expansion of $\mathcal{N} = 8$ supergravity amplitude in $D = 24/5$ are expressed as linear combinations of the eight master integrals shown in Fig. 3.21.

3.6.3   Result for ultraviolet divergences

As a first test for the full calculation, we used the reduction of the vacuum integrals to verify that our integrand exhibits the known ultraviolet properties in $D = 22/5$. We find that, as expected, all vacuum integrals cancel after IBP reduction, the five-loop four-point $\mathcal{N} = 8$ amplitude is ultraviolet finite,

$$\mathcal{M}_4^{(5)}\Big|_{\text{leading}}^{D=22/5} = 0\,. \tag{3.49}$$

With our new integrand there are few potential contributions because the naive double-copy terms are manifestly ultraviolet finite in $D = 22/5$ and only the contact terms give potential contributions. A similar check is performed for the earlier form of the integrand in Ref. [161], but that case only confirms the cancellation of the vacuum diagrams with the maximum cuts imposed.

As another test of our approach, we also recovered the leading divergence of $\mathcal{N} = 4$ super-Yang–Mills theory in its five-loop critical dimension, $D = 26/5$, originally found in [162]. Starting from our improved $\mathcal{N} = 4$ super-Yang–Mills integrand of Section 3.3, extracting the leading divergence in terms vacuum integrals and then substituting their expressions in terms of master integrals, we obtain

$$\mathcal{A}_4^{(5)}\Big|_{\text{leading}} = \frac{144}{5}g^{12}stA^{\text{tree}}N_c^3\left(N_c^2\includegraphics{box1} + 48\left(\frac{1}{4}\includegraphics{box2} + \frac{1}{2}\includegraphics{box3} + \frac{1}{4}\includegraphics{box4}\right)\right)$$
$$\times\left(t\,\tilde{f}^{a_1a_2b}\tilde{f}^{ba_3a_4} + s\,\tilde{f}^{a_2a_3b}\tilde{f}^{ba_4a_1}\right). \tag{3.50}$$

---

[7]We thank Andreas von Manteuffel and Robert Schabinger for providing us with this program.

111

The $\tilde{f}^{abc}$ are the group structure constants, as normalized below Eq. (3.2), and the s and t are the usual Mandelstam invariants. Here $A^{\mathrm{tree}} \equiv A^{\mathrm{tree}}(1, 2, 3, 4)$ is the color-ordered tree amplitude with the indicated ordering of external legs. This reproduces the result of Ref. [162], providing a nontrivial check of both our gauge-theory integrand construction and IBP reductions methods.

Interestingly, the thirteen master integrals in Fig. 3.6.2 that have vanishing coefficients in Eq. (3.50) violate a "no-one-loop-triangle" rule.[8] Indeed, diagrams (e)-(p) contain one-loop triangle subdiagrams while diagram (d) contains a loop momentum-dependent numerator in one-loop box subdiagrams, which upon expanding and reducing of that one-loop subintegral also leads to triangle subintegrals. Another interesting feature of these results is that the relative factors of the subleading-color term are given by the symmetry factors of the corresponding integrals. In the next section, we will show that these observations are part of a more general pattern.

Extracting the leading ultraviolet terms for $\mathcal{N} = 8$ supergravity in $D = 24/5$ follows the same strategy. After reducing the vacuum integrals obtained from our improved integrand to the basis of master integrals we find

$$\mathcal{M}_4^{(5)}\Big|_{\mathrm{leading}} = -\frac{16 \times 629}{25} \left(\frac{\kappa}{2}\right)^{12} (s^2 + t^2 + u^2)^2 stu M_4^{\mathrm{tree}} \left(\frac{1}{48} \, \boxplus + \frac{1}{16} \, \boxtimes \right). \quad (3.51)$$

This is the same result as obtained in the previous section by assuming that only vacuum diagrams with maximal-cuts contribute, and proves that Eq. (3.42) is complete. As in the case of the reduction of the expansion of the four-point five-loop $\mathcal{N} = 4$ super-Yang–Mills amplitude, all master integrals containing triangle subdiagrams, or with numerators which upon further one-loop reduction lead to triangle subdiagrams, enter with vanishing coefficients. Moreover, similarly to the subleading color in the gauge-theory case, the relative coefficients between the integrals are the symmetry factors of the vacuum diagrams. As we

---

[8]When counting the number of propagators around a loop, each dot should be counted as well.

discuss in the next section, these observations do not appear to be accidental.

The two Wick-rotated vacuum integrals in Eq. (3.51) are both positive definite, proving that no further hidden cancellations are present. We evaluated numerically, using FI-ESTA [278–280], the two master integrals entering Eq. (3.51), given by diagrams (a) and (b) in Fig. 3.21, and find

$$V_5^{(\mathrm{a})} = \frac{1}{(4\pi)^{12}} \frac{0.563}{\epsilon}, \qquad V_5^{(\mathrm{b})} = \frac{1}{(4\pi)^{12}} \frac{0.523}{\epsilon}. \tag{3.52}$$

The dimensional-regularization parameter is $\epsilon = (24/5 - D)/2$. Using Eq. (3.51), the numerical value of the divergence is

$$\mathcal{M}_4^{(5)}\Big|_{\mathrm{leading}} = -17.9 \left(\frac{\kappa}{2}\right)^{12} \frac{1}{(4\pi)^{12}} (s^2 + t^2 + u^2)^2 stu M_4^{\mathrm{tree}} \frac{1}{\epsilon}. \tag{3.53}$$

We leave as a problem for the future the question of obtaining an exact analytic expression instead of the numerical one found here.

3.7 Observations on ultraviolet consistency

Given the wealth of results from previous papers [61, 90, 145–149, 162, 281], as well as those from Section 3.6, we are in the position to search for useful structures that can lead to a more economic identification of the leading ultraviolet behavior of $\mathcal{N} = 4$ super-Yang-Mills theory and $\mathcal{N} = 8$ supergravity. In this section we analyze the available results in both these theories, observing remarkable consistency and recursive properties, whereby leading L-loop ultraviolet divergences in the L-loop critical dimension appear to be tightly constrained by the lower-loop vacuum diagrams describing leading behavior in the lower-loop critical dimension.

First we collect the known results for the leading ultraviolet behavior of both $\mathcal{N} = 4$ super-Yang–Mills theory and $\mathcal{N} = 8$ supergravity. We then demonstrate that appropriately-

defined subdiagrams of the vacuum diagrams are simply related to the vacuum diagrams describing lower-loop leading ultraviolet behavior.

Within the generalized-unitarity method, higher-loop scattering amplitudes are constructed in terms of lower-loop ones. The one-particle cut, setting on shell a single propagator, provides a direct link between L-loop n-point amplitudes and $(L-1)$-loop $(n+2)$-point amplitudes. One may therefore suspect that there may exist a relation between the leading ultraviolet properties of these amplitudes in their respective critical dimensions, which echoes the relation between the complete amplitudes. We will find, however, more surprising consistency relations between the leading ultraviolet behavior of L- and $(L-1)$-loop amplitudes with the same number of external legs for $L \leq 6$ for $\mathcal{N} = 4$ super-Yang-Mills theory and for $L \leq 5$ for $\mathcal{N} = 8$ supergravity. The nontrivial manipulations necessary for extracting the leading ultraviolet divergence adds to the surprising features of these relations. Indeed, without appropriate choices of integral bases, they would be obfuscated. They point to the possibility of a principle governing perturbative consistency in the ultraviolet. We close by noting the possibility that one may exploit these patterns to directly make detailed predictions of ultraviolet properties at higher loop orders.

3.7.1 Review of results

After IBP reduction, we obtain a simple description of the leading ultraviolet behavior in terms of a set of master vacuum integrals defined as

$$V = -i^{L+\sum_j A_j} \int \prod_{i=1}^{L} \frac{d^D \ell_i}{(2\pi)^D} \prod_j \frac{1}{(p_j^2 - m^2)^{A_j}} \, , \tag{3.54}$$

where the p_i are linear combinations of the independent loop momenta and the A_i are the propagators' exponents. The number of dots on propagator j is $A_j - 1$ for $A_j \geq 2$ The indices can be negative, in which case they represent irreducible numerators, as discussed in Section 3.6. While there is no need to explicitly introduce a mass regulator for carrying out

114

Loops	D_c for $\mathcal{N} = 4$ sYM	D_c for $\mathcal{N} = 8$ sugra
1	8	8
2	7	7
3	6	6
4	11/2	11/2
5	26/5	24/5
6	5	—

Table 3.2: The critical dimensions where ultraviolet divergences first occur in $\mathcal{N} = 4$ super Yang–Mills theory and $\mathcal{N} = 8$ supergravity, as determined by explicit calculations.

the IBP reductions, we do so here to make the integrals well defined in the infrared.

Collecting the results from Refs. [61, 90, 145–148] and from Eq. (3.51), the leading ultraviolet behavior of $\mathcal{N} = 8$ supergravity at each loop order through five loops is described by vacuum diagrams as

$$\mathcal{M}_4^{(1)}\Big|_{\text{leading}} = -3\,\mathcal{K}_{\text{G}}\left(\frac{\kappa}{2}\right)^4 \,\, \bigcirc \,\, ,$$

$$\mathcal{M}_4^{(2)}\Big|_{\text{leading}} = -8\,\mathcal{K}_{\text{G}}\left(\frac{\kappa}{2}\right)^6 (s^2 + t^2 + u^2)\left(\frac{1}{4}\,\ominus + \frac{1}{4}\,\ominus\right),$$

$$\mathcal{M}_4^{(3)}\Big|_{\text{leading}} = -60\,\mathcal{K}_{\text{G}}\left(\frac{\kappa}{2}\right)^8 \, stu\left(\frac{1}{6}\,\ominus + \frac{1}{2}\,\ominus\right),$$

$$\mathcal{M}_4^{(4)}\Big|_{\text{leading}} = -\frac{23}{2}\,\mathcal{K}_{\text{G}}\left(\frac{\kappa}{2}\right)^{10} (s^2 + t^2 + u^2)^2 \left(\frac{1}{4}\,\triangle + \frac{1}{2}\,\triangle + \frac{1}{4}\,\triangle\right),$$

$$\mathcal{M}_4^{(5)}\Big|_{\text{leading}} = -\frac{16 \times 629}{25}\,\mathcal{K}_{\text{G}}\left(\frac{\kappa}{2}\right)^{12} (s^2 + t^2 + u^2)^2 \left(\frac{1}{48}\,\boxdot + \frac{1}{16}\,\boxtimes\right), \quad (3.55)$$

where the universal factor is $\mathcal{K}_{\text{G}} \equiv stu\,M_4^{\text{tree}}(1, 2, 3, 4)$. For each loop order, the critical dimension is different and is summarized in Table 3.2.

We also collect all known vacuum graph expressions of the leading ultraviolet behavior

in the maximally supersymmetric $SU(N_c)$ Yang-Mills theory [61, 90, 145, 149, 162, 281],

$$\mathcal{A}_4^{(1)}\Big|_{\text{leading}} = g^4 \mathcal{K}_{\text{YM}} \left(N_c(\tilde{f}^{a_1 a_2 b}\tilde{f}^{b a_3 a_4} + \tilde{f}^{a_2 a_3 b}\tilde{f}^{b a_4 a_1}) - 3 B^{a_1 a_2 a_3 a_4} \right) \bigcirc ,$$

$$\mathcal{A}_4^{(2)}\Big|_{\text{leading}} = -g^6 \mathcal{K}_{\text{YM}} \left[F^{a_1 a_2 a_3 a_4}\left(N_c^2 \; \bigcirc + 48 \left(\frac{1}{4}\; \bigcirc + \frac{1}{4}\; \bigcirc \right)\right) \right.$$
$$\left. + 48\, N_c\, G^{a_1 a_2 a_3 a_4}\left(\frac{1}{4}\; \bigcirc + \frac{1}{4}\; \bigcirc \right)\right] ,$$

$$\mathcal{A}_4^{(3)}\Big|_{\text{leading}} = 2\, g^8 \mathcal{K}_{\text{YM}}\, N_c F^{a_1 a_2 a_3 a_4}\left(N_c^2 \; \bigcirc + 72\left(\frac{1}{6}\; \bigcirc + \frac{1}{2}\; \bigcirc \right)\right) , \qquad (3.56)$$

$$\mathcal{A}_4^{(4)}\Big|_{\text{leading}} = -6\, g^{10} \mathcal{K}_{\text{YM}}\, N_c^2 F^{a_1 a_2 a_3 a_4}\left(N_c^2 \; \bigcirc + 48\left(\frac{1}{4}\; \bigcirc + \frac{1}{2}\; \bigcirc + \frac{1}{4}\; \bigcirc \right)\right) ,$$

$$\mathcal{A}_4^{(5)}\Big|_{\text{leading}} = \frac{144}{5} g^{12}\mathcal{K}_{\text{YM}}\, N_c^3\, F^{a_1 a_2 a_3 a_4}\left(N_c^2 \; \bigcirc + 48\left(\frac{1}{4}\; \bigcirc + \frac{1}{2}\; \bigcirc + \frac{1}{4}\; \bigcirc \right)\right) ,$$

$$A_4^{(6)}\Big|_{\text{leading}} = -120 g^{14}\mathcal{K}_{\text{YM}}\, F^{a_1 a_2 a_3 a_4} N_c^6 \left(\frac{1}{2}\; \bigcirc + \frac{1}{4}(\ell_1 + \ell_2)^2 \; \bigcirc - \frac{1}{20}\; \bigcirc \right)$$
$$+ \mathcal{O}(N_c^4) ,$$

where the universal factor is $\mathcal{K}_{\text{YM}} \equiv st\, A_4^{\text{tree}}(1, 2, 3, 4)$, and

$$F^{a_1 a_2 a_3 a_4} \equiv t\, \tilde{f}^{a_1 a_2 b}\tilde{f}^{b a_3 a_4} + s\, \tilde{f}^{a_2 a_3 b}\tilde{f}^{b a_4 a_1} ,$$

$$G^{a_1 a_2 a_3 a_4} \equiv s\, \delta^{a_1 a_2}\delta^{a_3 a_4} + t\, \delta^{a_4 a_1}\delta^{a_2 a_3} + u\, \delta^{a_1 a_3}\delta^{a_2 a_4} ,$$

$$B^{a_1 a_2 a_3 a_4} \equiv \tilde{f}^{a_1 b_1 b_2}\tilde{f}^{a_2 b_2 b_3}\tilde{f}^{a_3 b_3 b_4}\tilde{f}^{a_4 b_4 b_1} . \qquad (3.57)$$

As before, $\tilde{f}^{abc}$ are the group structure constants, with normalization given below Eq. (3.2). As in the gravity case, the critical dimension at each loop order is different, and is included in Table 3.2.

Inspecting Eqs. (3.55) and (3.56) we already note a remarkable property in both the supergravity and subleading color gauge-theory expressions: the relative coefficients between

vacuum integrals in these representations, ignoring signs, are given by the symmetry factors of the corresponding vacuum graphs. For example, at five loops in Eq. (3.55), the first vacuum graph has 48 automorphisms and the second has 16 automorphisms, matching the relative factors. While the amplitude has such coefficients for each integral (see e.g. Eq. (3.23)), their appearance in the leading ultraviolet divergence is unexpected due to both the nontrivial manipulations and the choices of master integrals that are required to arrive at the final result.

Further inspection of Eqs. (3.55) and (3.56) reveals further interesting structures, showing that the relative coefficients of vacuum integrals are consistently related between the different loop orders.

3.7.2 Observed ultraviolet consistency

An L-loop (vacuum) integral has many $L' < L$ subintegrals. A way to isolate one and expose its associated ultraviolet properties is to take its loop momenta to be much larger than the other $(L - L')$ ones. We define an L'-loop subdiagram of an L-loop diagram as the sum over all of its L'-loop subintegrals. Since each subintegral may have a different critical dimension, the critical dimension of an L'-loop subdiagram is the minimum of the critical dimensions of all the L'-loop subintegrals.

With this definition, to compare the higher- and lower-loop leading ultraviolet properties of four-point amplitudes we carry out the following steps:

1. For each L-loop vacuum diagram construct its L'-loop subdiagram.

2. Keep only those contributions with leading ultraviolet behavior, i.e. those that are divergent in the lowest critical dimension

3. Apply IBP identities, as needed, to map the lower-loop vacuum integrals into the same vacuum integral basis as the one used in the ultraviolet expansion of the lower-loop amplitude.

117

As we now show by example, every result in Eqs. (3.55) and (3.56) supports the observation that the leading ultraviolet behavior at L and L' loops in their respective critical dimensions are consistent.

To see the power of this observation, consider the all-order constraints from one-loop subdiagrams. From Eqs. (3.55) and (3.56), we see that the one-loop leading ultraviolet divergence is given by a vacuum integral with four propagators. For the higher-loop vacuums this amounts to the statement that there exists an integral basis such that all one-loop subloops of any higher loop vacuum must contain at least four propagators.[9] This is equivalent to the no-triangle property of one-loop amplitudes in both $\mathcal{N} = 8$ and $\mathcal{N} = 4$ super-Yang–Mills amplitudes [282–285], except that here it applies to the reduction to an integral basis of the vacuum integrals describing the leading ultraviolet behavior. One-loop subgraphs with more than four propagators give a subleading behavior which we discard according to our procedure which focus on the leading ultraviolet properties. Because there is only a single type of leading one-loop subdiagram, this property of one-loop sub-graphs places no constraint on the relative coefficients of the higher loop vacuums. Nevertheless, the constraint that each one-loop subgraph has at least four propagators is extremely powerful. In particular, as discussed in Section 3.6, the only integrals in our basis of five-loop vacuum integrals without triangle subdiagrams are the two five-loop integrals contributing to Eq. (3.55). A similar property holds for $\mathcal{N} = 4$ super-Yang–Mills theory, where the only five-loop vacuum integral basis elements without any triangle or bubble subintegrals are the ones appearing in Eq. (3.56). This is quite a remarkable property because, in an appropriately-chosen integral basis that maximizes the number of one-loop triangle and bubble sub-integrals, it severely limits the vacuum integrals that can appear in the final expressions.

While the one-loop properties discussed above should hold for each one-loop subintegral at any loop order, understanding the consequences of higher-loop ultraviolet divergences

---

[9]In an arbitrary integral basis this property is not manifest and emerges only after the summation over all one-loop subintegrals of all diagrams and reduction to a one-loop integral basis.

in (3.55) and (3.56) can be best appreciated via a case by case analysis. We choose three illustrative examples. We begin by showing the consistency of subleading-color $\mathcal{N} = 4$ super-Yang–Mills between five and four loops. We focus on the subleading-color part, because it has a more complex structure than the leading-color part and it is similar to the supergravity case. We then examine the consistency of the four-loop ultraviolet divergences with those at lower loops, which are the same for the $\mathcal{N} = 4$ super-Yang–Mills theory at subleading color and the $\mathcal{N} = 8$ supergravity. Last, we discuss the five-to-four loop consistency of our results for the five-loop $\mathcal{N} = 8$ supergravity.

As mentioned earlier, not all terms in the sum that defines a lower-loop subdiagram have the same critical dimension. For example, when relating L and $(L - 1)$-loop diagrams, excluding a dotted propagator leads to a term with a lower critical dimension than one obtained by excluding an undotted one. Thus, when focusing on the ultraviolet critical dimension of lower-loop diagrams it suffices to keep only terms obtained by disconnecting the propagators with the largest number of dots. Once the subdiagrams are identified, we can compare them to the lower-loop result by treating the subdiagram as a new vacuum diagram where we have kept the leading order in small-momentum expansion for the excluded leg. This results in lower-loop vacuum diagrams with dots on the propagators where the excluded leg is connected to the subgraph.

For the $\mathcal{N} = 4$ super-Yang–Mills five-loop vacuum diagrams, the leading four-loop subdiagrams are all those that exclude the leg that carries the dot. Diagrammatically, we write

$$\text{(3.58)}$$

Excluding the propagator outside the dashed box and taking its momentum small compared

to the remaining ones leads to

$$\rightarrow \frac{1}{4} \quad + \frac{1}{2} \quad + \frac{1}{4} \quad . \tag{3.59}$$

This exactly matches the subleading-color four-loop vacuum diagrams describing their relative coefficients in Eq. (3.56).

Showing the consistency of the four loop expression with lower loops follows similar steps. Now there are two dotted legs that can be excluded. Summing over the two expansions of each subdiagram, we find

$$\rightarrow 2 \quad , \qquad \rightarrow 2 \quad , \qquad \rightarrow 2 \quad . \tag{3.60}$$

Using this we see that the subdiagrams match the relative factors and three-loop vacuum diagrams in Eq. (3.56),

$$\rightarrow 3 \left(\frac{1}{6} \quad + \frac{1}{2} \quad \right) . \tag{3.61}$$

Additionally, we can extract the two-loop subdiagrams in the four-loop divergence by expanding around both dotted propagators. This gives,

$$\rightarrow \quad , \qquad \rightarrow \quad , \qquad \rightarrow \quad . \tag{3.62}$$

Using this we find that with the relative coefficients from the four-loop expression, these subdiagrams are also consistent with the leading lower-loop behavior

$$\rightarrow \frac{1}{4} \quad + \frac{1}{4} \quad . \tag{3.63}$$

120

It is straightforward to confirm that the same relative coefficients arise by starting from the three-loop expression in Eq. (3.61) and extracting the leading two-loop subdiagrams.

Since master integrals giving the ultraviolet divergence of the five-loop supergravity amplitude in $D = 24/5$ do not have doubled propagators, all ways of excluding one propagator lead to integrals of the same critical dimension and must therefore be kept. The planar diagram is a cube, so all of its edges are equivalent. Summing over all the four-loop subintegrals leads to

$$\text{(diagram)} \rightarrow 12 \, \text{(diagram)}. \tag{3.64}$$

The nonplanar diagram has two inequivalent types of legs to exclude. There are eight legs that, when expanded around, lead to a planar four-loop subdiagram. The other four legs lead to a nonplanar subdiagram. Thus, after isomorphisms, the subintegrals of the nonplanar five-loop diagram contribute

$$\text{(diagram)} \rightarrow 8 \, \text{(diagram)} + 4 \, \text{(diagram)}. \tag{3.65}$$

After accounting for the relative symmetry factors of $1/48$ and $1/16$ between the two five-loop diagrams in Eq. (3.55), we get

$$\text{(diagram)} \rightarrow \frac{1}{4} \, \text{(diagram)} + \frac{1}{2} \, \text{(diagram)} + \frac{1}{4} \, \text{(diagram)}, \tag{3.66}$$

matching the relative factors between the four-loop vacuum diagrams also given in Eq. (3.55).

Through four loops super-Yang–Mills subleading-color and supergravity divergences follow the same pattern, being related between different loop orders by removing a dotted propagator. While in both theories the consistency relations hold at five loops as well, they now involve removing a dotted and an undotted propagator, respectively. The additional propagator in the gauge-theory expression raises its critical dimension to $D = 26/5$. It is re-

markable that, even though the various integrals and symmetry factors at five loops differ in the two theories, consistency requires that the relative coefficients for four-loop subdiagrams are the same.

Let us elaborate briefly on the structure of the planar $\mathcal{N} = 4$ super-Yang–Mills vacuum integrals at six loops. Unlike the previous examples, the lower-loop integrals given by our construction are not among the five-loop master integrals in Fig. 3.6.2 and a comparison with the five-loop expression (3.56) requires use of IBP identities. As in the five-to-four loop relation, the integrals with lowest critical dimension arise from subdiagrams that exclude the doubled propagator in the six-loop vacuum diagrams. Thus, the leading five-loop subdiagram result is

$$
\boxed{\bigcirc\!\!\!\bigcirc} \rightarrow \frac{1}{2}\, \bigcirc\!\!\!\diamondsuit\!\!\!\bigcirc + \frac{1}{4}\,(\ell_1 + \ell_2)^2 \underset{2\ \ \ \ 1}{\bigcirc\!\!\!\square\!\!\!\bigcirc} + \text{subleading color} . \tag{3.67}
$$

Using an integration-by-parts relation (see Eq. (4) of Ref. [162])

$$
\frac{1}{2}\, \bigcirc\!\!\!\diamondsuit\!\!\!\bigcirc + \frac{1}{4}(\ell_1 + \ell_2)^2 \underset{2\ \ \ \ 1}{\bigcirc\!\!\!\square\!\!\!\bigcirc} = \frac{6}{5}\, \bigcirc\!\!\!\square\!\!\!\bigcirc , \tag{3.68}
$$

to map (3.67) to the five-loop integral basis, we find that it is proportional to the five-loop leading color term in Eq. (3.56). It is gratifying that the subdiagram consistency holds even if not initially obvious.

3.7.3   Applications

The consistency observations discussed above give us additional confidence that we have correctly computed the leading ultraviolet behavior of $\mathcal{N} = 8$ supergravity at five loops by showing that in the sense discussed above, it fits the pattern of ultraviolet properties at all lower loops. The simple structures at the vacuum diagram level uncovered here also

offers the exciting possibility of probing seemingly out of reach ultraviolet properties at even higher loops. Apart from the possibility of imposing them on an ansatz for the leading ultraviolet terms of gauge and gravity amplitudes, we can use them to simplify the IBP system by focusing only on the vacuum integrals that are expected to appear. For example, in Section 3.5 we vastly simplified the five-loop $\mathcal{N} = 8$ IBP system by assuming that only the vacuum integrals with maximal cuts survive in the final result. As emphasized above, this condition follows from demanding consistency of the five-loop vacuum master diagrams with one-loop subdiagrams, which rules out one-loop triangle subgraphs and all but two five-loop master vacuum diagrams in the basis of Fig. 3.21. More importantly this condition eliminates nearly all integrals from the IBP system as well as a substantial part of the expansion of the integrand. The same strategy should continue to be fruitful at even higher loop orders. Alternatively, it may be possible to completely bypass the construction of the integrand, its ultraviolet expansion and integration, and instead extrapolate the final result in terms of vacuum diagrams to higher loop orders. We leave this task for future study.

We emphasize that the observed ultraviolet consistency is a property of the leading behavior after simplifying the integrals via Lorentz invariance and integration-by-parts relations. It relies on nontrivial simplifications that occur in the integral reduction and is manifest because we judiciously chose the vacuum integral bases. A key property of our IBP systems is that the space-time dimension enters only implicitly through the critical dimension where the integrals are logarithmically divergent. Had there been explicit dependence on the dimension, one would naturally expect a nontrivial dependence on dimension in the relative coefficients of master integrals and thus, given the differing critical dimensions at different loop orders, it would disrupt any systematic cross-loop-order relations. Simplifications based on Lorentz invariance in Eqs. (3.28) and (3.29) were used, and introduce explicit dependence on dimension. It is rather striking that this dependence drops out once the IBP relations are used and consequently it does not complicate relations between vacuum diagrams and their subdiagrams. These properties are worth investigating.

3.8 Conclusions and outlook

In this chapter we determined the ultraviolet behavior of the five-loop four-point amplitude of $\mathcal{N} = 8$ supergravity, finding the critical dimension where it first diverges to be $D_c = 24/5$. In analyzing the results we made the rather striking observation that the vacuum diagrams that describe the leading ultraviolet behavior satisfy certain nontrivial relations to the analogous lower-loop vacuum diagrams.

Previous work found examples of enhanced ultraviolet cancellations that render ultraviolet finite [4, 6] certain amplitudes in $\mathcal{N} = 4$ and $\mathcal{N} = 5$ supergravity in $D = 4$, despite the possibility of counterterms allowed by all known symmetry considerations [7–9, 144]. Related arguments suggest that $\mathcal{N} = 8$ supergravity should diverge at five loops in $D = 24/5$ [142, 143]. While one might have suspected that there could be corresponding enhanced cancellations in $\mathcal{N} = 8$ supergravity at five loops, our results conclusively demonstrate that, at this loop order, there are no further cancellations of ultraviolet divergences beyond those identified by symmetry arguments.

The divergence we find in $D = 24/5$ at five loops corresponds to a $D^8 R^4$ counterterm. This counterterm is especially interesting because it corresponds to a potential $D = 4$ divergence believed to be consistent with the $E_{7(7)}$ duality symmetry of maximal supergravity. It is, however, not clear that our result in $D = 24/5$ points towards a seven-loop divergence in $D = 4$, because the existence of counterterms does not transfer trivially between dimensions and loop orders. For example, one might be tempted to argue for a three-loop divergence in $\mathcal{N} = 4$ or $\mathcal{N} = 5$ supergravity in $D = 4$ based on the existence [5] of a nonvanishing one-loop R^4 counterterm in $D = 8$ in both theories; we know however that both theories are finite at three loops [4, 6]. Another result that indicates that further investigation of the ultraviolet structure of supergravities in four dimensions is warranted is the suspected link between anomalies and divergences in supergravity theories on the one hand, and the anticipated lack of anomalies in theories with $\mathcal{N} \geq 5$ supersymmetry on the other [2, 68–71, 111, 124].

Of course, not every divergence necessarily has an anomaly behind it. Nevertheless, it is surprising that $\mathcal{N} = 5$ supergravity at four loops in $D = 4$ appear to have additional cancellations beyond those predicted by symmetry considerations [6], while $\mathcal{N} = 8$ supergravity at five loops in $D = 24/5$ does not.

The ultraviolet properties of the amplitude were extracted, following standard methods [257–259], by expanding the integrand at large loop momenta or equivalently small external momenta, to identify the logarithmic divergences in various dimensions. The result was then reduced to a combination of master integrals; to this end we made use of modern ideas of organizing the system of IBP identities in terms of an $\mathrm{SL}(L)$ symmetry [108] (where L is the number of loops) and restricting to integrals with leading ultraviolet behavior. In addition to integrating the complete expansion of a new integrand in both $D = 22/5$ and $D = 24/5$, we also integrated the expansion of the previously-obtained integrand [161] in these dimensions, under the assumption that the only master integrals that appear in the final result have maximal cuts. These results, obtained by using unitarity-compatible integration-by-parts techniques [175, 183–188], agree with those of the full integration of the simpler integrand, thus providing a highly nontrivial check of our calculations.

The agreement of the two approaches highlights an important trend: the only integrals that contribute to the divergence of the four-point $1 \leq L \leq 5$ amplitudes in their critical dimensions are those with maximal cuts at the vacuum level. At higher loops we expect a systematic application of similar considerations to lead to a drastic reduction in the computational complexity. An approach based on exploiting these observations may make it possible to directly determine the critical dimension of the six- and seven-loop $\mathcal{N} = 8$ supergravity amplitudes.

An even greater efficiency gain may lie in the observed ultraviolet consistency relations described in Section 3.7. That is, L'-loop subdiagrams of the leading ultraviolet divergence in the L-loop critical dimension reproduce, upon reduction to master integrals, the combination of vacuum diagrams describing the leading ultraviolet behavior in the L'-loop critical

dimension. Moreover, in an appropriate basis, the relative coefficients of the vacuum master integrals are given by the order of the automorphism groups of the diagrams. We also observed similar patterns in the vacuum diagrams of $\mathcal{N} = 4$ super-Yang–Mills theory through six loops, suggesting that they will continue to hold to higher loop orders in both theories. While these observations are likely connected to standard consistency relations between multi-loop amplitudes and their subamplitudes, in our case they remain a conjecture due to the nontrivial steps needed to relate an amplitude to a basis of master vacuum graphs in the critical dimension. These vacuum diagram patterns should be very helpful to identify those terms in higher-loop amplitudes that are important for determining the leading ultraviolet behavior, and for enormously simplifying the integration-by-parts system. By enforcing the patterns described here, it may even be possible to obtain detailed higher-loop information including a determination of the critical dimensions, bypassing the construction of complete loop integrands.

In summary, the success of the newly-developed generalized double-copy construction [60, 161], and integration tools [108, 175–188, 274–277] used in our five-loop calculations, as well as our observed vacuum subdiagram consistency constraints, indicates that problems as challenging as seven-loop $\mathcal{N} = 8$ supergravity in four dimensions may now be within reach of direct investigations.

Bibliography

[1] Z. Bern, H.-H. Chi, L. Dixon, and A. Edison, "Two-Loop Renormalization of Quantum Gravity Simplified", Phys. Rev. **D95**, 046013 (2017), arXiv:1701.02422 [hep-th].

[2] Z. Bern, A. Edison, D. Kosower, and J. Parra-Martinez, "Curvature-squared multiplets, evanescent effects, and the U(1) anomaly in $N = 4$ supergravity", Phys. Rev. **D96**, 066004 (2017), arXiv:1706.01486 [hep-th].

[3] Z. Bern, J. J. Carrasco, W.-M. Chen, A. Edison, H. Johansson, J. Parra-Martinez, R. Roiban, and M. Zeng, "Ultraviolet Properties of $\mathcal{N} = 8$ Supergravity at Five Loops", Phys. Rev. **D98**, 086021 (2018), arXiv:1804.09311 [hep-th].

[4] Z. Bern, S. Davies, T. Dennen, and Y.-t. Huang, "Absence of Three-Loop Four-Point Divergences in N=4 Supergravity", Phys. Rev. Lett. **108**, 201301 (2012), arXiv:1202.3423 [hep-th].

[5] Z. Bern, S. Davies, T. Dennen, and Y.-t. Huang, "Ultraviolet Cancellations in Half-Maximal Supergravity as a Consequence of the Double-Copy Structure", Phys. Rev. **D86**, 105014 (2012), arXiv:1209.2472 [hep-th].

[6] Z. Bern, S. Davies, and T. Dennen, "Enhanced ultraviolet cancellations in $\mathcal{N} = 5$ supergravity at four loops", Phys. Rev. **D90**, 105011 (2014), arXiv:1409.3089 [hep-th].

[7] G. Bossard, P. S. Howe, and K. S. Stelle, "Anomalies and divergences in N=4 supergravity", Phys. Lett. **B719**, 424 (2013), arXiv:1212.0841 [hep-th].

[8] G. Bossard, P. S. Howe, and K. S. Stelle, "Invariants and divergences in half-maximal supergravity theories", JHEP **07**, 117 (2013), arXiv:1304.7753 [hep-th].

[9] Z. Bern, S. Davies, and T. Dennen, "The Ultraviolet Structure of Half-Maximal Supergravity with Matter Multiplets at Two and Three Loops", Phys. Rev. **D88**, 065007 (2013), arXiv:1305.4876 [hep-th].

[10] M. H. Goroff and A. Sagnotti, "QUANTUM GRAVITY AT TWO LOOPS", Phys. Lett. **160B**, 81 (1985).

[11] M. H. Goroff and A. Sagnotti, "The Ultraviolet Behavior of Einstein Gravity", Nucl. Phys. **B266**, 709 (1986).

[12] A. E. M. van de Ven, "Two loop quantum gravity", Nucl. Phys. **B378**, 309 (1992).

[13] Z. Bern, C. Cheung, H.-H. Chi, S. Davies, L. Dixon, and J. Nohle, "Evanescent Effects Can Alter Ultraviolet Divergences in Quantum Gravity without Physical Consequences", Phys. Rev. Lett. **115**, 211301 (2015), arXiv:1507.06118 [hep-th].

[14] G. 't Hooft and M. J. G. Veltman, "One loop divergencies in the theory of gravitation", Ann. Inst. H. Poincare Phys. Theor. **A20**, 69 (1974).

[15] M. J. Duff and P. van Nieuwenhuizen, "Quantum Inequivalence of Different Field Representations", Phys. Lett. **94B**, 179 (1980).

[16] E. Sezgin and P. van Nieuwenhuizen, "Renormalizability Properties of Antisymmetric Tensor Fields Coupled to Gravity", Phys. Rev. **D22**, 301 (1980).

[17] E. S. Fradkin and A. A. Tseytlin, "One Loop Infinities in Dimensionally Reduced Supergravities", Phys. Lett. **137B**, 357 (1984).

[18] W. Siegel, "Quantum Equivalence of Different Field Representations", Phys. Lett. **103B**, 107 (1981).

[19] E. S. Fradkin and A. A. Tseytlin, "Quantum Equivalence of Dual Field Theories", Annals Phys. **162**, 31 (1985).

[20] M. T. Grisaru, N. K. Nielsen, W. Siegel, and D. Zanon, "Energy Momentum Tensors, Supercurrents, (Super)traces and Quantum Equivalence", Nucl. Phys. **B247**, 157 (1984).

[21] A. J. Buras and P. H. Weisz, "QCD Nonleading Corrections to Weak Decays in Dimensional Regularization and 't Hooft-Veltman Schemes", Nucl. Phys. **B333**, 66 (1990).

[22] M. J. Dugan and B. Grinstein, "On the vanishing of evanescent operators", Phys. Lett. **B256**, 239 (1991).

[23] I. Jack, D. R. T. Jones, and K. L. Roberts, "Equivalence of dimensional reduction and dimensional regularization", Z. Phys. **C63**, 151 (1994), arXiv:`hep-ph/9401349` `[hep-ph]`.

[24] S. Herrlich and U. Nierste, "Evanescent operators, scheme dependences and double insertions", Nucl. Phys. **B455**, 39 (1995), arXiv:`hep-ph/9412375` `[hep-ph]`.

[25] R. Harlander, P. Kant, L. Mihaila, and M. Steinhauser, "Dimensional Reduction applied to QCD at three loops", JHEP **09**, 053 (2006), arXiv:`hep-ph/0607240` `[hep-ph]`.

[26] O. Aharony and Z. Komargodski, "The Effective Theory of Long Strings", JHEP **05**, 118 (2013), arXiv:`1302.6257` `[hep-th]`.

[27] D. M. Capper and M. J. Duff, "Trace anomalies in dimensional regularization", Nuovo Cim. **A23**, 173 (1974).

[28] D. M. Capper and M. J. Duff, "Conformal Anomalies and the Renormalizability Problem in Quantum Gravity", Phys. Lett. **A53**, 361 (1975).

[29] H.-S. Tsao, "Conformal Anomalies in a General Background Metric", Phys. Lett. **68B**, 79 (1977).

[30] G. W. Gibbons, S. W. Hawking, and M. J. Perry, "Path Integrals and the Indefiniteness of the Gravitational Action", Nucl. Phys. **B138**, 141 (1978).

[31] R. Critchley, "Trace Anomaly for Gravitons", Phys. Rev. **D18**, 1849 (1978).

[32] D. M. Capper and D. Kimber, "An Ambiguity in One Loop Quantum Gravity", J. Phys. **A13**, 3671 (1980).

[33] P. van Nieuwenhuizen and C. C. Wu, "On Integral Relations for Invariants Constructed from Three Riemann Tensors and their Applications in Quantum Gravity", J. Math. Phys. **18**, 182 (1977).

[34] M. L. Mangano and S. J. Parke, "Multiparton amplitudes in gauge theories", Phys. Rept. **200**, 301 (1991), arXiv:`hep-th/0509223` `[hep-th]`.

[35] Z. Bern, J. J. M. Carrasco, and H. Johansson, "New Relations for Gauge-Theory Amplitudes", Phys. Rev. **D78**, 085011 (2008), arXiv:`0805.3993` `[hep-ph]`.

[36] Z. Bern, J. J. M. Carrasco, and H. Johansson, "Perturbative Quantum Gravity as a Double Copy of Gauge Theory", Phys. Rev. Lett. **105**, 061602 (2010), arXiv:`1004.0476` `[hep-th]`.

[37] M. J. Duff, "Twenty years of the Weyl anomaly", Class. Quant. Grav. **11**, 1387 (1994), arXiv:`hep-th/9308075` `[hep-th]`.

[38] M. T. Grisaru, H. N. Pendleton, and P. van Nieuwenhuizen, "Supergravity and the S Matrix", Phys. Rev. **D15**, 996 (1977).

[39] M. T. Grisaru and H. N. Pendleton, "Some Properties of Scattering Amplitudes in Supersymmetric Theories", Nucl. Phys. **B124**, 81 (1977).

[40] S. J. Parke and T. R. Taylor, "Perturbative QCD Utilizing Extended Supersymmetry", Phys. Lett. **157B**, 81 (1985).

[41] E. Tomboulis, "On the Two Loop Divergences of Supersymmetric Gravitation", Phys. Lett. **67B**, 417 (1977).

[42] M. T. Grisaru, "Two Loop Renormalizability of Supergravity", Phys. Lett. **66B**, 75 (1977).

[43] Z. Bern, S. Davies, T. Dennen, Y.-t. Huang, and J. Nohle, "Color-Kinematics Duality for Pure Yang-Mills and Gravity at One and Two Loops", Phys. Rev. **D92**, 045041 (2015), arXiv:1303.6605 [hep-th].

[44] D. C. Dunbar and P. S. Norridge, "Calculation of graviton scattering amplitudes using string based methods", Nucl. Phys. **B433**, 181 (1995), arXiv:hep-th/9408014 [hep-th].

[45] D. C. Dunbar, G. R. Jehu, and W. B. Perkins, "Two-loop six gluon all plus helicity amplitude", Phys. Rev. Lett. **117**, 061602 (2016), arXiv:1605.06351 [hep-th].

[46] D. C. Dunbar, G. R. Jehu, and W. B. Perkins, "The two-loop n-point all-plus helicity amplitude", Phys. Rev. **D93**, 125006 (2016), arXiv:1604.06631 [hep-th].

[47] H. Kawai, D. C. Lewellen, and S. H. H. Tye, "A Relation Between Tree Amplitudes of Closed and Open Strings", Nucl. Phys. **B269**, 1 (1986).

[48] F. A. Berends, W. T. Giele, and H. Kuijf, "On relations between multi - gluon and multigraviton scattering", Phys. Lett. **B211**, 91 (1988).

[49] Z. Bern, L. Dixon, M. Perelstein, and J. S. Rozowsky, "Multileg one loop gravity amplitudes from gauge theory", Nucl. Phys. **B546**, 423 (1999), arXiv:hep-th/9811140 [hep-th].

[50] W. A. Bardeen, "Selfdual Yang-Mills theory, integrability and multiparton amplitudes", Prog. Theor. Phys. Suppl. **123**, 1 (1996).

[51] D. Cangemi, "Selfdual Yang-Mills theory and one loop like - helicity QCD multi - gluon amplitudes", Nucl. Phys. **B484**, 521 (1997), arXiv:hep-th/9605208 [hep-th].

[52] D. Cangemi, "Selfduality and maximally helicity violating QCD amplitudes", Int. J. Mod. Phys. **A12**, 1215 (1997), arXiv:hep-th/9610021 [hep-th].

[53] S. Weinberg, "Infrared photons and gravitons", Phys. Rev. **140**, B516 (1965).

[54] S. G. Naculich and H. J. Schnitzer, "Eikonal methods applied to gravitational scattering amplitudes", JHEP **05**, 087 (2011), arXiv:1101.1524 [hep-th].

[55] S. G. Naculich, H. Nastase, and H. J. Schnitzer, "All-loop infrared-divergent behavior of most-subleading-color gauge-theory amplitudes", JHEP **04**, 114 (2013), arXiv:1301.2234 [hep-th].

[56] R. Akhoury, R. Saotome, and G. Sterman, "Collinear and Soft Divergences in Perturbative Quantum Gravity", Phys. Rev. **D84**, 104040 (2011), arXiv:1109.0270 [hep-th].

[57] R. S. Ward, "Integrable and solvable systems, and relations among them", Phil. Trans. Roy. Soc. Lond. **A315**, 451 (1985).

[58] Q.-H. Park, "A Master equation for multidimensional nonlinear field theories", Phys. Lett. **B297**, 266 (1992), arXiv:hep-th/9211037 [hep-th].

[59] K. Krasnov, "Self-Dual Gravity", Class. Quant. Grav. **34**, 095001 (2017), arXiv:1610.01457 [hep-th].

[60] Z. Bern, J. J. Carrasco, W.-M. Chen, H. Johansson, and R. Roiban, "Gravity Amplitudes as Generalized Double Copies of Gauge-Theory Amplitudes", Phys. Rev. Lett. **118**, 181602 (2017), arXiv:1701.02519 [hep-th].

[61] Z. Bern, J. J. M. Carrasco, L. Dixon, H. Johansson, and R. Roiban, "Simplifying Multiloop Integrands and Ultraviolet Divergences of Gauge Theory and Gravity Amplitudes", Phys. Rev. **D85**, 105014 (2012), arXiv:1201.5366 [hep-th].

[62] R. Monteiro, D. O'Connell, and C. D. White, "Black holes and the double copy", JHEP **12**, 056 (2014), arXiv:1410.0239 [hep-th].

[63] A. Luna, R. Monteiro, D. O'Connell, and C. D. White, "The classical double copy for Taub–NUT spacetime", Phys. Lett. **B750**, 272 (2015), arXiv:1507.01869 [hep-th].

[64] A. Luna, R. Monteiro, I. Nicholson, D. O'Connell, and C. D. White, "The double copy: Bremsstrahlung and accelerating black holes", JHEP **06**, 023 (2016), arXiv:`1603.05737 [hep-th]`.

[65] W. D. Goldberger and A. K. Ridgway, "Radiation and the classical double copy for color charges", Phys. Rev. **D95**, 125010 (2017), arXiv:`1611.03493 [hep-th]`.

[66] A. Luna, R. Monteiro, I. Nicholson, A. Ochirov, D. O'Connell, N. Westerberg, and C. D. White, "Perturbative spacetimes from Yang-Mills theory", JHEP **04**, 069 (2017), arXiv:`1611.07508 [hep-th]`.

[67] D. C. Dunbar, G. R. Jehu, and W. B. Perkins, "Two-Loop Gravity amplitudes from four dimensional Unitarity", Phys. Rev. **D95**, 046012 (2017), arXiv:`1701.02934 [hep-th]`.

[68] N. Marcus, "Composite Anomalies in Supergravity", Phys. Lett. **157B**, 383 (1985).

[69] J. J. M. Carrasco, R. Kallosh, R. Roiban, and A. A. Tseytlin, "On the U(1) duality anomaly and the S-matrix of N=4 supergravity", JHEP **07**, 029 (2013), arXiv:`1303.6219 [hep-th]`.

[70] R. Kallosh, "Cancellation of Conformal and Chiral Anomalies in $\mathcal{N} \geq 5$ supergravities", Phys. Rev. **D95**, 041701 (2017), arXiv:`1612.08978 [hep-th]`.

[71] Z. Bern, S. Davies, T. Dennen, A. V. Smirnov, and V. A. Smirnov, "Ultraviolet Properties of N=4 Supergravity at Four Loops", Phys. Rev. Lett. **111**, 231302 (2013), arXiv:`1309.2498 [hep-th]`.

[72] G. 't Hooft and M. J. G. Veltman, "Regularization and Renormalization of Gauge Fields", Nucl. Phys. **B44**, 189 (1972).

[73] D. C. Dunbar, J. H. Ettle, and W. B. Perkins, "Perturbative expansion of N $\leq$ 8 Supergravity", Phys. Rev. **D83**, 065015 (2011), arXiv:`1011.5378 [hep-th]`.

[74] P. Tourkine and P. Vanhove, "One-loop four-graviton amplitudes in $\mathcal{N} = 4$ supergravity models", Phys. Rev. **D87**, 045001 (2013), arXiv:1208.1255 [hep-th].

[75] Z. Bern, C. Boucher-Veronneau, and H. Johansson, "$N \geq 4$ Supergravity Amplitudes from Gauge Theory at One Loop", Phys. Rev. **D84**, 105035 (2011), arXiv:1107.1935 [hep-th].

[76] C. Boucher-Veronneau and L. Dixon, "N $\geq$- 4 Supergravity Amplitudes from Gauge Theory at Two Loops", JHEP **12**, 046 (2011), arXiv:1110.1132 [hep-th].

[77] A. Ochirov and P. Tourkine, "BCJ duality and double copy in the closed string sector", JHEP **05**, 136 (2014), arXiv:1312.1326 [hep-th].

[78] S. Ferrara and M. Villasante, "Curvatures, Gauss-Bonnet and Chern-simons Multiplets in Old Minimal $N = 1$ Supergravity", J. Math. Phys. **30**, 104 (1989).

[79] S. Ferrara, S. Sabharwal, and M. Villasante, "Curvatures and Gauss-Bonnet Theorem in New Minimal Supergravity", Phys. Lett. **B205**, 302 (1988).

[80] D. Butter, B. de Wit, S. M. Kuzenko, and I. Lodato, "New higher-derivative invariants in N=2 supergravity and the Gauss-Bonnet term", JHEP **12**, 062 (2013), arXiv:1307.6546 [hep-th].

[81] D. Butter, "The $\mathcal{N} = 2$ Gauss-Bonnet from conformal supergravity", Phys. Part. Nucl. Lett. **11**, 941 (2014).

[82] S. M. Kuzenko and J. Novak, "On curvature squared terms in N=2 supergravity", Phys. Rev. **D92**, 085033 (2015), arXiv:1507.04922 [hep-th].

[83] E. Bergshoeff, M. de Roo, and B. de Wit, "Extended Conformal Supergravity", Nucl. Phys. **B182**, 173 (1981).

[84] F. Ciceri and B. Sahoo, "Towards the full $N = 4$ conformal supergravity action", JHEP **01**, 059 (2016), arXiv:1510.04999 [hep-th].

[85] D. Butter, F. Ciceri, B. de Wit, and B. Sahoo, "Construction of all N=4 conformal supergravities", Phys. Rev. Lett. **118**, 081602 (2017), arXiv:1609.09083 [hep-th].

[86] R. H. Boels and R. Medina, "Graviton and gluon scattering from first principles", Phys. Rev. Lett. **118**, 061602 (2017), arXiv:1607.08246 [hep-th].

[87] J. J. M. Carrasco, M. Chiodaroli, M. Günaydin, and R. Roiban, "One-loop four-point amplitudes in pure and matter-coupled N $\leq$ 4 supergravity", JHEP **03**, 056 (2013), arXiv:1212.1146 [hep-th].

[88] H. Johansson and A. Ochirov, "Pure Gravities via Color-Kinematics Duality for Fundamental Matter", JHEP **11**, 046 (2015), arXiv:1407.4772 [hep-th].

[89] H. Johansson and A. Ochirov, "Color-Kinematics Duality for QCD Amplitudes", JHEP **01**, 170 (2016), arXiv:1507.00332 [hep-ph].

[90] M. B. Green, J. H. Schwarz, and L. Brink, "N=4 Yang-Mills and N=8 Supergravity as Limits of String Theories", Nucl. Phys. **B198**, 474 (1982).

[91] E. W. N. Glover and M. E. Tejeda-Yeomans, "Two loop QCD helicity amplitudes for massless quark massless gauge boson scattering", JHEP **06**, 033 (2003), arXiv:hep-ph/0304169 [hep-ph].

[92] Z. Bern, L. Dixon, and D. A. Kosower, "Dimensionally regulated pentagon integrals", Nucl. Phys. **B412**, 751 (1994), arXiv:hep-ph/9306240 [hep-ph].

[93] O. V. Tarasov, "Connection between Feynman integrals having different values of the space-time dimension", Phys. Rev. **D54**, 6479 (1996), arXiv:hep-th/9606018 [hep-th].

[94] A. V. Smirnov, "Algorithm FIRE – Feynman Integral REduction", JHEP **10**, 107 (2008), arXiv:0807.3243 [hep-ph].

[95] A. V. Smirnov, "FIRE5: a C++ implementation of Feynman Integral REduction", Comput. Phys. Commun. **189**, 182 (2015), arXiv:1408.2372 [hep-ph].

[96] Z. Bern, L. Dixon, and D. A. Kosower, "Dimensionally regulated one loop integrals", Phys. Lett. **B302**, 299 (1993), arXiv:`hep-ph/9212308` `[hep-ph]`.

[97] M. Berg, I. Buchberger, and O. Schlotterer, "From maximal to minimal supersymmetry in string loop amplitudes", JHEP **04**, 163 (2017), arXiv:`1603.05262` `[hep-th]`.

[98] M. B. Green, J. H. Schwarz, and E. Witten, *SUPERSTRING THEORY. VOL. 1: INTRODUCTION*, Cambridge Monographs on Mathematical Physics (1988).

[99] P. Tourkine, "Results in perturbative quantum supergravity from string theory", PhD thesis (Paris U., VI-VII, 2014).

[100] M. B. Green and A. Rudra, "Type I/heterotic duality and M-theory amplitudes", JHEP **12**, 060 (2016), arXiv:`1604.00324` `[hep-th]`.

[101] M. de Roo, H. Suelmann, and A. Wiedemann, "Supersymmetric R**4 actions in ten-dimensions", Phys. Lett. **B280**, 39 (1992).

[102] J. Broedel and L. Dixon, "Color-kinematics duality and double-copy construction for amplitudes from higher-dimension operators", JHEP **10**, 091 (2012), arXiv:`1208.0876` `[hep-th]`.

[103] S. He and Y. Zhang, "New Formulas for Amplitudes from Higher-Dimensional Operators", JHEP **02**, 019 (2017), arXiv:`1608.08448` `[hep-th]`.

[104] N. E. J. Bjerrum-Bohr, "Generalized string theory mapping relations between gravity and gauge theory", Nucl. Phys. **B673**, 41 (2003), arXiv:`hep-th/0305062` `[hep-th]`.

[105] N. E. J. Bjerrum-Bohr, "String theory and the mapping of gravity into gauge theory", Phys. Lett. **B560**, 98 (2003), arXiv:`hep-th/0302131` `[hep-th]`.

[106] Z. Bern, C. Cheung, H.-H. Chi, S. Davies, L. Dixon, and J. Nohle.

[107] S. M. Christensen and M. J. Duff, "Axial and Conformal Anomalies for Arbitrary Spin in Gravity and Supergravity", Phys. Lett. **B76**, 571 (1978).

[108] Z. Bern, M. Enciso, J. Parra-Martinez, and M. Zeng, "Manifesting enhanced cancellations in supergravity: integrands versus integrals", JHEP **05**, 137 (2017), arXiv:`1703.08927` [`hep-th`].

[109] S. Deser and P. van Nieuwenhuizen, "One Loop Divergences of Quantized Einstein-Maxwell Fields", Phys. Rev. **D10**, 401 (1974).

[110] S. Deser, H.-S. Tsao, and P. van Nieuwenhuizen, "One Loop Divergences of the Einstein Yang-Mills System", Phys. Rev. **D10**, 3337 (1974).

[111] D. Z. Freedman, R. Kallosh, D. Murli, A. Van Proeyen, and Y. Yamada, "Absence of U(1) Anomalous Superamplitudes in $\mathcal{N} \geq 5$ Supergravities", JHEP **05**, 067 (2017), arXiv:`1703.03879` [`hep-th`].

[112] B. de Wit and S. Ferrara, "On Higher Order Invariants in Extended Supergravity", Phys. Lett. **81B**, 317 (1979).

[113] E. Cremmer, J. Scherk, and S. Ferrara, "SU(4) Invariant Supergravity Theory", Phys. Lett. **74B**, 61 (1978).

[114] H. Nicolai and P. K. Townsend, "N=3 Supersymmetry Multiplets with Vanishing Trace Anomaly: Building Blocks of the N>3 Supergravities", Phys. Lett. **98B**, 257 (1981).

[115] H. Elvang and Y.-t. Huang, "Scattering Amplitudes", (2013), arXiv:`1308.1697` [`hep-th`].

[116] D. Z. Freedman, P. van Nieuwenhuizen, and S. Ferrara, "Progress Toward a Theory of Supergravity", Phys. Rev. **D13**, 3214 (1976).

[117] S. Deser and B. Zumino, "Consistent Supergravity", Phys. Lett. **B62**, 335 (1976).

[118] Z. Bern, L. J. Dixon, and R. Roiban, "Is N = 8 supergravity ultraviolet finite?", Phys. Lett. **B644**, 265 (2007), arXiv:`hep-th/0611086` [`hep-th`].

[119] Z. Bern, J. J. Carrasco, D. Forde, H. Ita, and H. Johansson, "Unexpected Cancellations in Gravity Theories", Phys. Rev. **D77**, 025010 (2008), arXiv:`0707.1035` [`hep-th`].

[120] E. Herrmann and J. Trnka, "Gravity On-shell Diagrams", JHEP **11**, 136 (2016), arXiv:1604.03479 [hep-th].

[121] A. K. Das, "SO(4) Invariant Extended Supergravity", Phys. Rev. **D15**, 2805 (1977).

[122] E. Cremmer and J. Scherk, "Algebraic Simplifications in Supergravity Theories", Nucl. Phys. **B127**, 259 (1977).

[123] B. de Wit and H. Nicolai, "Extended Supergravity With Local SO(5) Invariance", Nucl. Phys. **B188**, 98 (1981).

[124] Z. Bern, J. Parra-Martinez, and R. Roiban, "Canceling the U(1) Anomaly in the S Matrix of N=4 Supergravity", Phys. Rev. Lett. **121**, 101604 (2018), arXiv:1712.03928 [hep-th].

[125] E. Cremmer, B. Julia, and J. Scherk, "Supergravity Theory in Eleven-Dimensions", Phys. Lett. **B76**, 409 (1978).

[126] E. Cremmer and B. Julia, "The N=8 Supergravity Theory. 1. The Lagrangian", Phys. Lett. **B80**, 48 (1978).

[127] E. Cremmer and B. Julia, "The SO(8) Supergravity", Nucl. Phys. **B159**, 141 (1979).

[128] P. S. Howe and U. Lindstrom, "Higher Order Invariants in Extended Supergravity", Nucl. Phys. **B181**, 487 (1981).

[129] R. E. Kallosh, "Counterterms in extended supergravities", Phys. Lett. **99B**, 122 (1981).

[130] M. T. Grisaru and W. Siegel, "Supergraphity. 2. Manifestly Covariant Rules and Higher Loop Finiteness", Nucl. Phys. **B201**, 292 (1982).

[131] N. Marcus and A. Sagnotti, "The Ultraviolet Behavior of $N = 4$ Yang-Mills and the Power Counting of Extended Superspace", Nucl. Phys. **B256**, 77 (1985).

[132] G. Chalmers, "On the finiteness of N=8 quantum supergravity", (2000), arXiv:hep-th/0008162 [hep-th].

[133] N. Berkovits, "New higher-derivative R**4 theorems", Phys. Rev. Lett. **98**, 211601 (2007), arXiv:`hep-th/0609006` [`hep-th`].

[134] M. B. Green, J. G. Russo, and P. Vanhove, "Non-renormalisation conditions in type II string theory and maximal supergravity", JHEP **02**, 099 (2007), arXiv:`hep-th/0610299` [`hep-th`].

[135] M. B. Green, J. G. Russo, and P. Vanhove, "Ultraviolet properties of maximal supergravity", Phys. Rev. Lett. **98**, 131602 (2007), arXiv:`hep-th/0611273` [`hep-th`].

[136] G. Bossard, P. S. Howe, and K. S. Stelle, "The Ultra-violet question in maximally supersymmetric field theories", Gen. Rel. Grav. **41**, 919 (2009), arXiv:`0901.4661` [`hep-th`].

[137] R. Kallosh, "N=8 Supergravity on the Light Cone", Phys. Rev. **D80**, 105022 (2009), arXiv:`0903.4630` [`hep-th`].

[138] N. Berkovits, M. B. Green, J. G. Russo, and P. Vanhove, "Non-renormalization conditions for four-gluon scattering in supersymmetric string and field theory", JHEP **11**, 063 (2009), arXiv:`0908.1923` [`hep-th`].

[139] G. Bossard, P. S. Howe, and K. S. Stelle, "On duality symmetries of supergravity invariants", JHEP **01**, 020 (2011), arXiv:`1009.0743` [`hep-th`].

[140] N. Beisert, H. Elvang, D. Z. Freedman, M. Kiermaier, A. Morales, and S. Stieberger, "E7(7) constraints on counterterms in N=8 supergravity", Phys. Lett. **B694**, 265 (2011), arXiv:`1009.1643` [`hep-th`].

[141] P. Vanhove, "The Critical ultraviolet behaviour of N=8 supergravity amplitudes", (2010), arXiv:`1004.1392` [`hep-th`].

[142] J. Bjornsson and M. B. Green, "5 loops in 24/5 dimensions", JHEP **08**, 132 (2010), arXiv:`1004.2692` [`hep-th`].

[143] J. Bjornsson, "Multi-loop amplitudes in maximally supersymmetric pure spinor field theory", JHEP **01**, 002 (2011), arXiv:1009.5906 [hep-th].

[144] G. Bossard, P. S. Howe, K. S. Stelle, and P. Vanhove, "The vanishing volume of D=4 superspace", Class. Quant. Grav. **28**, 215005 (2011), arXiv:1105.6087 [hep-th].

[145] Z. Bern, L. J. Dixon, D. C. Dunbar, M. Perelstein, and J. S. Rozowsky, "On the relationship between Yang-Mills theory and gravity and its implication for ultraviolet divergences", Nucl. Phys. **B530**, 401 (1998), arXiv:hep-th/9802162 [hep-th].

[146] Z. Bern, J. J. Carrasco, L. J. Dixon, H. Johansson, D. A. Kosower, and R. Roiban, "Three-Loop Superfiniteness of N=8 Supergravity", Phys. Rev. Lett. **98**, 161303 (2007), arXiv:hep-th/0702112 [hep-th].

[147] Z. Bern, J. J. M. Carrasco, L. J. Dixon, H. Johansson, and R. Roiban, "Manifest Ultraviolet Behavior for the Three-Loop Four-Point Amplitude of N=8 Supergravity", Phys. Rev. **D78**, 105019 (2008), arXiv:0808.4112 [hep-th].

[148] Z. Bern, J. J. Carrasco, L. J. Dixon, H. Johansson, and R. Roiban, "The Ultraviolet Behavior of N=8 Supergravity at Four Loops", Phys. Rev. Lett. **103**, 081301 (2009), arXiv:0905.2326 [hep-th].

[149] Z. Bern, J. J. M. Carrasco, L. J. Dixon, H. Johansson, and R. Roiban, "The Complete Four-Loop Four-Point Amplitude in N=4 Super-Yang-Mills Theory", Phys. Rev. **D82**, 125040 (2010), arXiv:1008.3327 [hep-th].

[150] F. Gliozzi, J. Scherk, and D. I. Olive, "Supersymmetry, Supergravity Theories and the Dual Spinor Model", Nucl. Phys. **B122**, 253 (1977).

[151] L. Brink, J. H. Schwarz, and J. Scherk, "Supersymmetric Yang-Mills Theories", Nucl. Phys. **B121**, 77 (1977).

[152] S. Mandelstam, "Light-cone Superspace and the Finiteness of the $N = 4$ Model", J. Phys. Colloq. **43**, 331 (1982).

[153] S. Mandelstam, "Light Cone Superspace and the Ultraviolet Finiteness of the N=4 Model", Nucl. Phys. **B213**, 149 (1983).

[154] L. Brink, O. Lindgren, and B. E. W. Nilsson, "The Ultraviolet Finiteness of the N=4 Yang-Mills Theory", Phys. Lett. **123B**, 323 (1983).

[155] P. S. Howe, K. S. Stelle, and P. K. Townsend, "The Relaxed Hypermultiplet: An Unconstrained N=2 Superfield Theory", Nucl. Phys. **B214**, 519 (1983).

[156] Z. Bern, L. J. Dixon, D. C. Dunbar, and D. A. Kosower, "One loop n point gauge theory amplitudes, unitarity and collinear limits", Nucl. Phys. **B425**, 217 (1994), arXiv:`hep-ph/9403226 [hep-ph]`.

[157] Z. Bern, L. J. Dixon, D. C. Dunbar, and D. A. Kosower, "Fusing gauge theory tree amplitudes into loop amplitudes", Nucl. Phys. **B435**, 59 (1995), arXiv:`hep-ph/9409265 [hep-ph]`.

[158] Z. Bern, L. J. Dixon, and D. A. Kosower, "One loop amplitudes for e+ e- to four partons", Nucl. Phys. **B513**, 3 (1998), arXiv:`hep-ph/9708239 [hep-ph]`.

[159] R. Britto, F. Cachazo, and B. Feng, "Generalized unitarity and one-loop amplitudes in N=4 super-Yang-Mills", Nucl. Phys. **B725**, 275 (2005), arXiv:`hep-th/0412103 [hep-th]`.

[160] Z. Bern, J. J. M. Carrasco, H. Johansson, and D. A. Kosower, "Maximally supersymmetric planar Yang-Mills amplitudes at five loops", Phys. Rev. **D76**, 125020 (2007), arXiv:`0705.1864 [hep-th]`.

[161] Z. Bern, J. J. M. Carrasco, W.-M. Chen, H. Johansson, R. Roiban, and M. Zeng, "Five-loop four-point integrand of $N = 8$ supergravity as a generalized double copy", Phys. Rev. **D96**, 126012 (2017), arXiv:`1708.06807 [hep-th]`.

[162] Z. Bern, J. J. M. Carrasco, H. Johansson, and R. Roiban, "The Five-Loop Four-Point Amplitude of N=4 super-Yang-Mills Theory", Phys. Rev. Lett. **109**, 241602 (2012), arXiv:1207.6666 [hep-th].

[163] P. A. Baikov, K. G. Chetyrkin, and J. H. Kühn, "Five-Loop Running of the QCD coupling constant", Phys. Rev. Lett. **118**, 082002 (2017), arXiv:1606.08659 [hep-ph].

[164] F. Herzog, B. Ruijl, T. Ueda, J. A. M. Vermaseren, and A. Vogt, "The five-loop beta function of Yang-Mills theory with fermions", JHEP **02**, 090 (2017), arXiv:1701.01404 [hep-ph].

[165] T. Luthe, A. Maier, P. Marquard, and Y. Schroder, "Complete renormalization of QCD at five loops", JHEP **03**, 020 (2017), arXiv:1701.07068 [hep-ph].

[166] K. G. Chetyrkin and F. V. Tkachov, "Integration by Parts: The Algorithm to Calculate beta Functions in 4 Loops", Nucl. Phys. **B192**, 159 (1981).

[167] S. Laporta, "High precision calculation of multiloop Feynman integrals by difference equations", Int. J. Mod. Phys. **A15**, 5087 (2000), arXiv:hep-ph/0102033 [hep-ph].

[168] S. Laporta and E. Remiddi, "The Analytical value of the electron (g-2) at order alpha**3 in QED", Phys. Lett. **B379**, 283 (1996), arXiv:hep-ph/9602417 [hep-ph].

[169] C. Anastasiou and A. Lazopoulos, "Automatic integral reduction for higher order perturbative calculations", JHEP **07**, 046 (2004), arXiv:hep-ph/0404258 [hep-ph].

[170] A. von Manteuffel and C. Studerus, "Reduze 2 - Distributed Feynman Integral Reduction", (2012), arXiv:1201.4330 [hep-ph].

[171] R. N. Lee, "Presenting LiteRed: a tool for the Loop InTEgrals REDuction", (2012), arXiv:1212.2685 [hep-ph].

[172] B. Ruijl, T. Ueda, and J. A. M. Vermaseren, "Forcer, a FORM program for the parametric reduction of four-loop massless propagator diagrams", (2017), arXiv:1704.06650 [hep-ph].

[173] P. Maierhöfer, J. Usovitsch, and P. Uwer, "Kira—A Feynman integral reduction program", Comput. Phys. Commun. **230**, 99 (2018), arXiv:1705.05610 [`hep-ph`].

[174] V. A. Smirnov, "Analytic tools for Feynman integrals", Springer Tracts Mod. Phys. **250**, 1 (2012).

[175] J. Gluza, K. Kajda, and D. A. Kosower, "Towards a Basis for Planar Two-Loop Integrals", Phys. Rev. **D83**, 045012 (2011), arXiv:1009.0472 [`hep-th`].

[176] D. A. Kosower and K. J. Larsen, "Maximal Unitarity at Two Loops", Phys. Rev. **D85**, 045017 (2012), arXiv:1108.1180 [`hep-th`].

[177] S. Caron-Huot and K. J. Larsen, "Uniqueness of two-loop master contours", JHEP **10**, 026 (2012), arXiv:1205.0801 [`hep-ph`].

[178] M. Søgaard, "Global Residues and Two-Loop Hepta-Cuts", JHEP **09**, 116 (2013), arXiv:1306.1496 [`hep-th`].

[179] H. Johansson, D. A. Kosower, and K. J. Larsen, "Maximal Unitarity for the Four-Mass Double Box", Phys. Rev. **D89**, 125010 (2014), arXiv:1308.4632 [`hep-th`].

[180] M. Søgaard and Y. Zhang, "Multivariate Residues and Maximal Unitarity", JHEP **12**, 008 (2013), arXiv:1310.6006 [`hep-th`].

[181] M. Sogaard and Y. Zhang, "Unitarity Cuts of Integrals with Doubled Propagators", JHEP **07**, 112 (2014), arXiv:1403.2463 [`hep-th`].

[182] S. Abreu, R. Britto, C. Duhr, and E. Gardi, "Cuts from residues: the one-loop case", JHEP **06**, 114 (2017), arXiv:1702.03163 [`hep-th`].

[183] R. M. Schabinger, "A New Algorithm For The Generation Of Unitarity-Compatible Integration By Parts Relations", JHEP **01**, 077 (2012), arXiv:1111.4220 [`hep-ph`].

[184] H. Ita, "Two-loop Integrand Decomposition into Master Integrals and Surface Terms", Phys. Rev. **D94**, 116015 (2016), arXiv:1510.05626 [`hep-th`].

[185] K. J. Larsen and Y. Zhang, "Integration-by-parts reductions from unitarity cuts and algebraic geometry", Phys. Rev. **D93**, 041701 (2016), arXiv:1511.01071 [hep-th].

[186] A. Georgoudis, K. J. Larsen, and Y. Zhang, "Azurite: An algebraic geometry based package for finding bases of loop integrals", Comput. Phys. Commun. **221**, 203 (2017), arXiv:1612.04252 [hep-th].

[187] Z. Bern, M. Enciso, H. Ita, and M. Zeng, "Dual Conformal Symmetry, Integration-by-Parts Reduction, Differential Equations and the Nonplanar Sector", Phys. Rev. **D96**, 096017 (2017), arXiv:1709.06055 [hep-th].

[188] D. A. Kosower, "Direct Solution of Integration-by-Parts Systems", Phys. Rev. **D98**, 025008 (2018), arXiv:1804.00131 [hep-ph].

[189] Y. Zhang, "Lecture Notes on Multi-loop Integral Reduction and Applied Algebraic Geometry", in (2016), arXiv:1612.02249 [hep-th].

[190] G. Mogull and D. O'Connell, "Overcoming Obstacles to Colour-Kinematics Duality at Two Loops", JHEP **12**, 135 (2015), arXiv:1511.06652 [hep-th].

[191] J. J. Carrasco and H. Johansson, "Five-Point Amplitudes in N=4 Super-Yang-Mills Theory and N=8 Supergravity", Phys. Rev. **D85**, 025006 (2012), arXiv:1106.4711 [hep-th].

[192] Z. Bern, S. Davies, and J. Nohle, "Double-Copy Constructions and Unitarity Cuts", Phys. Rev. **D93**, 105015 (2016), arXiv:1510.03448 [hep-th].

[193] Z. Bern, T. Dennen, Y.-t. Huang, and M. Kiermaier, "Gravity as the Square of Gauge Theory", Phys. Rev. **D82**, 065003 (2010), arXiv:1004.0693 [hep-th].

[194] M. Tolotti and S. Weinzierl, "Construction of an effective Yang-Mills Lagrangian with manifest BCJ duality", JHEP **07**, 111 (2013), arXiv:1306.2975 [hep-th].

[195] N. E. J. Bjerrum-Bohr, P. H. Damgaard, T. Sondergaard, and P. Vanhove, "The Momentum Kernel of Gauge and Gravity Theories", JHEP **01**, 001 (2011), arXiv:1010.3933 [hep-th].

[196] C. R. Mafra, O. Schlotterer, and S. Stieberger, "Explicit BCJ Numerators from Pure Spinors", JHEP **07**, 092 (2011), arXiv:1104.5224 [hep-th].

[197] Y.-J. Du and C.-H. Fu, "Explicit BCJ numerators of nonlinear simga model", JHEP **09**, 174 (2016), arXiv:1606.05846 [hep-th].

[198] N. E. J. Bjerrum-Bohr, J. L. Bourjaily, P. H. Damgaard, and B. Feng, "Manifesting Color-Kinematics Duality in the Scattering Equation Formalism", JHEP **09**, 094 (2016), arXiv:1608.00006 [hep-th].

[199] Y.-J. Du and F. Teng, "BCJ numerators from reduced Pfaffian", JHEP **04**, 033 (2017), arXiv:1703.05717 [hep-th].

[200] Y.-J. Du, B. Feng, and F. Teng, "Expansion of All Multitrace Tree Level EYM Amplitudes", JHEP **12**, 038 (2017), arXiv:1708.04514 [hep-th].

[201] J. J. M. Carrasco and H. Johansson, "Generic multiloop methods and application to N=4 super-Yang-Mills", J. Phys. **A44**, 454004 (2011), arXiv:1103.3298 [hep-th].

[202] J. J. M. Carrasco, "Gauge and Gravity Amplitude Relations", in Proceedings, Theoretical Advanced Study Institute in Elementary Particle Physics: Journeys Through the Precision Frontier: Amplitudes for Colliders (TASI 2014): Boulder, Colorado, June 2-27, 2014 (WSP, 2015), pp. 477–557, arXiv:1506.00974 [hep-th].

[203] M. Chiodaroli, "Simplifying amplitudes in Maxwell-Einstein and Yang-Mills-Einstein supergravities", in (2018), pp. 266–287, arXiv:1607.04129 [hep-th].

[204] C. Cheung, "TASI Lectures on Scattering Amplitudes", in Proceedings, Theoretical Advanced Study Institute in Elementary Particle Physics : Anticipating the Next

Discoveries in Particle Physics (TASI 2016): Boulder, CO, USA, June 6-July 1, 2016 (2018), pp. 571–623, arXiv:1708.03872 [`hep-ph`].

[205] J. J. M. Carrasco, C. R. Mafra, and O. Schlotterer, "Abelian Z-theory: NLSM amplitudes and α'-corrections from the open string", JHEP **06**, 093 (2017), arXiv:1608.02569 [`hep-th`].

[206] R. H. Boels, B. A. Kniehl, O. V. Tarasov, and G. Yang, "Color-kinematic Duality for Form Factors", JHEP **02**, 063 (2013), arXiv:1211.7028 [`hep-th`].

[207] C. R. Mafra and O. Schlotterer, "Two-loop five-point amplitudes of super Yang-Mills and supergravity in pure spinor superspace", JHEP **10**, 124 (2015), arXiv:1505.02746 [`hep-th`].

[208] S. He, R. Monteiro, and O. Schlotterer, "String-inspired BCJ numerators for one-loop MHV amplitudes", JHEP **01**, 171 (2016), arXiv:1507.06288 [`hep-th`].

[209] G. Yang, "Color-kinematics duality and Sudakov form factor at five loops for N=4 supersymmetric Yang-Mills theory", Phys. Rev. Lett. **117**, 271602 (2016), arXiv:1610.02394 [`hep-th`].

[210] R. H. Boels, T. Huber, and G. Yang, "Four-Loop Nonplanar Cusp Anomalous Dimension in N=4 Supersymmetric Yang-Mills Theory", Phys. Rev. Lett. **119**, 201601 (2017), arXiv:1705.03444 [`hep-th`].

[211] H. Johansson, G. Kälin, and G. Mogull, "Two-loop supersymmetric QCD and half-maximal supergravity amplitudes", JHEP **09**, 019 (2017), arXiv:1706.09381 [`hep-th`].

[212] G. Cardoso, S. Nagy, and S. Nampuri, "Multi-centered $\mathcal{N} = 2$ BPS black holes: a double copy description", JHEP **04**, 037 (2017), arXiv:1611.04409 [`hep-th`].

[213] T. Adamo, E. Casali, L. Mason, and S. Nekovar, "Scattering on plane waves and the double copy", Class. Quant. Grav. **35**, 015004 (2018), arXiv:1706.08925 [`hep-th`].

[214] N. Bahjat-Abbas, A. Luna, and C. D. White, "The Kerr-Schild double copy in curved spacetime", JHEP **12**, 004 (2017), arXiv:`1710.01953` [`hep-th`].

[215] M. Carrillo-González, R. Penco, and M. Trodden, "The classical double copy in maximally symmetric spacetimes", JHEP **04**, 028 (2018), arXiv:`1711.01296` [`hep-th`].

[216] W. D. Goldberger, S. G. Prabhu, and J. O. Thompson, "Classical gluon and graviton radiation from the bi-adjoint scalar double copy", Phys. Rev. **D96**, 065009 (2017), arXiv:`1705.09263` [`hep-th`].

[217] J. Li and S. G. Prabhu, "Gravitational radiation from the classical spinning double copy", Phys. Rev. **D97**, 105019 (2018), arXiv:`1803.02405` [`hep-th`].

[218] W. D. Goldberger and A. K. Ridgway, "Bound states and the classical double copy", Phys. Rev. **D97**, 085019 (2018), arXiv:`1711.09493` [`hep-th`].

[219] N. E. J. Bjerrum-Bohr, J. F. Donoghue, B. R. Holstein, L. Planté, and P. Vanhove, "Bending of Light in Quantum Gravity", Phys. Rev. Lett. **114**, 061301 (2015), arXiv:`1410.7590` [`hep-th`].

[220] N. E. J. Bjerrum-Bohr, J. F. Donoghue, B. R. Holstein, L. Planté, and P. Vanhove, "Light-like Scattering in Quantum Gravity", JHEP **11**, 117 (2016), arXiv:`1609.07477` [`hep-th`].

[221] N. E. J. Bjerrum-Bohr, B. R. Holstein, J. F. Donoghue, L. Planté, and P. Vanhove, "Illuminating Light Bending", PoS **CORFU2016**, 077 (2017), arXiv:`1704.01624` [`gr-qc`].

[222] L. Borsten, M. J. Duff, L. J. Hughes, and S. Nagy, "Magic Square from Yang-Mills Squared", Phys. Rev. Lett. **112**, 131601 (2014), arXiv:`1301.4176` [`hep-th`].

[223] A. Anastasiou, L. Borsten, M. J. Duff, L. J. Hughes, and S. Nagy, "A magic pyramid of supergravities", JHEP **04**, 178 (2014), arXiv:`1312.6523` [`hep-th`].

[224] A. Anastasiou, L. Borsten, M. J. Duff, L. J. Hughes, and S. Nagy, "Yang-Mills origin of gravitational symmetries", Phys. Rev. Lett. **113**, 231606 (2014), arXiv:1408.4434 [hep-th].

[225] M. Chiodaroli, M. Günaydin, H. Johansson, and R. Roiban, "Scattering amplitudes in $\mathcal{N} = 2$ Maxwell-Einstein and Yang-Mills/Einstein supergravity", JHEP **01**, 081 (2015), arXiv:1408.0764 [hep-th].

[226] M. Chiodaroli, M. Gunaydin, H. Johansson, and R. Roiban, "Explicit Formulae for Yang-Mills-Einstein Amplitudes from the Double Copy", JHEP **07**, 002 (2017), arXiv:1703.00421 [hep-th].

[227] M. Chiodaroli, M. Gunaydin, H. Johansson, and R. Roiban, "Spontaneously Broken Yang-Mills-Einstein Supergravities as Double Copies", JHEP **06**, 064 (2017), arXiv:1511.01740 [hep-th].

[228] M. Chiodaroli, M. Gunaydin, H. Johansson, and R. Roiban, "Complete construction of magical, symmetric and homogeneous N=2 supergravities as double copies of gauge theories", Phys. Rev. Lett. **117**, 011603 (2016), arXiv:1512.09130 [hep-th].

[229] A. Anastasiou, L. Borsten, M. J. Duff, M. J. Hughes, A. Marrani, S. Nagy, and M. Zoccali, "Twin supergravities from Yang-Mills theory squared", Phys. Rev. **D96**, 026013 (2017), arXiv:1610.07192 [hep-th].

[230] A. Anastasiou, L. Borsten, M. J. Duff, A. Marrani, S. Nagy, and M. Zoccali, "Are all supergravity theories Yang–Mills squared?", Nucl. Phys. **B934**, 606 (2018), arXiv:1707.03234 [hep-th].

[231] M. Chiodaroli, M. Gunaydin, H. Johansson, and R. Roiban, "Gauged Supergravities and Spontaneous Supersymmetry Breaking from the Double Copy Construction", Phys. Rev. Lett. **120**, 171601 (2018), arXiv:1710.08796 [hep-th].

[232] T. Bargheer, S. He, and T. McLoughlin, "New Relations for Three-Dimensional Super-symmetric Scattering Amplitudes", Phys. Rev. Lett. **108**, 231601 (2012), arXiv:1203.0562 [hep-th].

[233] Y.-t. Huang and H. Johansson, "Equivalent D=3 Supergravity Amplitudes from Double Copies of Three-Algebra and Two-Algebra Gauge Theories", Phys. Rev. Lett. **110**, 171601 (2013), arXiv:1210.2255 [hep-th].

[234] Y.-t. Huang, H. Johansson, and S. Lee, "On Three-Algebra and Bi-Fundamental Matter Amplitudes and Integrability of Supergravity", JHEP **11**, 050 (2013), arXiv:1307.2222 [hep-th].

[235] G. Chen and Y.-J. Du, "Amplitude Relations in Non-linear Sigma Model", JHEP **01**, 061 (2014), arXiv:1311.1133 [hep-th].

[236] F. Cachazo, S. He, and E. Y. Yuan, "Scattering Equations and Matrices: From Einstein To Yang-Mills, DBI and NLSM", JHEP **07**, 149 (2015), arXiv:1412.3479 [hep-th].

[237] F. Cachazo, P. Cha, and S. Mizera, "Extensions of Theories from Soft Limits", JHEP **06**, 170 (2016), arXiv:1604.03893 [hep-th].

[238] C. R. Mafra and O. Schlotterer, "Non-abelian Z-theory: Berends-Giele recursion for the α'-expansion of disk integrals", JHEP **01**, 031 (2017), arXiv:1609.07078 [hep-th].

[239] J. J. M. Carrasco, C. R. Mafra, and O. Schlotterer, "Semi-abelian Z-theory: NLSM+ϕ^3 from the open string", JHEP **08**, 135 (2017), arXiv:1612.06446 [hep-th].

[240] C. Cheung, C.-H. Shen, and C. Wen, "Unifying Relations for Scattering Amplitudes", JHEP **02**, 095 (2018), arXiv:1705.03025 [hep-th].

[241] C. Cheung and C.-H. Shen, "Symmetry for Flavor-Kinematics Duality from an Action", Phys. Rev. Lett. **118**, 121601 (2017), arXiv:1612.00868 [hep-th].

[242] J. Broedel, O. Schlotterer, and S. Stieberger, "Polylogarithms, Multiple Zeta Values and Superstring Amplitudes", Fortsch. Phys. **61**, 812 (2013), arXiv:`1304.7267` [`hep-th`].

[243] S. Stieberger and T. R. Taylor, "Closed String Amplitudes as Single-Valued Open String Amplitudes", Nucl. Phys. **B881**, 269 (2014), arXiv:`1401.1218` [`hep-th`].

[244] Y.-t. Huang, O. Schlotterer, and C. Wen, "Universality in string interactions", JHEP **09**, 155 (2016), arXiv:`1602.01674` [`hep-th`].

[245] C. R. Mafra and O. Schlotterer, "Double-Copy Structure of One-Loop Open-String Amplitudes", Phys. Rev. Lett. **121**, 011601 (2018), arXiv:`1711.09104` [`hep-th`].

[246] T. Azevedo, M. Chiodaroli, H. Johansson, and O. Schlotterer, "Heterotic and bosonic string amplitudes via field theory", JHEP **10**, 012 (2018), arXiv:`1803.05452` [`hep-th`].

[247] H. Johansson and J. Nohle, "Conformal Gravity from Gauge Theory", (2017), arXiv:`1707.02965` [`hep-th`].

[248] V. P. Nair, "A Current Algebra for Some Gauge Theory Amplitudes", Phys. Lett. **B214**, 215 (1988).

[249] H. Elvang, D. Z. Freedman, and M. Kiermaier, "Recursion Relations, Generating Functions, and Unitarity Sums in N=4 SYM Theory", JHEP **04**, 009 (2009), arXiv:`0808.1720` [`hep-th`].

[250] Z. Bern, J. J. M. Carrasco, H. Ita, H. Johansson, and R. Roiban, "On the Structure of Supersymmetric Sums in Multi-Loop Unitarity Cuts", Phys. Rev. **D80**, 065029 (2009), arXiv:`0903.5348` [`hep-th`].

[251] C. Cheung and D. O'Connell, "Amplitudes and Spinor-Helicity in Six Dimensions", JHEP **07**, 075 (2009), arXiv:`0902.0981` [`hep-th`].

[252] T. Dennen, Y.-t. Huang, and W. Siegel, "Supertwistor space for 6D maximal super Yang-Mills", JHEP **04**, 127 (2010), arXiv:`0910.2688` [`hep-th`].

[253] Z. Bern, J. J. Carrasco, T. Dennen, Y.-t. Huang, and H. Ita, "Generalized Unitarity and Six-Dimensional Helicity", Phys. Rev. **D83**, 085022 (2011), arXiv:`1010.0494` `[hep-th]`.

[254] S. H. Henry Tye and Y. Zhang, "Dual Identities inside the Gluon and the Graviton Scattering Amplitudes", JHEP **06**, 071 (2010), arXiv:`1003.1732` `[hep-th]`.

[255] N. E. J. Bjerrum-Bohr, P. H. Damgaard, T. Sondergaard, and P. Vanhove, "Monodromy and Jacobi-like Relations for Color-Ordered Amplitudes", JHEP **06**, 003 (2010), arXiv:`1003.2403` `[hep-th]`.

[256] Z. Bern, J. S. Rozowsky, and B. Yan, "Two loop four gluon amplitudes in N=4 superYang-Mills", Phys. Lett. **B401**, 273 (1997), arXiv:`hep-ph/9702424` `[hep-ph]`.

[257] A. A. Vladimirov, "Method for Computing Renormalization Group Functions in Dimensional Renormalization Scheme", Theor. Math. Phys. **43**, 417 (1980).

[258] N. Marcus and A. Sagnotti, "A Simple Method for Calculating Counterterms", Nuovo Cim. **A87**, 1 (1985).

[259] M. Beneke and V. A. Smirnov, "Asymptotic expansion of Feynman integrals near threshold", Nucl. Phys. **B522**, 321 (1998), arXiv:`hep-ph/9711391` `[hep-ph]`.

[260] T. Luthe, "Fully massive vacuum integrals at 5 loops", PhD thesis (Bielefeld, 2015).

[261] A. Pak, "The Toolbox of modern multi-loop calculations: novel analytic and semi-analytic techniques", J. Phys. Conf. Ser. **368**, 012049 (2012), arXiv:`1111.0868` `[hep-ph]`.

[262] J. Hoff, "The Mathematica package TopoID and its application to the Higgs boson production cross section", J. Phys. Conf. Ser. **762**, 012061 (2016), arXiv:`1607.04465` `[hep-ph]`.

[263] J. Bosma, M. Sogaard, and Y. Zhang, "Maximal Cuts in Arbitrary Dimension", JHEP **08**, 051 (2017), arXiv:`1704.04255` `[hep-th]`.

[264] M. Harley, F. Moriello, and R. M. Schabinger, "Baikov-Lee Representations Of Cut Feynman Integrals", JHEP **06**, 049 (2017), arXiv:1705.03478 [`hep-ph`].

[265] S. Abreu, F. Febres Cordero, H. Ita, M. Jaquier, B. Page, and M. Zeng, "Two-Loop Four-Gluon Amplitudes from Numerical Unitarity", Phys. Rev. Lett. **119**, 142001 (2017), arXiv:1703.05273 [`hep-ph`].

[266] S. Abreu, F. Febres Cordero, H. Ita, B. Page, and M. Zeng, "Planar Two-Loop Five-Gluon Amplitudes from Numerical Unitarity", Phys. Rev. **D97**, 116014 (2018), arXiv:1712.03946 [`hep-ph`].

[267] H. Johansson, D. A. Kosower, K. J. Larsen, and M. Søgaard, "Cross-Order Integral Relations from Maximal Cuts", Phys. Rev. **D92**, 025015 (2015), arXiv:1503.06711 [`hep-th`].

[268] G. Chen, J. Liu, R. Xie, H. Zhang, and Y. Zhou, "Syzygies Probing Scattering Amplitudes", JHEP **09**, 075 (2016), arXiv:1511.01058 [`hep-th`].

[269] G. P. W. Decker G.-M. Greuel and H. Schönemann, SINGULAR 4-1-1 — A COMPUTER ALGEBRA SYSTEM FOR POLYNOMIAL COMPUTATIONS, `http://www.singular.uni-kl.de`, 2018.

[270] P. A. Baikov, "Explicit solutions of the three loop vacuum integral recurrence relations", Phys. Lett. **B385**, 404 (1996), arXiv:`hep-ph/9603267` [`hep-ph`].

[271] P. A. Baikov, "Explicit solutions of the multiloop integral recurrence relations and its application", Nucl. Instrum. Meth. **A389**, 347 (1997), arXiv:`hep-ph/9611449` [`hep-ph`].

[272] R. E. Cutkosky, "Singularities and discontinuities of Feynman amplitudes", J. Math. Phys. **1**, 429 (1960).

[273] A. G. Grozin, "Integration by parts: An Introduction", Int. J. Mod. Phys. **A26**, 2807 (2011), arXiv:1104.3993 [`hep-ph`].

[274] A. von Manteuffel and R. M. Schabinger, "A novel approach to integration by parts reduction", Phys. Lett. **B744**, 101 (2015), arXiv:1406.4513 [hep-ph].

[275] T. Peraro, "Scattering amplitudes over finite fields and multivariate functional reconstruction", JHEP **12**, 030 (2016), arXiv:1608.01902 [hep-ph].

[276] J. Dumas, T. Gautier, M. Giesbrecht, P. Giorgi, B. Hovinen, E. Kaltofen, B. D. Saunders, W. J. Turner, and G. Villard, LINBOX: *A generic library for exact linear algebra.* http://www.linalg.org, July 2002.

[277] A. von Manteuffel and R. M. Schabinger, "Quark and gluon form factors to four-loop order in QCD: the N_f^3 contributions", Phys. Rev. **D95**, 034030 (2017), arXiv:1611.00795 [hep-ph].

[278] A. V. Smirnov and M. N. Tentyukov, "Feynman Integral Evaluation by a Sector decomposiTion Approach (FIESTA)", Comput. Phys. Commun. **180**, 735 (2009), arXiv:0807.4129 [hep-ph].

[279] A. V. Smirnov, V. A. Smirnov, and M. Tentyukov, "FIESTA 2: Parallelizeable multiloop numerical calculations", Comput. Phys. Commun. **182**, 790 (2011), arXiv:0912.0158 [hep-ph].

[280] A. V. Smirnov, "FIESTA 3: cluster-parallelizable multiloop numerical calculations in physical regions", Comput. Phys. Commun. **185**, 2090 (2014), arXiv:1312.3186 [hep-ph].

[281] Z. Bern, J. J. Carrasco, L. J. Dixon, M. R. Douglas, M. von Hippel, and H. Johansson, "D=5 maximally supersymmetric Yang-Mills theory diverges at six loops", Phys. Rev. **D87**, 025018 (2013), arXiv:1210.7709 [hep-th].

[282] Z. Bern, N. E. J. Bjerrum-Bohr, and D. C. Dunbar, "Inherited twistor-space structure of gravity loop amplitudes", JHEP **05**, 056 (2005), arXiv:hep-th/0501137 [hep-th].

[283] N. E. J. Bjerrum-Bohr and P. Vanhove, "Explicit Cancellation of Triangles in One-loop Gravity Amplitudes", JHEP **04**, 065 (2008), arXiv:0802.0868 [hep-th].

[284] N. E. J. Bjerrum-Bohr and P. Vanhove, "Absence of Triangles in Maximal Supergravity Amplitudes", JHEP **10**, 006 (2008), arXiv:0805.3682 [hep-th].

[285] N. Arkani-Hamed, F. Cachazo, and J. Kaplan, "What is the Simplest Quantum Field Theory?", JHEP **09**, 016 (2010), arXiv:0808.1446 [hep-th].